Modeling, Control & Performance Evaluation of Bottom-up Motorized Shade

Konstantinos Kapsis

A Thesis in the Department of

Building, Civil, and Environmental Engineering

Presented in Partial Fulfillment of the Requirements for the Degree of Master of Applied Science (Building Engineering) at Concordia University

Montreal, Quebec, Canada

July 2009

Your file Votre référence
ISBN: 978-0-494-80161-1
Our file Notre référence
ISBN: 978-0-494-80161-1

Abstract

Modeling, Control & Performance Evaluation of Bottom-up Motorized Shade

by Konstantinos Kapsis

Integration of daylighting into buildings using motorized interior shades is challenging. If it is done properly, reduction of energy for artificial lighting and eventually building cooling demand can be achieved, while providing an improved visual and thermal office environment, beneficial for the occupants' health and performance. If it is poorly done, it can lead to increased cooling demand due to overheating, thermal discomfort and glare problems.

In this study, the daylighting and thermal performance of "bottom-up" shades was presented. The bottom-up is a motorized roller shade that operates in reverse of a conventional roller shade (opens from top to bottom), so as to cover the bottom part of the window, providing privacy to the occupants, while allowing daylight to enter from the top section.

A daylighting simulation model, validated with experimental results, was developed in order to establish correlations between the shade position, outdoor illuminance and work plane illuminance for different outdoor conditions as well as to allow a sensitivity analysis of the impact of shade optical properties on the results. Moreover, the model was used to compare "bottom-up" shades with conventional roller shades. The results showed that the Daylight Autonomy (DA) for the bottom-up is 8%-58% higher than the DA for a conventional roller shade, with a difference of 46% at the back part of the room, away from the façade, where the use of artificial lighting is usually more needed, proving the advantage

of bottom-up shade versus conventional roller shades, by allowing the natural light to enter from the top section of the façade deep into the room

Thermal experiments were conducted to examine the possible advantages of the use of a bottom-up shade's "sealed" cavity, showing increase of the effective thermal resistance of the fenestration, compared with no shades and with conventional roller shades

Finally, a methodology is proposed for the development of a control algorithm for a bottom-up shade, applicable for any location and orientation

Acknowledgments

I would like to express my gratitude to my supervisors Dr. A. K. Athienitis and Dr. R. Zmeureanu whose expertise and encouragement added to my graduate studies. This thesis would not appear in its present form without their kind assistance and support.

I am also indebted to Dr. A. Tzempelikos for his assistance and provision of critical thinking.

Special thanks to my friends and colleagues in the Solar Lab for their friendship and assistance.

I would also like to thank my family, without whom none of this would have been even possible. I am forever grateful.

Financial support of this work was provided by NSERC through the Solar Buildings Research Network and by Natural Resources Canada through the Innovative Research Initiative and the Technology and Innovation Program as part of the Climate Change Plan for Canada.

Στη Φεβρωνία, το Γιάννη, την Αγγελική

Στην Ελένη

Table of Contents

List of Figures

List of Tables

Nomenclature

A	correlation constant
$\mathbf{A_{sunlit}}$	sunlit area of the facade, m^2
c	atmospheric extinction coefficient
Control	Position of the bottom-up shade due to a control strategy
d	profile angle
D	depth, m
DA	Daylight Autonomy
E	illuminance, lx
$\mathbf{E_{corr}}$	correlation illuminance (lx) or solar radiation (W/m^2) value
$\mathbf{E_{sc}}$	solar illuminance constant, lx
$\mathbf{F_{ij}}$	view factor between surfaces i and j
$\mathbf{F_{trans}}$	transmittance factor
H	height, m
L(x, y, z)	Cartesian coordinates
$\mathbf{M_{facade}}$	total illuminance (lx) or solar radiant (W/m^2), as measured by the sensor
$\mathbf{M_i}$	luminous exitance of surface i
n	Julian day number
SHGC	Solar Heat Gain Coefficient (W/m^2K)
UDI	Useful Daylight Illuminance
U-Value	overall heat transfer coefficient, $W/m^2 \cdot K$
W	width, m
W(x ,y ,z)	Cartesian coordinates

Greek letters

α_s	solar altitude
γ	surface solar azimuth
δ	percentage of perforation
ΔT	temperature difference
ε	emissivity
θ	angle of incidence
ϱ	effective reflectance
τ	effective transmittance

Subscripts

0	initial
AWI	due to "Acceptable Workplane Illuminance" control strategy
bottom-up	bottom-up shade
ceiling	ceiling
clear	due to clear sky
diffuse	due to diffuse daylight
direct	due to direct daylight
dn	at the sea level
ext	exterior, incident on the façade
façade	façade
floor	floor
frame	frame
GFZ	due to "Glare-Free Zone" control strategy

glass	glass
ground	due to the ground
h	horizontal
overcast	due to overcast sky
rm	room
roller	conventional roller shade
setpoint	setpoint
shaded	shaded part of the façade
sky	due to the sky
solar	solar spectrum
sp	spandrel
sun	due to the direct sunlight
visible	visible spectrum
wall	interior wall
win	window
xt	extraterrestrial
$\perp$	perpendicular to a source of light
//	parallel to a source of light

Chapter 1: Introduction

1.1 Background

In 2005, lighting energy consumption amounted to 30% of total global electricity used in the commercial building sector, an estimated 1133 TWh (Waide & Tanishima, 2006). In Canada this percentage is less but still significant at 9.4% of national total electricity consumption in the sector, an estimated of 30 TWh (NRCan, 2007). Moreover, artificial lighting is not only responsible for considerable amount of electrical loads on commercial sector, but it can also cause excessive cooling loads as a side effect of its extensive use.

As commercial buildings with largely transparent facades become mainstream, daylighting is experiencing renewed attention as an important aspect of building lighting design; an architectural statement that is part of an overall sustainable design able to contribute to the energy and environmental solution. In addition, the benefits of daylighting extend beyond energy and architecture. Research confirms that daylighting improves health and well-being, and increases the occupants' productivity (Heschong, 2002). However, daylighting design requires careful system integration, as it can lead to design failure (e.g. overheating due to excessive solar gains, glare problems due to over-illuminated spaces, thermal discomfort due to radiant asymmetry caused by highly-glazed surfaces, etc.).

In order to properly integrate daylighting into a building, shading devices should be considered as an integral part of the HVAC and lighting system of the building. Ability to control the solar gains, optimize lighting levels and protect the occupants from visual and thermal discomfort, well-designed and controlled shading devices can drastically reduce building cooling energy demand and electric energy consumption.

1.2 Bottom-Up Roller Shade

The bottom up (see Figure 1 1) is a motorized roller shade that operates in the opposite direction of a conventional roller shade (opens from top to bottom) Its advantage, compared to conventional roller shades, is that it covers the bottom part of the window, providing shade and glare protection as well as privacy to the occupants, while allowing daylight to enter from the top section and illuminate the space (see Figure 1 2)

Figure 1 1 Comparison of a conventional roller shade (on the left) with a bottom-up roller shade (on the right), emphasizing the operational direction

The concept of three section façade, where the lower part is the spandrel, the middle section is the "viewing section" and the upper section is the section used for daylight benefits, is not new Previous research has been made (Galasiu *et al*, 2004, Tzempelikos *et al*, 2007), demonstrating the advantages of using this advanced dynamic fenestration configuration in office daylighting performance

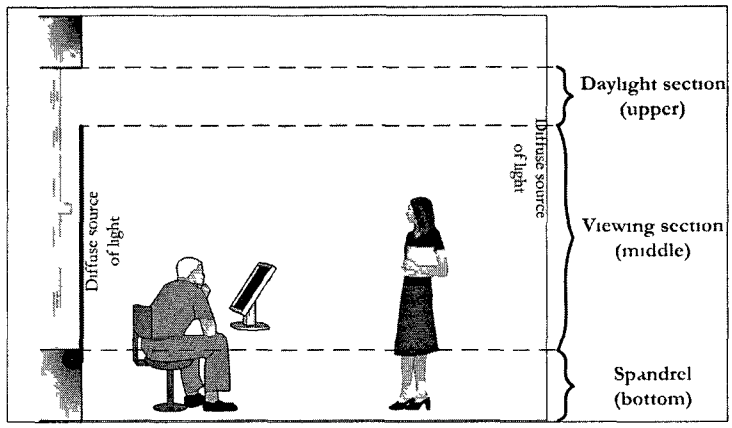

Figure 1 2 Using bottom-up shades in a three-section façade concept

Somfy Canada Inc manufactured a prototype bottom-up roller shade, donated to Concordia University for daylighting and thermal performance experiments The prototype shade has a single motor, positioned at the top part of the shading device (similar to conventional motorized roller shades) that drives the shade in both directions, through cords attached on the two upper corners of the shade It moves between vertical aluminum tracks (that contain the cords) attached to the window frame, keeping the fabric taut during shade extension and retraction Hence, as part of the frame, the bottom up shade is able to nearly seal the cavity between the glazing and the shade, compared to the loose sides of a conventional roller shade (see Figure 1 3)

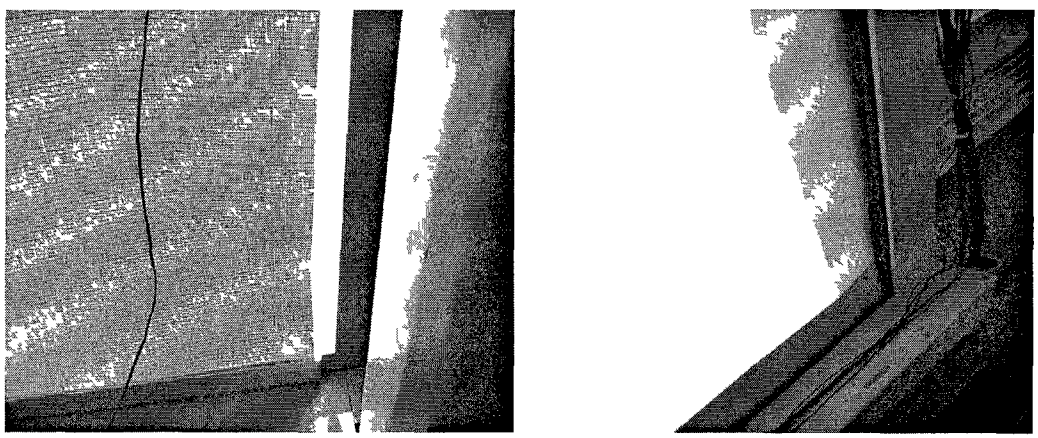

Figure 1 3 Comparison of a conventional roller shade (on the left) with a bottom-up roller shade (on the right), emphasizing the "sealed" cavity

1.3 Motivation

Ongoing development of new fenestration systems results in a wide variation of shading devices in the market. Despite the broad range of computer software available, most of them use simplified models to simulate shading devices' thermal and daylight performance, without considering their specific properties (e g. specular reflectance or transmittance, solar angular dependence on visual or thermal properties, etc.), that can differ their overall performance and make one shading device more suitable for a specific application. In addition, the variation of control strategies available in the majority of computer software is poor, further reducing the value of the comparison between shading devices and proper integrated control strategies.

The bottom-up is a new kind of shade with significant potential to improve comfort while reducing energy consumption through increased daylight utilization. However, to achieve this potential mathematical models and methods need to be developed for the design and control of bottom-up shades, as it is difficult, if not impractical, to use available software to simulate its daylighting and thermal performance. Thus, there is a clear need for work that will support the design of daylighting systems that incorporate bottom-up shade, as well as control algorithms for their control - both alone and in conjunction with lighting and HVAC.

1.4 Thesis Objectives

The main objectives of the thesis are the following:

- Study the daylighting performance of bottom-up roller shades as well as their effect on artificial lighting energy consumption, in commercial building applications.

- Develop control algorithms for automatically moving the shade so as to avoid direct sunlight on the occupant at all times, while maximizing daylight provision and outdoor view, and maintaining the workplane illuminance levels within acceptable range.
- Investigate the possible thermal advantages of the use of the "sealed" cavity on the thermal performance of the fenestration.

1.5 Thesis Overview

Chapter 2 presents a general overview on literature related to the control and performance of dynamic shading devices, integrated into commercial buildings' fenestration. Furthermore, an essential review on the nature of light and its effects on human health and performance is presented.

Chapter 3 presents a daylighting/lighting numerical model, for office spaces with bottom-up or conventional roller shades, developed based on radiosity (Athienitis & Tzempelikos, 2002; Murdoch, 2003) and ray tracing (Glassner, 1989) theories . Two control strategies are introduced in order to ensure proper lighting conditions: the 'Glare-Free Zone' (GFZ) and the Acceptable Workplane Illuminance (AWI). A general methodology is proposed in order to obtain control algorithms for bottom-up motorized shades, applicable for any location and orientation around the world. Finally, a sensitivity analysis of the impact of bottom-up shade optical properties on the annual daylighting and lighting energy demand is presented as well as an annual comparison of a bottom-up shade with a conventional roller shade of equal transmittance, in terms of daylight performance and energy consumption on artificial lighting.

Chapter 4 presents the experimental study of a prototype bottom-up roller shade The results of this study are used for the verification of the daylighting/lighting numerical model. The thermal performance of this innovative shading device is investigated as well and a comparison with a conventional roller shade is made. Finally, a third control strategy is introduced, applied when the occupants are absent, giving priority to the thermal performance of the fenestration.

Chapter 5 presents the conclusions of this study and recommendations for future work.

Chapter 2: Literature Review

2.1 Introduction

This chapter gives an overview of significant literature related to the control and performance of dynamic shading devices, integrated in fenestration commercial buildings. Due to the lack of any literature related to bottom-up shades, this review focuses on the daylighting, thermal and energy performance of various shading devices (roller shades and venetian blinds) which have been previous studied. The knowledge gained from these studies can be generalized and applied to the modeling and evaluation of daylighting performance of new innovative shading devices (e.g. bottom-up shade), as well as to the development of control algorithms.

In addition, this chapter presents an essential review on the nature of light and its effects on human health and performance.

2.2 Sun and Daylight

Our solar system consists of the sun and several celestial bodies (planets, asteroid belts etc.) -that are on gravitational orbit around the sun- all of which formed from the collapse of a giant molecular cloud approximately 4.57 billion years ago (Lang, 2001).

Despite its relatively small star size, the sun has a diameter of $1.39x10^6$ Km and constitutes about 98.6% of the solar system mass. It generates its energy by nuclear fusion of hydrogen nuclei into helium, therefore its temperature varies from $40x10^6$K (core) to 5800K (photosphere).

As the nearest star to the earth, the sun is the dominant source of energy on earth. The photosphere is the source of most solar radiation (Sen, 2008). As a result, the solar radiation

at the top of the earth's atmosphere is similar to that which a perfect black body emits at a temperature of 5800K, with the solar spectrum peak occurring between wavelengths of 380–770 nm (visible range). As the sunlight penetrates the earth's atmosphere, some of the wavelengths are absorbed by atmospheric constituents (ozone layer, water vapour, CO_2, etc.), reducing the solar radiation that reaches the earth's surface (see Figure 2.1). Hence, the power intercepted by the earth at the top of the atmosphere has an average value of 1360 W/m^2, where at sea level it varies from 80 W/m^2 to 1200 W/m^2 during the solar noon, due to latitude, season and weather conditions.

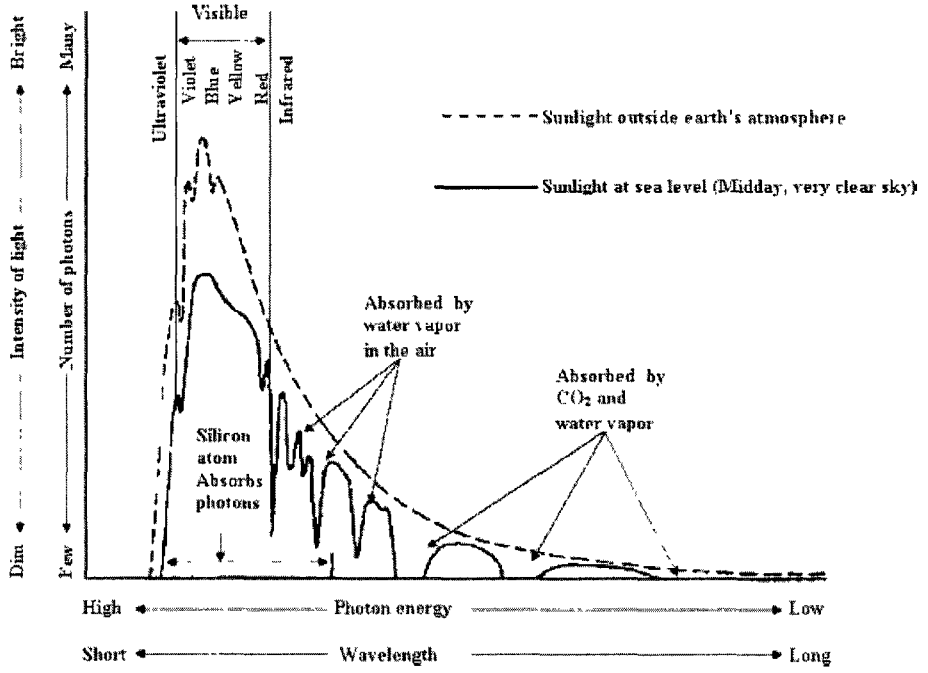

Figure 2.1: Solar electromagnetic spectrum (Sen, 2008)

In terms of luminous efficacy (lm/W), sunlight is more efficient than the majority of artificial lighting used in commercial buildings (see Table 2.1), providing a broad electromagnetic spectrum with excellent colour rendering that creates interesting, dynamic interiors supportive of human health and performance (Leslie, 2003).

Table 2 1 Light sources used for commercial buildings (U S DOE[1])

Incandescent lamp	2600-3000	10-18	750-2000
Tungsten-Halogen lamp (TH)	2800 3400	15 20	3000-4000
Linear Fluorescent lamp	2900 7000	50 100	20000-30000
Compact Fluorescent lamp	2900 7000	35 60	8000-10000
Solid state lamp (LED)	2600-6000	25-100	35000-50000
Direct Beam Sunlight	5800	80-120	--

2.3 Visual Comfort

Most lighting standards require an office workplane illuminance of at least 500 lx where paper work is carried out However, when visual display units (VDUs) such as computer monitors are used, the workplane illuminance should be lower than 500 lx (Rea, 2000) In all cases the work plane illuminance should never be below 100 lx and should not exceed 2000 lx, as this is likely to produce glare (Nabil & Mardaljevic, 2006)

"Glare is the sensation produced by luminances within the visual field that are sufficiently greater than the luminance to which eyes are adapted" (Murdoch, 2003). There are two types of glare which can occur in an office space· Disability and Discomfort Disability glare is a physiological effect that reduces visibility caused by a reduction of contrast, due to a bright light source (e g direct sun or an unshaded bright window reflected on a VDU) Discomfort glare is a psychological effect – therefore, a subjective phenomenon – which produces annoyance due to high contrast between luminous sources and room surfaces (e g light fixtures, windows and reflections from shiny surfaces) but usually without affecting the visual task It is highly affected by the angular displacement of the source from the observer's line of sight as well as by the size of source of glare (Osterhaus & Bailey,

[1] www eere energy gov

1992). Discomfort glare can lead to headaches and eyestrain, due to the continuous effort of the eyes to adapt on the highly contrast lighting conditions.

When disability glare occurs, occupants react by re-positioning themselves or utilizing any shading devices available (Osterhaus, 2005). On the other hand, occupants have higher tolerance to discomfort glare, often without taking any actions to prevent it This tolerance is even higher when it comes to daylighting (Fisekis *et al.*, 2003; Sutter *et al.*, 2006).

When looking at lighting standards, there is research evidence that the proposed lighting levels are too low, and considering the findings on the non-visual effects of light these standards are not sufficient to maintain health and well-being of the occupants. Thus, these illuminance requirements should be regarded as minimum lighting requirements

2.4 Non-Visual Effects of Light

Artificial lighting is designed for a consistent and controlled visual environment, allowing suitable visual performance for the occupants. However, its spectral characteristics differ from sunlight, lacking the spectral distribution needed for complete biological functions of the neuroendocrine system. Eyestrain and ability to refocus are related to the poor spectrum of light present in a workspace due to artificial lighting (Edwards *et al.*, 2002). Circadian rhythm of hormone secretions and core body temperature as well as Vitamin D production, are strongly connected with sunlight exposure. Diminution or disruption of these cycles affects the alertness, mood and human behaviour, and can cause temporary jet lag and Seasonal Affective Disorder (SAD) (Webb, 2006). Luminous modulation of light source output, or flicker, can reduce visual performance (Veitch & McColl, 1995), causing headaches and eyestrain as well Finally, Leppamaki & Partonen [as cited by Veitch (2006)]

reported improved feelings of vitality and well-being in healthy adults, when they were exposed to high doses of light (2400-4000 lx), two to three times a week.

2.5 Thermal Comfort

Thermal comfort refers to "that condition of mind that express satisfaction with the thermal environment" [ASHRAE *standard 55*; as cited on ASHRAE (2005)]. Thermal comfort occurs in narrow temperature ranges, at low skin moisture levels and with minimal physiological effort of regulation. It is strongly dependent on the levels of activity, physiological and psychological state, nature of clothing as well as the surrounding environment.

When it comes to fenestration, thermal comfort is affected in three ways (Huizenga *et al.*, 2006): (i) through transmitted solar radiation, (ii) by long-wave radiation exchange between the occupant and the interior glass surface and (iii) from convective drafts caused by temperature difference between the glass surface and the room air. Hence, effective thermal resistance and effective solar transmittance of the fenestration [usually expressed as solar heat gain coefficient (SHGC)] can influence not only the building energy consumption, but also the thermal comfort. Hodder & Parsons (2007) reported for direct exposure of solar radiation transmitted though glazing, "slightly warm" to "warm" mean overall thermal sensation for actual mean vote (AMV). Moreover, the higher the solar transmittance, the higher the actual percentage of dissatisfied (APD).

Ge & Fazio (2004) measured temperature and velocity profiles on large cold windows. Better insulated systems induce less forceful cold draft than conventional windows and with higher glass and room air temperatures. The cold window-induced air motion could reach values of 1 m/s near the window, to 0.15 m/s 1.2 m away from it, with a temperature from

1.8°C (close to the window) to 0.8°C (1.2 m away) lower than the room air temperature. According to Lyons *et al.* (2000) at 20°C indoor temperature, more than 0.1 m/s mean air velocity leads to greater than 10% predicted percentage of dissatisfied (PPD)

An effective way to reduce radiant asymmetry, solar radiation, and possibly downward cold drafts, is with the use of shading devices Carmody *et al.* (2004) and Bessoudo *et al.* (2007) carried out studies on highly-glazed perimeter zones, showing the beneficial use of shading devices on maintaining thermal comfort, with no additional perimeter heating required, when high performance commercial building facades were used. Moreover, several studies have shown how the energy performance of a fenestration system increases by using shading devices (Carmody *et al.*, 2004; Shahid & Naylor, 2005, Tzempelikos & Athienitis, 2007), consequently leading to better thermal comfort performance.

2.6 Dynamic Fenestration

Fenestration is an architectural term that refers to windows, skylights and door systems within a building (ASHRAE, 2005). These building components provide a physical barrier between the building interior microclimate and the natural elements (wind, rain, humidity, solar radiation) while at the same time retaining a physical and visual connection to the outdoors.

In recent years, there is a trend towards the design of highly transparent building envelopes and there has been great deal of interest to optimize fenestration, using dynamic components to control and optimize the thermal heat transfer, solar heat gains, daylighting, ventilation and energy demand of buildings. Conventional and innovative shading devices, electrochromic windows, double-skin facades and semi-transparent photovoltaics are some of the components that make the fenestration not just a static envelope element, but a

dynamic one, able to provide visual and thermal comfort to occupants under various weather conditions, increasing the building energy performance as well.

Dubois (2001) investigated the daylight performance of four exterior shading devices for several desk positions and viewing directions using *Radiance* Three design days (21st of June, September and December), under CIE Clear Sky model, were used to verify their performance based on simple performance metrics. Overall, dynamic shading devices (retractable awning and venetian blinds) performed better than static ones (overhang, screen), and due to their ability to adjust to exterior lighting conditions they provided better workplane illuminance uniformity and achieved a higher percentage of the required luminance ratios between the workplane, VDT and the surroundings , thus illustrating the advantageous use of dynamic shading devices.

2.6.1 Interior Shading Devices

Interior shading devices (roller shades, venetian blinds, drapes and curtains) are widely adapted in commercial buildings, due to their low initial cost, easy maintenance and control (ASHRAE, 2005), as well as their relatively small influence on the building's exterior appearance. Innovative or conventional, manually or automatically controlled, shading devices should not only be considered as an integral part of fenestration system design (Athienitis & Santamouris, 2002) but also as a vital component of the HVAC system of the building. Mainly used to control daylight into the space and provide visual quality to the occupants by controlling glare and reducing contrast ratios, interior shading has a strong impact on building thermal and energy performance. Well-designed and controlled shading devices can drastically reduce a building's peak heat gains and cooling energy demand (see section 2.8), while maintaining thermal comfort. Automated shades incorporated with

controlled artificial lighting can reduce the electric energy demand by substituting artificial lighting with daylight (for the impact of daylight on human health and performance, see section 2 4).

A major factor in the evaluation of the performance of dynamic shading systems is their detailed and unique optical and thermal properties These properties are usually not provided by manufacturers and computer software normally use simplified models to simulate shading devices' thermal and daylight performance, without considering their specific properties. This practice can give similar performance for completely different shades or for shades under different control strategies, which can lead the user to unsuitable shading selection. Therefore, in order to optimize the system performance, preliminary daylighting and thermal studies are required in order to adapt an appropriate shading control strategy.

Breitenbach *et al.*(2001), through experimental measurements, addressed the importance of calculating the total solar energy transmittance and luminous transmittance of advanced fenestration system as a function of solar angles, instead of using oversimplified constant values. Klems (2000) dealt with similar issues and developed a methodology for solar angular dependent solar heat gain coefficients (SHGC) for advanced fenestration systems and Kuhn (Kuhn *et al*, 2001, Kuhn, 2006) developed a methodology to calculate the angular dependent total solar energy transmittance (g-value). Athienitis & Tzempelikos (2002) developed a methodology for solar angular dependent luminous transmittance for similar fenestration systems. Only after the lighting and thermal properties of the shading devices are known can the control strategies be applied.

2.6.2 Control Strategies for Shades

Despite the ongoing technological developments in digital control systems, manually controlled shading and manually controlled lighting are the norm. However, as the use of highly-glazed building surfaces is increasingly adapted in commercial buildings (most of the times as an architectural statement, less often as an envelope component that will add to building energy performance), the need for more sophisticated and dynamic controlled shading systems is apparent.

The variation in control strategies for shades is as wide as the variation of shading devices themselves. However, all control strategies have one thing in common: they all aim to provide acceptable visual and thermal conditions to the occupants as well as to reduce a building's energy demand. Figure 2.2 summarizes these requirements, many of which are in conflict (e.g. advantageous high solar heat gains in winter dictates an open shade, a decision than will cause glare during a sunny day).

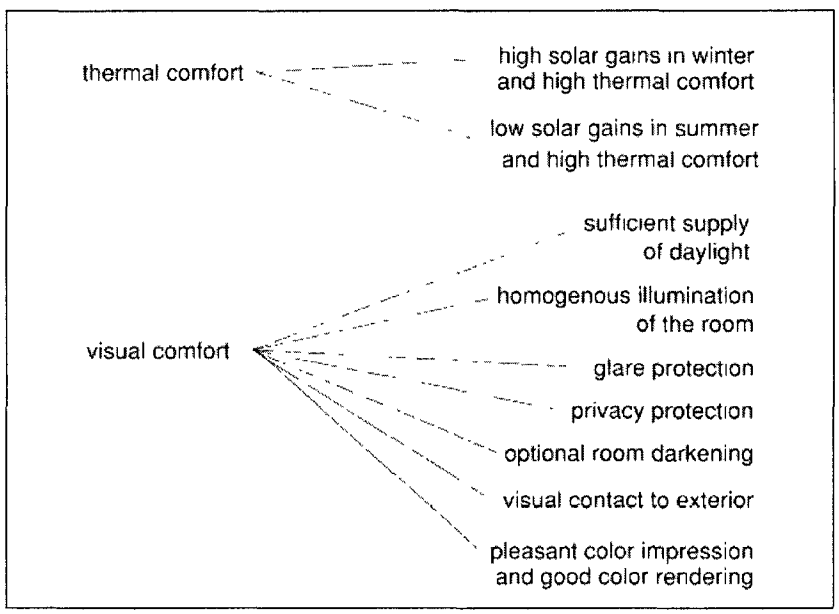

Figure 2.2: Daylighting and thermal requirements for shading devices (Kuhn et al., 2001)

Control systems for shades are classified as either open-loop or closed-loop. An open-loop controller computes the position of the shade through control algorithms, using a single input (e.g. from a sensor monitoring the exterior solar radiation incident on the façade), without using feedback to determine if the output (e.g. workplane illuminance level) has achieved the desired goal. On the other hand, a closed-loop controller uses a sensor to monitor the output (e.g. workplane illuminance level) and feeds the data to the controller which adjusts the position of the shade appropriately.

If the relationship between input (e.g. exterior solar radiation incident on the façade), the position of the shading system and the output (e.g. workplane illuminance level) can be modeled by mathematical correlations, open-loop controller can be more effective than a closed-loop one, as it is independent from the interior environment and is more cost effective as with one sensor several shading systems can be controlled. In contrast, a closed-loop controller achieves higher response and accuracy at the output if the interior environment is long-standing (e.g. reposition of the office furniture or change of the office carpet can destabilize a closed-loop controller). However, multiple sensors required to control multiple shading systems, increasing the initial cost.

Several studies have been conducted on control strategies for roller shades and venetian blinds. Rosenfeld & Selkowitz (1977) considered direct beam daylight as an alternative illumination technique, by proposing the use of venetian blinds that redirected the light onto the ceiling which illuminated not only the perimeter zone of an office but further away from the window, where artificial lighting is mainly used to maintain workplane illuminance at desirable levels.

Athienitis & Tzempelikos (2002) proposed an open-loop control strategy for motorized venetian blinds, using an exterior vertical illuminance sensor at window orientation. The tilt

angle of the blinds was calculated in order to transmit the maximum possible amount of daylight and to eliminate at the same time the direct sunlight entering the room (cut-off angle), providing the maximum view to outside. Twelve representative days were simulated (one for each month of the year) under CIE Clear and Overcast Sky conditions, to illustrate the ability of venetian blinds to provide sufficient lighting conditions throughout the workplane, when the appropriate control strategies were applied However, the authors called attention to sunny days, where the workplane illuminance could reach values above 2000 lx, leading to glare.

Galasiu *et al.*(2004) studied the daylight performance of several blind position configurations, using venetian blinds. Of these configurations, there were two that drew attention: (i) "*top blind*" configuration in which the top blinds were controlled for daylight admission and the bottom blinds were closed to provide shading to occupants (similar principal with the bottom-up shade) and, (ii) "*bottom blind*" configuration in which the bottom blinds were controlled for daylight admission and the top blinds were closed. Despite the fact that bottom windows were twice the size of the top ones, the "*top blind*" configuration performed significantly better than the "*bottom blind*" configuration, in terms of artificial energy consumption – regardless of the lighting control strategy applied – illustrating the advantage of daylight penetration into the room from the upper window section

For the evaluation of roller shades, Roche (2002) conducted experiments to develop and evaluate an open-loop control shading system, incorporated with dimmable lights. The system used inputs from two sensors to control the installation: one exterior vertical illuminance sensor at window orientation, providing input for the exterior lighting conditions and sun position, and one mounted on the ceiling facing the workplane,

providing input for the workplane conditions. The system was able to control the roller shades' position (two shades were used, controlled independently) in order to eliminate direct solar penetration into the room and maintain workplane illuminance levels within a desirable range (700 lx - 1800 lx). The system performed a nightly autocalibration routine once a week in order to ensure proper performance in case of furniture rearrangements or faulty performance of shading and lighting systems. The results showed adequate visual quality performance of the workplane illuminance as it was kept in the range of 400 lx – 1800 lx. The actual minimum was less than the minimum target limit (700 lx), due to the overestimated workplane illuminance levels given from the control algorithms. However, it was apparent that conventional roller shades impede sufficient penetration of daylight into the room. In addition, the system had higher savings using continuous dimmable lights than if it used automated on/off control. Finally, the author addressed the problem of the control system to deal with "the more variable classes of weather", illustrating the need for predictive weather control of shading devices.

Lee & Selkowitz (2006) performed a field study on the performance of automated roller shades and a dimmable lighting system, in an unoccupied, fully furnished mockup of the New York Times building. Two different proportional control systems were used, in different areas of the office: (i) an open-loop (*area A*) and (ii) a closed-loop (*area B*). In *area A* all lighting zones were controlled using a single photosensor, whereas in *area B* each lighting zone was controlled by its own individual photosensor (in both case, the photosensors were ceiling-mounted, but at different angles). The workplane illuminance setpoint range was 400 lx – 538 lx. Overall, *area A* performed better than *area B,* which had difficulties meeting the control performance requirements In terms of cost effectiveness, *area A* was also better, due to the ability to control several zones with a single photosensor.

Guillemin (Guillemin & Molteni, 2002; Guillemin & Morel, 2002) developed an open-loop fuzzy controller for roller shades that had the capability of adapting to user's wishes (EDIFICIO system). The system was incorporated with a weather predictor, heating controller and dimmable lighting system, in order to maximize its performance. The controller used as inputs the global and direct vertical illuminance incident on the façade and the average outside temperature of the last 24 hours. The controller was divided into two modes: when users were absent, priority was given to thermal aspects, and when users were present, priority was given to visual comfort as well as the users' preferences. Despite the fact that the EDIFICIO system was able to take into account several parameters (visual and thermal comfort, energy savings, short-term user's wishes) and provide a comfortable indoor environment to the users, authors stated that "only one of the two users was satisfied" and that control systems "should take into account, on a long-term basis, the particular preferences of the occupants".

Similar observations were made by Velds (2002). Automated venetian blinds were used to block direct sunlight from entering the room and an automated daylight responsive artificial lighting system was incorporated to maintain workplane illuminance levels at 500 lx. The study showed that users expressed complaints with respect to the lack of control of the shading and artificial lighting systems (24% for the blind control and 44% for the artificial lighting control). Both studies delivered the importance of manual override control available on both automated shading and artificial lighting systems.

2.7 Artificial Lighting

Despite the fact that artificial lighting controls are widely available on the market, manual on/off lighting control is still the norm. This is the case even though, field studies show that occupants switch on the lights if needed, but hardly ever switch them off (even if the available daylight is adequate), until the space is unoccupied (Hunt, 1979) Rosenfeld & Selkowitz (1977) reported than one of five lights was left on at the end of the work day.

In addition, artificial lighting is responsible for 5% - 15% of annual cooling energy demand and about 30% of the electric energy consumption in commercial buildings. Zmeureanu & Peragine (1999) simulated the energy impact of a retrofitted lighting system on the HVAC system of an existing energy efficient office building. The model was calibrated for the actual energy performance of the building based on the utility bills Parametric analysis was carried out for various types of fluorescent fixture lamps and various installed electric power densities as well as under two different climatic conditions (Montreal & Phoenix). The results showed that the net energy savings from retrofit of lighting systems, using more efficient ones was less energy effective than initially expected (the net energy savings are only about 70% of the gross lighting energy savings, for most cases). Similar results on the artificial lighting/ HVAC interaction, were found from Sezgen & Koomey (2000), for several building types and climates around U.S

On the other hand, advanced lighting systems (e g automated on/off or dimmable lights, with integrated occupancy sensors and photosensors) can result in significant energy savings. Newsham (2009), in a survey of offices, found that dimmable lights can reduce light levels by 80% (starting from a baseline of 400 lx), often undetected by occupants. Despite the extreme level of dimming, 40% of the occupants did not notice the difference with relatively low prevailing daylight and with high prevailing daylight the percentage was

increased to 60% By gradually dimming the lights over a period of 15-30 min, electric energy reductions of up to 23% were achieved (for dimming levels of up to 30%)

Energy savings can be substantial when artificial lighting controls are incorporated with daylight control systems (e.g. interior shading devices). Athienitis & Tzempelikos (2002) reported lighting energy savings of 76% for overcast days and 92% for clear days, using dynamic venetian blinds incorporated with dimmable lights. In both studies, the study cases were compared down with the reference case, where the lights were on at 100% output during working hours

Galasiu *et al.*(2004) investigated the daylight performance and its effect on artificial lighting energy consumption for several blind configurations, using venetian blinds. Continuous dimming and on/off control strategies were applied on artificial lighting, for static and photocontrolled venetian blinds The performance of the shading systems was monitored for several short periods of days through a year (from 6:00 to 18:00), in order to include various sky conditions and solar geometries. The minimum workplane illuminance requirements were 570 lx, below which the artificial lighting was controlled. Overall, both lighting control strategies achieved greater savings for the case of the photocontrolled venetian blinds over the static ones. However, the photocontrolled venetian blinds showed response failures under sunny clear sky and overcast sky conditions (extreme case scenarios).

2.8 Daylighting/HVAC System Interaction

Shading devices lower the building cooling demand, due to the reduction of building solar gains Moreover, with the development of dimmable lighting systems integrated with shading control systems, electric lighting energy consumption should be considered along

with cooling loads as an indicator for the overall performance of the shading devices and their impact on buildings and environment.

Lee *et al.* (1998) conducted a full-scale study on an automated venetian blind system incorporated with controlled dimmable lighting system installed in a cooling-load dominated office building The system controlled the venetian blind/lighting system in order to maintain the workplane illuminance levels within an acceptable range (510 lx -700 lx), block the direct beam sunlight, maximize the view to the outside while minimizes the artificial lighting use and glare Under these requirements, the system achieved 28% reductions in cooling load and in peak cooling load and a 22-86% reduction in lighting energy, when compared to a static horizontal blind with no daylighting controls. Moreover, the workplane illuminance levels were within the design range 70% of the time (with 15% of the year exceeded and 15% falling-short) and the view to outside was possible on average 56% of the day, throughout the year.

Tzempelikos & Athienitis (2007) simulated the impact of roller shades on daylighting and thermal performance of a typical office . Two types of control strategies were used for roller shades: (i) passive control in which the roller shades remain closed during working hours to ensure privacy/reduce glare and, (ii) active on/off control in which roller shades were open during overcast sky conditions (beam solar radiation incident on the window was less than 20 W/m^2) and closed under other sky conditions. The findings indicated that passive shading control resulted in poor Daylight Autonomy (DA) (see section 2.9) while automatic on/off (open/close) control increased annual DA ratio by 20% on average. In both cases, a sensitivity analysis was carried out showing that the "optimal" shade transmittance was 20% above this transmittance the daylight performance of the shades would not significantly change, increasing at the same time the possibility for glare to occur

and increasing the cooling demand, due to increased solar gains. The annual electric lighting energy consumption for this configuration was reduced by 40% for passive shading control and by 60% for active on/off automatic shading control (passive lighting control). In addition, it was estimated that a 50% reduction in annual cooling energy demand occurred when compared with the base case without shades, resulting in a total annual energy demand reduction of 12%.

Guillemin (Guillemin & Molteni, 2002; Guillemin & Morel, 2002) used a fuzzy controller for roller shades (EDIFICIO system), achieving net value savings of 19% (heating + artificial lighting + electrical appliances, considering as well the energy consumption from the EDIFICIO system), compared to a conventional controller (no automatic shade control, no automatic artificial lighting control, proportional controller with saturation). Better performance was obtained in thermal comfort, based on predicted mean vote (PMV) calculations (66% of the time the room is comfortable) and in visual comfort, based on PIECLE method, avoiding very bad visual conditions (97% of time acceptable visual comfort for EDIFICIO compared to 85% for the conventional).

2.9 Daylight Performance Metrics

Due to the variation of dynamic shading devices available and possible control strategies applied, there is a need for standard daylight performance metrics. Performance metrics can be used for comparative studies to guide building designers, owners and users on effective decisions based on their daylight requirements. However, as mentioned by Reinhart *et al.* (2006): "Daylighting is a notoriously difficult building performance strategy to evaluate", as "daylight quality cannot be measured in the same sense as one measures length, mass or

lumen output" (Veitch & Newsham, 1998), but can only be assessed indirectly using behavioural measures.

Daylight Autonomy (DA), redefined by Reinhart & Walkenhorst (2001), is the percentage of the occupied hours per year when the minimum illuminance requirement is met by daylight alone, in a specific point When it comes to workplane illuminance, it is usually presented for several points on the centre line of a room, from the façade to the back wall, giving an overall indicator of the performance of the room and illustrating the ability of the shading device to illuminate the back part of the room where there is a greater requirement for artificial lighting

Useful Daylight Illuminance (UDI), proposed by Nabil & Mardaljevic (2006) is the percentage of the occupied hours per year when the daylight levels are useful for the occupants For offices, the suggested range of useful daylight levels is 100 lx to 2000 lx. The UDI is presented as a three-value metric: for when the UDI is achieved (100-2000 lx), falls-short (<100 lx) and is exceeded (> 2000 lx). When it comes to workplane illuminance, it is presented for several points on the centre line of a room, from the façade to the back wall or as a metric for the average workplane illuminance.

The Daylight Glare Index (DGI), developed at the Building Research Station in England and at Cornell University, is the only available discomfort glare index that is developed to evaluate glare due to daylighting (the rest of discomfort glare indices are developed for artificial lighting). Revised from Nazzal (2001) (DGI_N) and experimentally verified by Fisekis *et al.* (2003), DGI_N is an empirically derived model that assesses the degree of visual discomfort, based on source luminance, solid angle of the glare source, angular displacement of the source from the observer's line of sight and background luminance.

However, many researchers argue that there is not enough solid evidence that DGI_N is a reliable generic index to predict discomfort glare from windows. Lee & Kim (2007) reported different glare perceptivity between Caucasians and Asians Kim *et al* (2008) reported difference in glare sensation between uniform and non-uniform glare sources Therefore, as it is based on an empirical model, it should be used carefully, taking into account its limitations (Osterhaus, 2005).

Chapter 3: Numerical Model of Bottom-up Roller Shade

3.1 Introduction

In order to evaluate the daylight performance of the bottom-up motorized shade and propose proper control strategies that will enhance office daylight utilization, a daylighting/lighting numerical model was developed based on radiosity and ray tracing theories in **Mathcad14®**[1] . The model uses as inputs:

- the geographic location (latitude, longitude);
- the room geometry and orientation;
- the visible reflectance of the room elements, and
- the visible reflectance and transmittance of the façade and the shading device;

in order to determine the daylighting potential of bottom-up shades on space's visual performance and energy savings in artificial lighting. Assuming that:

- the room geometry is orthogonal parallelepiped;
- all the room surfaces are perfectly diffuse reflective (Lambertian);
- there are no exterior obstacles; and
- there is no furniture in the room;

the model calculates the position of the sun and the amount of daylight incident on a defined office façade. Then, the workplane illuminance distribution is computed, as well as the amount of artificial lighting required to keep the workplane illuminance in acceptable levels (500 lx). Control correlations and optimization of the bottom-up shades' properties are derived from the model's outputs and corresponding inputs. The general methodology

[1] www ptc com

followed is presented in Figure 3.1. Finally, the numerical model developed is presented in appendices A to I.

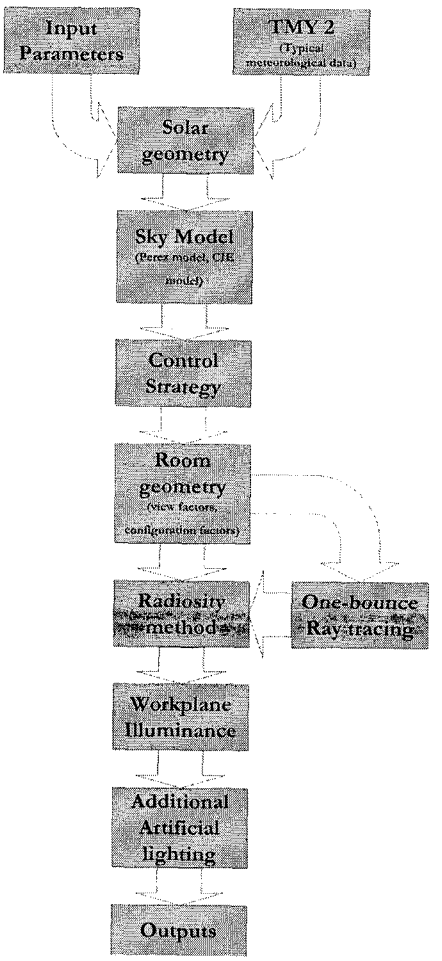

Figure 3.1: Flowchart of simulation methodology

3.2 Solar Geometry

The determination of the solar geometry is well defined (Duffie & Beckmann, 2006) and strongly linked with daylighting simulations as well as control strategies implemented for shading devices. Thus, four basic solar angles are presented and used (see Figure 3.2):

- Solar altitude (α_s): is the angle between the sun's rays and their projection on the horizontal plane

- Surface solar azimuth (γ): is the angle between the normal (n) to the surface and the projection of the sun's rays on the horizontal plane
- Angle of incidence (θ): is the angle between the sun's rays and the normal to the surface
- Profile angle (d): is the projection of the solar altitude angle (α_s) on the vertical plane perpendicular to the surface

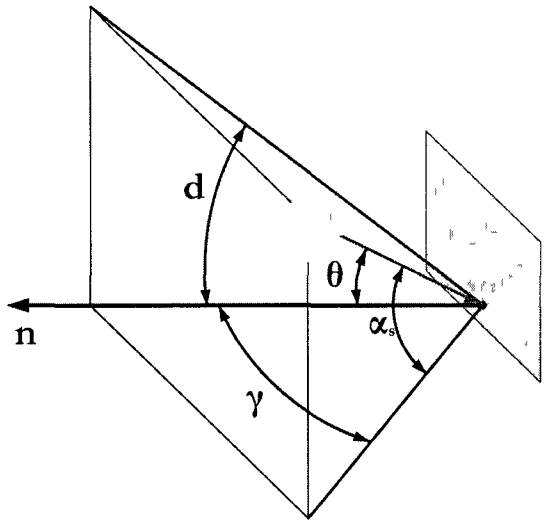

Figure 3.2: Solar geometry schematic

3.3 CIE Sky Models

The International Illumination Commission (CIE) has developed mathematical models of ideal luminous distributions under clear and overcast sky conditions, from where the daylight incident on a window of any orientation and tilt angle can be calculated. These standard models were used to illustrate the performance of bottom-up shades under extreme case scenarios (clear sunny day & overcast day).

3.3.1 CIE Clear Sky

In a clear day, the daylight incident on a vertical window consists of three components: direct sunlight (E_{direct}), diffuse light from the sky (E_{sky}) and reflected light from the ground (E_{ground}).

In order to calculate the direct (solar) component, the average illuminance outside the earth's atmosphere on a surface perpendicular to the sun's rays (E_{sc}), called the solar illuminance constant, is used:

$$E_{sc} = 1275 \ \text{lx} \qquad (3.1)$$

The elliptical shape of the earth's orbit around the sun should be considered. Therefore, the solar illuminance constant is multiplied with a correction factor in order to estimate the illuminance outside the earth's atmosphere on a surface perpendicular to the sun's rays (E_{xt}), as follows:

$$E_{xt} = E_{sc}\left[1 + 0.034\cos\left(\frac{360}{365}(n-2)\right)\right] \ (\text{lx}) \qquad (3.2)$$

where n is the Julian day number (1-365).

To obtain the solar illuminance corresponding to sea level (E_{dn}), the atmospheric attenuation is taken into account:

$$E_{dn} = E_{xt}\exp\left(\frac{-c}{\sin\alpha_s}\right) \ (\text{lx}) \qquad (3.3)$$

where c is the atmospheric extinction coefficient, equals to 0.21 for a clear day.

For a given moment, the higher the solar altitude, the higher the illuminance on a perpendicular surface, as the length of the atmospheric path traversed by the sun's rays increases, as the solar altitude decreases.

Finally, the solar illuminance incident on a window is given by:

$$E_{direct} = E_{dn} \cos\theta \ \text{(lx)} \qquad (3.4)$$

Similarly, the solar illuminance incident on a horizontal plane is given by:

$$E_{direct\_h} = E_{dn} \sin\alpha_s \ \text{(lx)} \qquad (3.5)$$

An experimentally derived equation (Murdoch, 2003) is used to estimate the horizontal illuminance due to a clear sky ($E_{sky\_h_{clear}}$):

$$E_{sky\_h_{clear}} = 800 + 15500\sqrt{\sin\alpha_s} \ \text{(lx)} \qquad (3.6)$$

The first term represents the horizontal illuminance values expected during sunrise and sunset, the second one, the horizontal sky illuminance based on the solar geometry. Assuming that the view factor between a vertical window and the sky, as well as between a vertical window and the ground is 0.5, the illuminance incident on a vertical window due to the diffuse light from the sky is given by:

$$E_{sky_{clear}} = 0.5E_{sky\_h_{clear}} \ \text{(lx)} \qquad (3.7)$$

The illuminance incident on a vertical window due to the reflected light from the ground is given by:

$$E_{ground_{clear}} = 0.5 \cdot \rho_{ground}(E_{sky_{clear}} + E_{direct\_h_{clear}}) \ \text{(lx)} \qquad (3.8)$$

where ρ_{ground} is the effective reflectance of the ground.

Hence, the total illuminance incident on a vertical window equals to:

$$E_{total_{clear}} = E_{direct} + E_{sky_{clear}} + E_{ground_{clear}} \ \text{(lx)} \qquad (3.9)$$

Finally, the luminous exitance of the window equals to:

$$M_{win_{clear}} = \tau_{direct}(\theta) \cdot E_{direct} + \tau_{diffuse}(\theta) \cdot (E_{sky_{clear}} + E_{ground_{clear}}) \ \text{(lx)} \qquad (3.10)$$

where:

$\tau_{direct}(\theta)$ is the visible beam transmittance of the glazing as a function of angle of incidence (θ)

$\tau_{diffuse}(\theta)$ is the visible diffuse transmittance of the glazing as a function of θ

3.3.2 CIE Overcast Sky

The Overcast Sky is based on a completely cloud covered sky where the sun and its position are not apparent. Thus, the daylight incident on a vertical window consists of two components: diffuse light from the sky and reflected light from the ground.

Similar to CIE Clear sky, an empirical equation (Murdoch, 2003) is used to estimate the horizontal illuminance due to an overcast sky ($E_{sky\_h_{overcast}}$):

$$E_{sky\_h_{overcast}} = 300 + 21000 \sin \alpha_s \ (lx) \qquad (3.11)$$

Therefore, the illuminance incident on a vertical window due to the diffuse light from the sky is a product of the view factor and the horizontal illuminance and is given by:

$$E_{sky_{overcast}} = 0.5 E_{sky\_h_{overcast}} \ (lx) \qquad (3.12)$$

Similarly, the illuminance incident on a vertical window due to the reflected light from the ground is given by:

$$E_{ground_{overcast}} = 0.5 \cdot \rho_{ground} E_{sky\_h_{overcast}} \ (lx) \qquad (3.13)$$

Therefore, the total illuminance incident on a vertical window equals to:

$$E_{total_{overcast}} = E_{sky_{overcast}} + E_{ground_{overcast}} \ (lx) \qquad (3.14)$$

Finally, the luminous exitance of the window equals to:

$$M_{win_{overcast}} = \tau_{diffuse}(\theta) \cdot (E_{sky_{overcast}} + E_{ground_{overcast}}) \ (lx) \qquad (3.15)$$

3.4 "All-weather" Sky Model

The Perez "all-weather" sky model (Perez *et al.*, 1990) was used to determine the daylighting performance of a bottom-up shade. The model inputs consist of hourly direct and global irradiance, dry-bulb and dew point temperatures. A typical meteorological year (TMY2) was used, derived from the 1961-1990 National Solar Radiation Data Base hourly weather observations and extracted from TRNSYS®[2].

The model considers atmospheric phenomena such as atmospheric turbidity, local atmospheric pressure, cloud type and density that affect the daylight quantities. Therefore, the model is able to generate comprehensive and realistic illuminance values relevant to the performance of bottom-up shades.

3.5 Control Strategy

Knowing the luminous exitance of the window (M_{win}), a control strategy for the bottom-up shades was implemented, to ensure that occupants' visual comfort is attained, following the concepts below:

- Glare-Free Zone (GFZ)
- Acceptable Workplane Illuminance (AWI)

3.5.1 Glare-Free Zone

The concept of a 'Glare-Free Zone' (GFZ), alternatively described as a cubic space within a space (Kapsis *et al.*, 2008; Park *et al.*, 2008), where glare caused by direct daylight is eliminated, providing visual comfort to the occupants, is introduced (see Figure 3.3) .

[2] www trnsys com

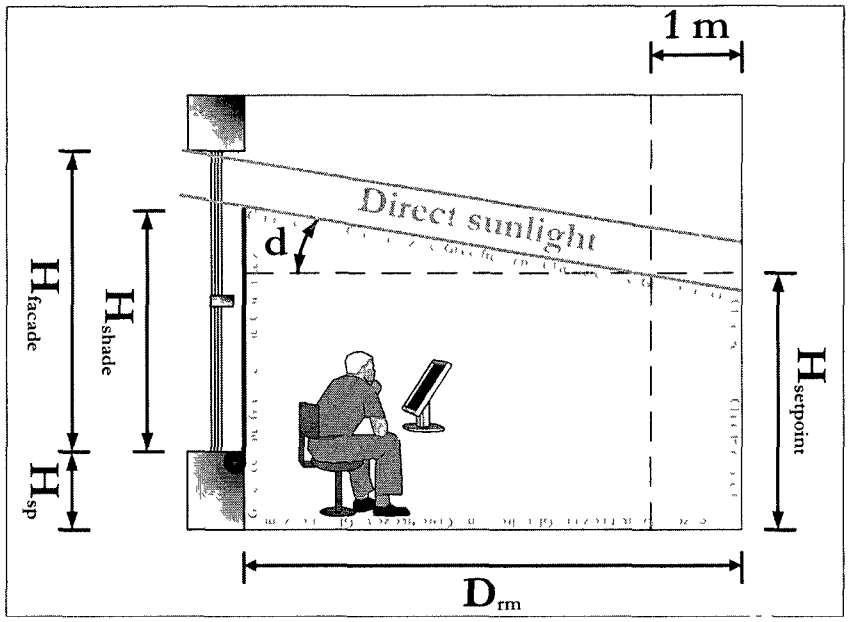

Figure 3.3: Glare-Free Zone (GFZ) schematic

In order to achieve a GFZ, the interior shading devices should be positioned in such a way as to block the direct daylight from entering into the occupied area. Hence, the solar and room geometry should be taken into consideration, giving the position of a bottom-up shade as follows:

$$\text{Control}_{GFZ} = \frac{H_{shade}}{H_{facade}} = \frac{(D_{rm} - 1.00\text{m})\tan d - H_{sp} + H_{setpoint}}{H_{facade}} \qquad (3.16)$$

where:

Control_{GFZ} is the position of the shade due to GFZ concept, a fraction of one (1) (where 0 refers to open shade and 1 to closed shade)

D_{rm} is the depth of the room

H_{sp} is the height of the spandrel

$H_{setpoint}$ equals to 1.50 m for seated occupants and 1.80 m for standing occupants

H_{facade} is the height of the façade

The $H_{setpoint}$ indicates the height of the GFZ, ensuring that below that height on the office space, there is no direct glare Moreover, the GFZ based on equation (3 16) extends from the fenestration wall until 1 00 m away from the inside wall (wall parallel to the fenestration-wall), since that area is rarely used as a workplane in a typical office (e g room entrance and bookshelves are often placed in that wall) However, by specifying the position of the workstation into the room, the GFZ could be different (e g changing the parameter in equation (3 16) from 1 00 m to 0 00 m, the entire room is characterized as a GFZ)

3.5.2 Acceptable Workplane Illuminance (AWI)

Based on the numerical model, control correlations for the bottom up shades were developed (Kapsis *et al*, 2009) between the shade position and outdoor illuminance, in order to maintain the average workplane illuminance at acceptable levels (500 lx) and do not exceed the value of 1000 lx locally on the workplane

When the AWI correlations are applied, an input to an open-loop control system from a photometer of pyranometer positioned parallel to the façade or curtain wall, could position the bottom-up shades properly However, at the AWI control strategy no glare concerns are taken into consideration, thus the correlations should always be used in relation with other control strategies that ensure glare free conditions for the occupants (see Figure 3 4)

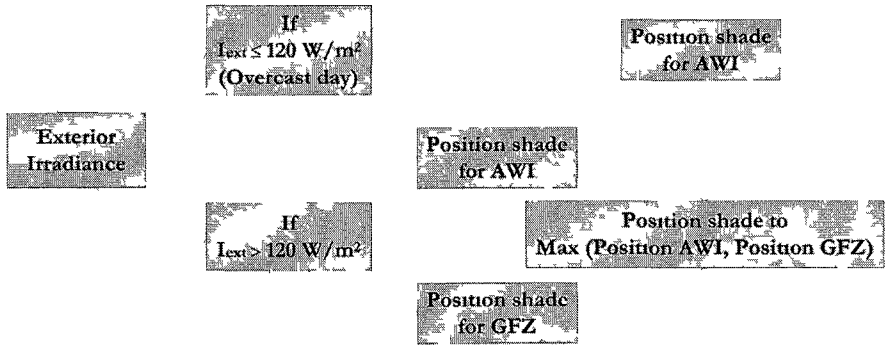

Figure 3 4 Recommended control strategy for bottom-up shades

The Levenberg-Marquardt method was used to employ the correlations (see Figure 3.5). The following design days were used (from 6:00-18:00), to develop the control correlations:

- Equinox
- Summer and Winter Solstice
- Summer and Winter typical clear day
- Summer and Winter typical overcast day

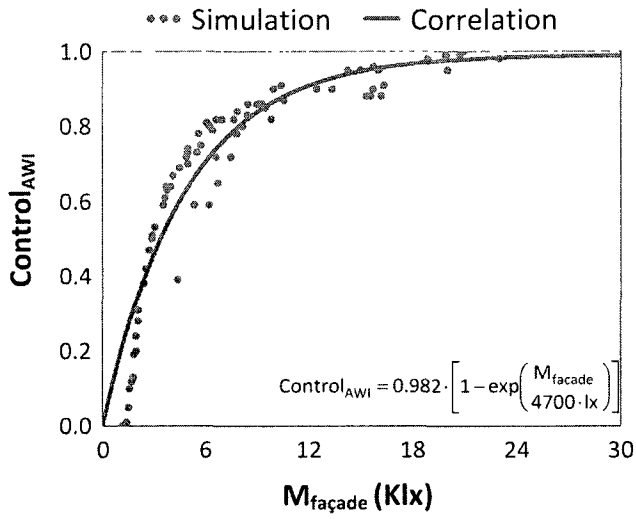

*Figure 3.5: An example of curve-fitting correlation for a WxDxH=4 m x 4 m x 4 m typical office with a shade transmittance of 5%, using **Mathcad®** built-in function for the Levenberg-Marquardt method*

The correlations have a common structure given by:

$$\text{Control}_{AWI} = A \cdot \left[1 - \exp\left(\frac{-F_{trans} \cdot M_{facade}}{E_{corr}} \right) \right] \qquad (3.17)$$

where:

Control_{AWI} is the position of the shade due to AWI concept, a fraction of one (1) (where 0 refers to open shade and 1 to closed shade)

A is the correlation constant (see Table 3.1), related with the measured quantity (illuminance or solar radiation)

M_{facade} is the total illuminance (lx) or solar irradiance (W/m^2), as measured by the sensor

E_{corr} is the correlation illuminance (lx) or solar radiation (W/m^2) value (see Table 3.1), related with the room geometry and shade transmittance

F_{trans} is the transmittance factor, related with the glass façade properties and the relative position of the sensor used to control the bottom-up shade. If the sensor is an exterior photometer (measuring lx) oriented parallel to the façade, the F_{trans} equals to: $F_{trans} = \tau_{visible\_glass}(\theta)$. If the sensor is an exterior pyranometer (measuring W/m^2) oriented parallel to the façade, the F_{trans} equals to: $F_{trans} = \tau_{solar\_glass}(\theta)$. If the transmittance of the glass façade is not available, the sensor could be placed behind the glass, facing outside (interior sensor). In that case, the F_{trans} equals to: $F_{trans} = 1$

$\tau_{visible\_glass}(\theta)$ is the visible transmittance of the glass as a function of angle of incidence (θ)

$\tau_{solar\_glass}(\theta)$ is the solar transmittance of the glass as a function of θ

Table 3.1 presents the correlation constants and values for bottom-up shades, for various transmittances and various room geometries for a typical office, based on which an AWI control strategy can be applied to ensure proper lighting conditions for the occupants.

Table 3.1: AWI correlation constants and values for bottom-up shades

E_{corr} (lx) if the sensor measures lx				E_{corr} (W/m²) if the sensor measures W/m²			
A=0.982				**A=0.97**			
	D=4 m	D=5 m	D=6 m		D=4 m	D=5 m	D=6 m
W=4 m	5400	6600	7000	W=4 m	47	58	61
W=5 m	5000	5600	6500	W=5 m	44	49	57
W=6 m	4600	5400	6200	W=6 m	40	47	54
	D=4 m	D=5 m	D=6 m		D=4 m	D=5 m	D=6 m
W=4 m	4700	5700	6000	W=4 m	41	50	53
W=5 m	4300	5050	5650	W=5 m	38	44	49
W=6 m	4000	4700	5500	W=6 m	35	41	48
	D=4 m	D=5 m	D=6 m		D=4 m	D=5 m	D=6 m
W=4 m	3950	4800	5300	W=4 m	34	42	46
W=5 m	3700	4100	4600	W=5 m	32	36	40
W=6 m	3500	4000	4400	W=6 m	30	35	38

Note. W: is the room width along façade
D: is the room depth
τ: is the transmittance of the bottom-up shade

The correlations are developed for a typical office height of 4 m, spandrel height of 0.8 m and reflectance values equal to: ϱ_{walls}=0.7, ϱ_{floor}=0.3 and $\varrho_{ceiling}$=0.8.

For example, if a bottom-up shade of $\tau = 5\%$ is installed in a typical office of WxDxH=5 m x 4 m x 4 m and an exterior pyranometer parallel to the façade is used to control the shade, then equation (3.17), based on Table 3.1, takes the following form:

$$\text{Control}_{AWI} = 0.97 \cdot \left[1 - \exp\left(\frac{-\tau_{solar\_glass}(\theta) \cdot M_{facade}}{38}\right)\right] \qquad (3.18)$$

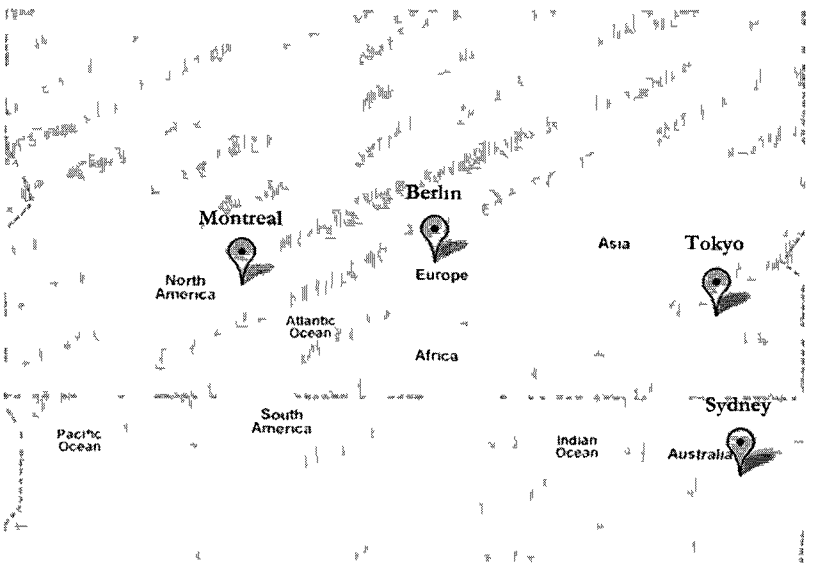

Figure 3 6 Cities used for the parametric analysis[3]

Parametric analysis was carried out for a typical office of WxDxH=4 m x 5 m x 4 m with a bottom-up shade transmittance of $\tau = 5\%$, to examine the dependence of the correlation values (E_{corr}) from the nature of daylight (beam & diffuse), the solar geometry, the geographic location and the orientation of the office Based on the numerical model, correlation values were developed for four cities around the world (see Figure 3 6) as well as for five different orientations in Montreal The analysis showed that the dependence of the correlation values from the geographic location and eventually from the nature of daylight and the solar geometry (see Table 3 2) as well as the office orientation (see Table 3 3) can be considered negligible, due to low standard deviation Therefore, the values given in Table 3 1 can be used under any daylight conditions and for any city and office orientation around the world

[3] maps google com

Table 3 2 Correlation values for four different cities around the world as well as the mean and standard deviation values

	Montreal	**Berlin**	**Tokyo**	**Sydney**		
E_{corr}(lx)	5700	5719	5678	5732	5707 3	23 5
E_{corr}(W/m^2)	50	50 19	49 85	50 32	50 1	0 2

Table 3 3 Correlation values for five different orientations in Montreal as well as the mean and standard deviation values

	E	**SE**	**S**	**SW**	**W**		
E_{corr}(lx)	5700	5704	5700	5711	5692	5701.4	6 9
E_{corr}(W/m^2)	49 8	49 93	50	49 94	49 81	49 9	0.1

In addition, further analysis was performed to examine the relation between the correlation values (E_{corr}) and the bottom-up shade transmittance. The analysis was made for two different typical office geometries (WxDxH=6 m x 4 m x 4 m & 4 m x 5 m x 4 m) and for four bottom-up shade transmittances ($\tau_{bottom-up}$=0%, 5%, 10% & 15%) The simulation results showed that the relation between the E_{corr} and the bottom-up shade transmittance is linear (see Figure 3 7 & Figure 3.8). Hence, the E_{corr}, for different bottom-up shade transmittances than the ones provided on Table 3 1, could be specified through interpolation/extrapolation method

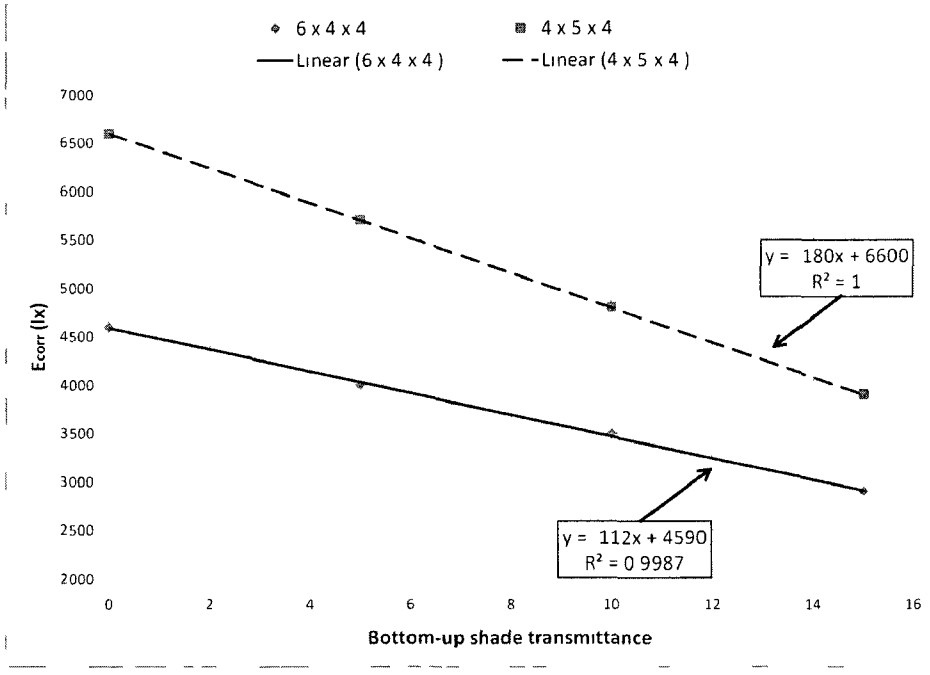

Figure 3 7 E_{corr}(lx) as a function of bottom-up shade transmittance for two different room geometries (WxDxH)

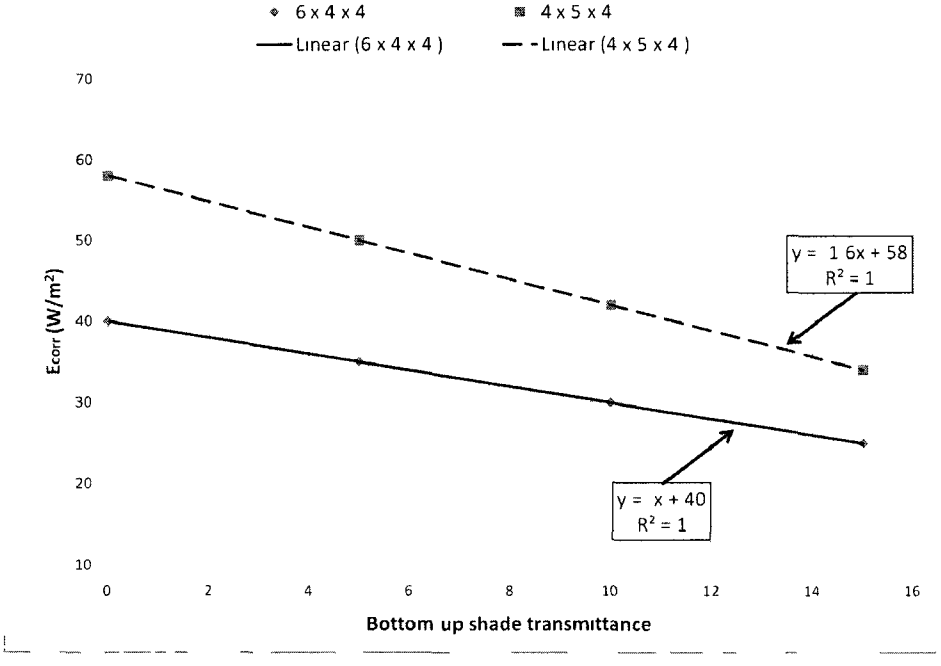

Figure 3 8 E_{corr}(W/m²) as a function of bottom-up shade transmittance for two different room geometries (WxDxH)

3.6 Radiosity Method

The radiosity method, also known as multiple-bounce flux transfer (Athienitis & Tzempelikos, 2002; Murdoch, 2003; Park & Athienitis, 2003), was used to predict the workplane illuminance levels due to diffuse daylighting The method assumes diffuse light source and diffuse reflective (Lambertian) surfaces in order to calculate the final luminous exitance of the interior room surfaces after an infinite number of multiple reflections. Thus, the radiosity method is applied to the following quantities:

- diffuse daylighting transmitted through the unshaded part of the window
- total daylighting transmitted through the shaded part of the window
- direct daylighting reflected from interior surfaces (e.g. sun patch on a wall)

The amount of the light leaving a surface consists of the initial luminous exitance of the surface and the amount of light reflected from that surface, as follows:

$$M_i = M_{i,0} + \rho_i \sum_j M_j F_{ij} \qquad (3.19)$$

where:

M_i is the final luminous exitance of surface i (lx)

$M_{i,0}$ is the initial luminous exitance of surface i (lx) (zero in the case of a non self-emitting surface)

ρ_i is the diffuse reflectance of surface i

M_j is the final luminous exitance of surface j (lx)

F_{ij} is the view factor between surfaces i and j (fraction of flux emitted by surface i that falls on surface j)

Matrix algebra is employed to solve the system of equations above. An eight-surface room enclosure is considered (four vertical walls, floor, ceiling, unshaded and shaded part of the window) for the calculations.

In addition, a five by five (5x5) point-array is used (see Figure 3.9) to predict the workplane illuminance levels as follows:

$$E_{\perp} = \frac{M_1}{\pi} \iint \frac{u \cdot w}{(u^2 + v^2 + w^2)^2} dudv \quad (lx) \qquad (3.20\ a)$$

$$E_{//} = \frac{M_1}{\pi} \iint \frac{w^2}{(u^2 + v^2 + w^2)^2} dudv \quad (lx) \qquad (3.20\ b)$$

where:

$E_{\perp}$ is the illuminance at a workplane point, if the point lies in a plane perpendicular to the source

$E_{//}$ is the illuminance at a workplane point, if the point lies in a plane parallel to the source

u, v are the "dimensions" of the source (see Figure 3.10)

w is the distance of the point from the source plane

Finally, the sun patch is treated separately from the room surfaces, using superposition principles.

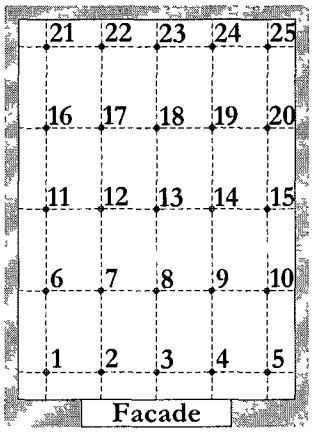

Figure 3.9: Plan view of the office, illustrating the five by five point-array for the workplane

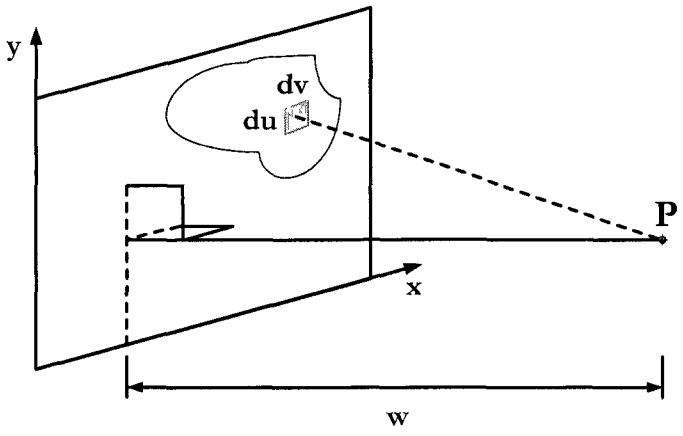

Figure 3.10: Relative position of a workplane point to a source that lies in the x-y plane

3.7 Ray Tracing

The direct daylight that penetrates a room through an unshaded window is an essential component on the prediction of the workplane illuminance as well as, the control strategy implemented for the bottom-up shades. Consequently, one-bounce ray tracing (Glassner, 1989) was used to trace the path of the direct sunlight and detect the final shape and position of the sun patch, into the room. After locating the sun patch, it was treated as a Lambertian source, using the radiosity method to calculate its lighting contribution to the workplane.

Initially, a sun-ray vector, based on solar geometry, equals to:

$$(x_0,\ y_0,\ z_0) = \left(1,\ \tan\gamma,\ -\tan\alpha_s\sqrt{1+\tan^2\gamma}\right) \qquad (3.21)$$

Moreover, a sun-ray can be represented through a parametric form (Williams, 2008) as:

$$L_A + (L_B - L_A)t \qquad t \in \Re \qquad (3.22)$$

where:

$L_A = (x_A,\ y_A,\ z_A)$, coordinates of a window corner; and

$L_B = (x_A + x_0,\ y_A + y_0,\ z_A + z_0)$, a point along the sun-ray that passes through L_A.

Similarly, a room surface (e.g. wall) can be represented as:

$$W_1 + (W_2 - W_1)u + (W_3 - W_1)v \qquad u, v \in \Re \qquad (3.23)$$

where:

$W_k = (x_k,\ y_k,\ z_k)$ $\quad k = 1,2,3$, three non co-linear points on the room surface.

The point at which the sun-ray intersects with the room surface is therefore described by setting equal the two parametric equations:

$$L_A + (L_B - L_A)t = W_1 + (W_2 - W_1)u + (W_3 - W_1)v \qquad (3.24)$$

which can be simplified to:

$$L_A - W_1 = (L_A - L_B)t + (W_2 - W_1)u + (W_3 - W_1)v \qquad (3.25)$$

and expressed in matrix form as:

$$\begin{bmatrix} x_A - x_1 \\ y_A - y_1 \\ z_A - z_1 \end{bmatrix} = \begin{bmatrix} -x_0 & x_2 - x_1 & x_3 - x_1 \\ -y_0 & y_2 - y_1 & y_3 - y_1 \\ -z_0 & z_2 - z_1 & z_3 - z_1 \end{bmatrix} \begin{bmatrix} t \\ u \\ v \end{bmatrix} \qquad (3.26)$$

Inverting the matrix, the parameter t can be specified as follows:

$$\begin{bmatrix} t \\ u \\ v \end{bmatrix} = \begin{bmatrix} -x_0 & x_2 - x_1 & x_3 - x_1 \\ -y_0 & y_2 - y_1 & y_3 - y_1 \\ -z_0 & z_2 - z_1 & z_3 - z_1 \end{bmatrix}^{-1} \begin{bmatrix} x_A - x_1 \\ y_A - y_1 \\ z_A - z_1 \end{bmatrix} \qquad (3.27)$$

Consequently, the intersection point (P) equals to:

$$P = L_A + (L_B - L_A)t \qquad (3.28)$$

Repeating the steps above for all the four corners of the unshaded window, the sun patch can be located (see Figure 3.11). As the room surfaces are not infinite planes, but well-defined geometric areas, some constraints have to be taken into account. Therefore, a sun-ray intersects with a room surface only if the intersection point lies within the surface.

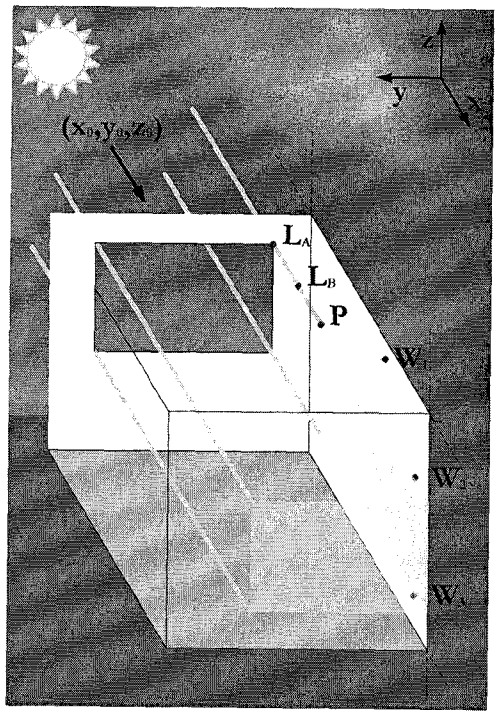

Figure 3.11: Ray tracing schematic, demonstrating the intersection between a sun-ray and a room surface

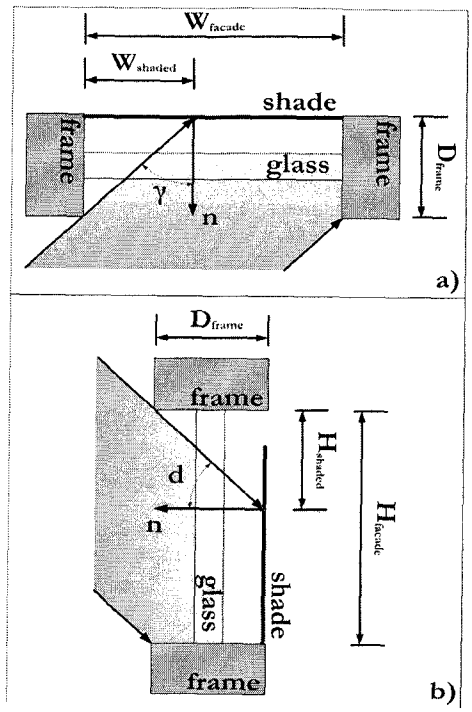

Figure 3.12: a) Plan view of the façade, showing the shading due to vertical frame, b) Cross section of the façade, showing the shading due to horizontal frame

3.8 Correction due to frame shading

The fenestration frame is taken into consideration as, depending on the solar geometry, it can shade – partly or fully – the window, reducing substantially the luminous exitance of the façade (O'Neill, 2008). Thus, the shaded areas, due to vertical and upper horizontal frame (see Figure 3.12), are determined as follows:

$$W_{shaded} = D_{frame} \tan \gamma \qquad (3.29) \qquad \text{and} \qquad H_{shaded} = D_{frame} \tan d \qquad (3.30)$$

where:

D_{frame} is the depth of the frame

W_{shaded} is the width of the shaded part of the façade, due to horizontal frame

H_{shaded} is the height of the shaded part of the façade, due to vertical frame

Hence, the sunlit area of the façade equals to:

$$A_{sunlit} = (W_{facade} - W_{shaded})(H_{facade} - H_{shaded}) \qquad (3.31)$$

where:

W_{facade} is the width of the window

H_{facade} is the height of the window

3.9 Artificial Lighting

After predicting the workplane illuminance levels, the electric lights were controlled in order to provide the necessary amount of light in order to achieve the minimum workplane illuminance requirements.

The selected luminaire for the simulation were the dimmable Lightolier Energos 2-light T8 per 4' louver (EG2-2N). The luminaire specifications and the candlepower curve, as provided by the manufacturer's specification sheet, follow (see Table 3.4 and Figure 3.13).

Table 3.4: Luminaire specifications[4]

Lamp Type	T8 DIM
Ballast Factor (BF)	1.0 / .05 (max / min)
Lamp Rated Wattage	32
Lamp Rated Output	2850
Lamp Color (Kelvin)	830
IES Output (Lumens)	2850 / 143 (max / min)
System Input Watts	34 / 8 (max / min)
System Efficacy (lum/watt)	83.8
Start Type	Program

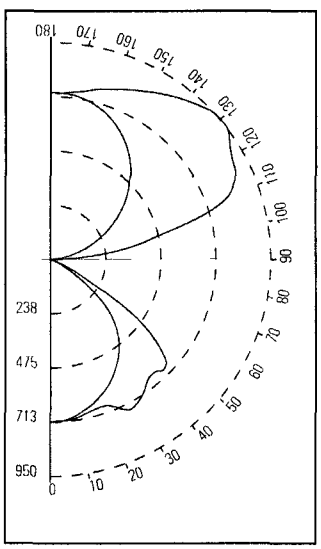

Figure 3.13. : Luminaire candlepower curve

[4] www lightolier com

RadianceIES®[5] was used to calculate the number of luminaires needed, as well as the workplane illuminance distribution due to electric lighting. These outputs were used as inputs to the numerical model, to estimate the energy consumption attributable to electric lighting.

3.9.1 Control Strategies

Two different control strategies for electric lighting were implemented and compared down to annual energy consumption, as follows:

- **Active On-off control**: The lights are turned on when the average workplane illuminance is lower than 500 lx and they are turned off if it exceeds 500 lx
- **Continuous dimming control**: The lights are continually dimmed in order to meet the minimum workplane illuminance requirements, based on average workplane illuminance.

In order to estimate the energy consumption of the electric lighting at the dimming control cases, an experimental linear correlation was used between luminaire power consumption and percent luminous flux output (see Figure 3.14).

[5] www.iesve.com

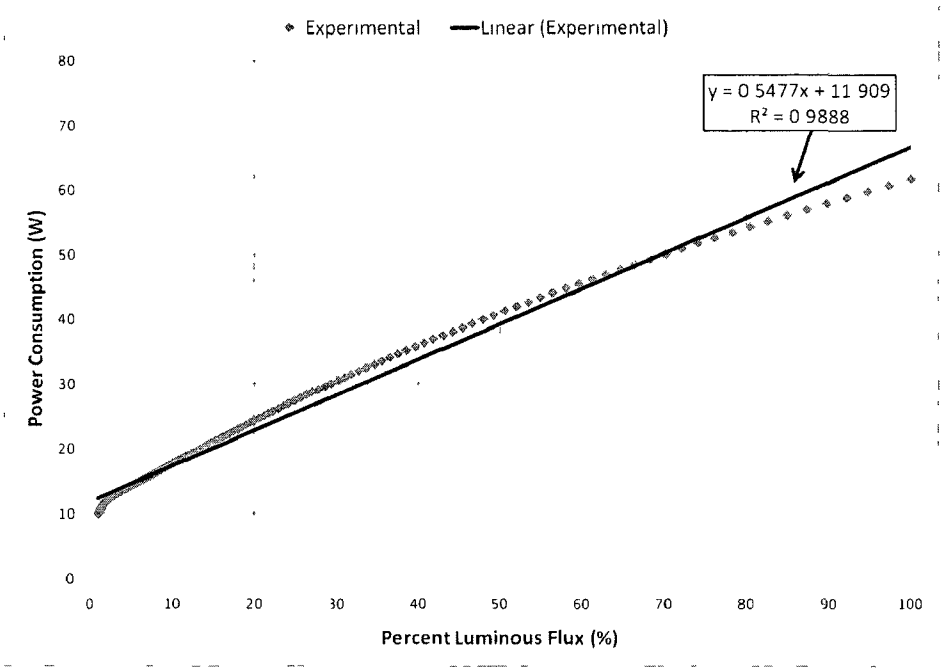

Figure 3.14: Luminaire power consumption versus percent luminous flux output (O'Neill, 2008)

3.10 Results and Discussion

A sensitivity analysis was performed of the impact of shade's optical properties on the workplane illuminance levels as well as on lighting energy consumption. Furthermore, a comparison between a bottom-up shade and a conventional roller shade was made in order to evaluate the daylighting performance of bottom-up shades and the control strategies applied.

3.10.1 Sensitivity Analysis

A sensitivity analysis about the impact of bottom-up transmittance on the annual daylighting performance was performed. Three different transmittance values were simulated ($\tau_{bottom-up}$ =0%, 5% and 10%) for a typical, south facing, office in Montreal, Canada (from 6:00-18:00). The dimensions of the office were: WxDxH=4 m x 5 m x 4 m. The typical clear glazing used for the window office simulations was: ASHRAE 17a LE CLR (3mm, Low-e

Double Glazing, e = 0 2 on surface 2) (ASHRAE, 2005) In all cases, GFZ and AWI control strategies were applied, to eliminate direct glare for the occupants and to ensure proper daylighting conditions The position step of the shades was 5% This step was chosen in order to reduce fluctuations at the workplane illuminance levels

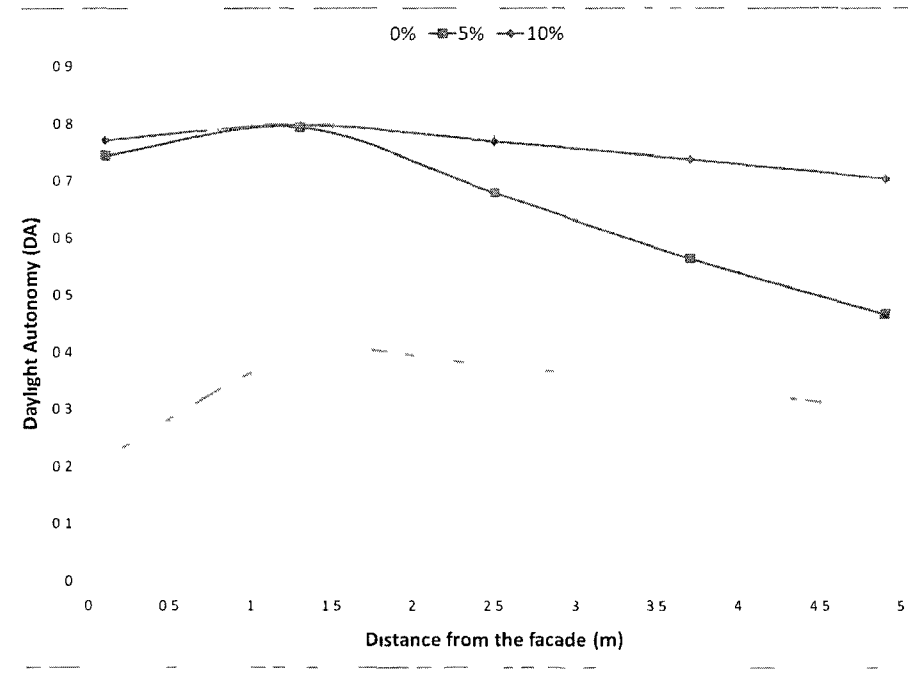

Figure 3 15 Daylight Autonomy distribution for three configurations of bottom-up shade $\tau_{bottom\ up}$=0%, 5% and 10%

Daylight Autonomies (Reinhart *et al.*, 2006) were calculated on the centre line (see Figure 3 9) at distances of 0.1 m, 1 3 m, 2.5 m, 3 7 m and 4.9 m from the façade (points 3, 8, 13, 18 & 23) Moreover, the Useful Daylight Illuminances (Nabil & Mardaljevic, 2006) were determined as well as the annual relative frequency of the position of the shade The results showed that· The daylighting performance of the bottom-up with $\tau = 0\%$ is relatively inadequate (see Figure 3.15), as the Daylight Autonomy (DA) does not exceed the value of 40% On the other hand, both $\tau = 5\%$ and $\tau = 10\%$ have adequate performance, with the DA for the bottom-up of $\tau = 10\%$ to be higher than 70% through the entire length of the

centre line of the office, increasing though the possibility of reflected glare to appear on VDU's oriented facing the façade, because of the high shading transmittance. For $\tau = 5\%$, the DA obtains similar values with the $\tau = 10\%$ until 2 m away from the façade, where it starts to decrease linearly until it reaches the value of 47%, 4.9 m away from the façade.

Table 3.5: Useful Daylight Illuminance for three configurations of bottom-up shade: $\tau_{bottom\text{-}up}$=0%, 5% and 10%

	τ=0%	τ=5%	τ=10%
<100 lx	35.8%	14.6%	14.6%
100-2000 lx	64.2%	85.4%	84.6%
> 2000 lx	0.0%	0.0%	0.8%

Comparing the Useful Daylight Illuminance (UDI) (see Table 3.5), the two cases of $\tau = 5\%$ and 10% have adequate identical performance. In contrast, the $\tau = 0\%$ is fell-short 35.8% of the time (twice as much as the other two cases). Finally, in all cases, the time that the average workplane illuminance exceeds the value of 2000 lx is negligible, due to AWI control strategy applied.

In addition, a comparison was made between the three cases, in terms of lighting energy consumption, for two control strategies of artificial lighting (see Figure 3.16). In the case of active on-off control strategy, the configuration of $\tau = 10\%$ consumes 47% less energy for artificial lighting than the $\tau = 5\%$ and 66% less than the $\tau = 0\%$. At the case of continuous dimming control strategy, the differences are 18% and 70%, respectively. At the same time, it is clear that using continuous dimming control for the artificial lighting, energy savings of 32%-61% could be achieved.

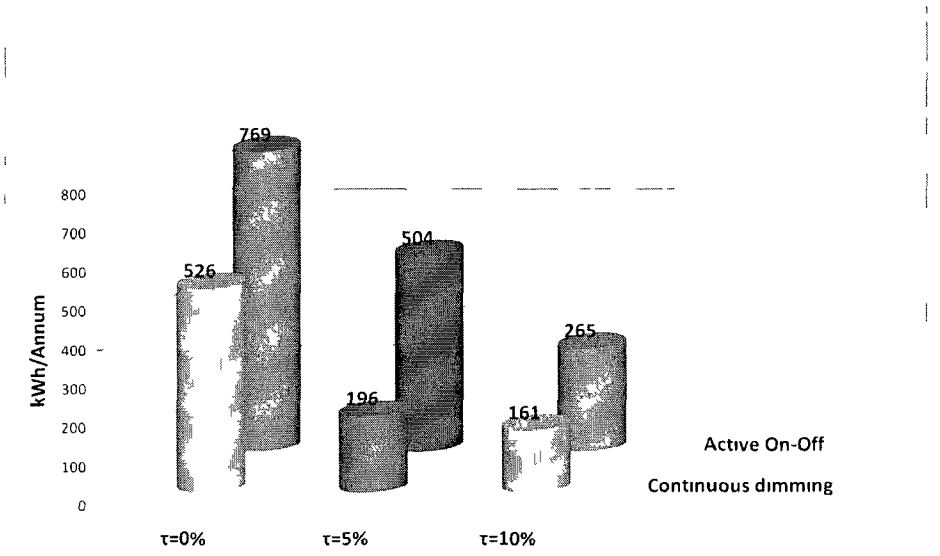

Figure 3.16 Annual lighting energy consumption for three configurations of bottom-up shade. $\tau_{bottom\ up}$=0%, 5% and 10% and two different control strategies for artificial lighting: Active On-Off and continuous dimming

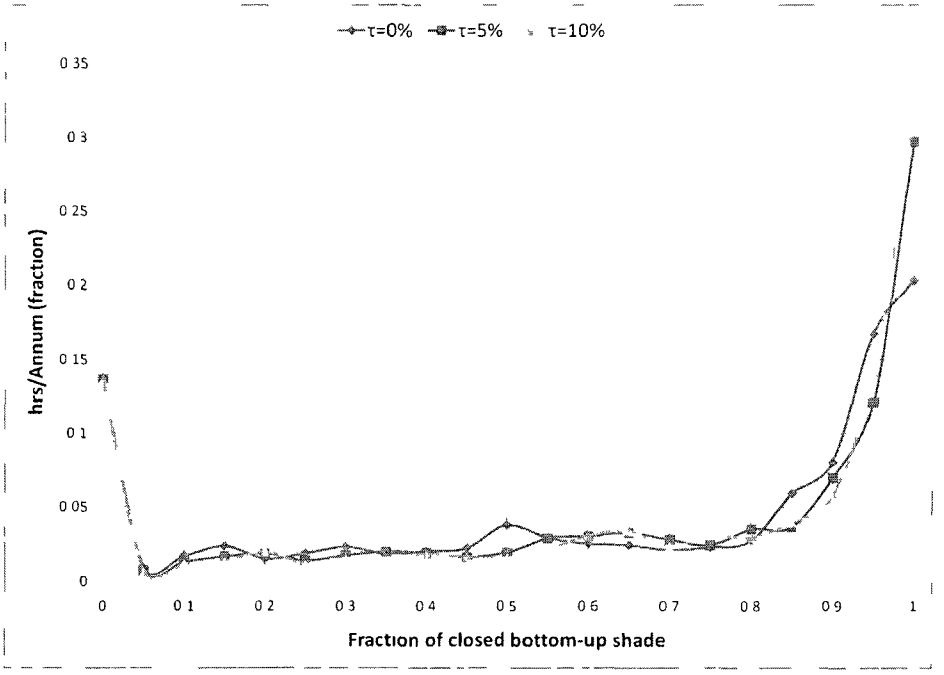

Figure 3 17. Annual relative frequency of the position of the bottom-up shade, for three configurations $\tau_{bottom\ up}$=0%, 5% and 10%

Finally, the annual relative frequency of the position of the bottom-up shades (see Figure 3.17) demonstrates the importance of continuous shade control instead of open-closed control, in order for acceptable workplane illuminance levels to be achieved, using daylight. Between 55%-66% of the time (>2600 working hours) the shades are positioned between 5%-95% closed, when 14% of the time the shades are totally open and between 20%-31% are totally closed. Assuming that the occupants' (seated or standing) line of sight is at a minimum height of 1 4 m and considering the annual relative frequency of the position of the bottom-up shades, 19% of the time occupants have a full view outside (shades positioned lower that 20% closed), where 44%-49% of the time they have a relative view outside (shades positioned lower than 80% closed).

In conclusion, the bottom-up of $\tau = 10\%$ performs better, in terms of daylight and energy consumption for artificial lighting. However, the combination of continuous dimming control for artificial lighting and the bottom-up of $\tau = 5\%$, could give similar results, minimizing the possibility of reflected glare to occur. Moreover, orienting the VDU's perpendicular to the façade, when possible, could eliminate reflected glare and veiling issues (Osterhaus, 2005).

3.10.2 Comparison with a Conventional Roller Shade

A comparison was made between a bottom-up shade and a conventional roller shade of the same transmittance ($\tau = 5\%$), for the previous office. GFZ and AWI control strategies were applied for the bottom-up shade. On the other hand, the control strategy followed for the conventional roller shade was:

- fully-open roller shade when the solar radiation incident on the façade is equal or lower than 120 W/m^2 (Tzempelikos & Athienitis, 2007); and

- fully-closed roller shade when the solar radiation incident on the façade is higher than 120 W/m^2;

to ensure glare-free conditions for the occupants, by blocking the direct sunlight incident on the workplane.

The results showed that: the DA for the bottom-up is 8%-58% higher than the DA for the conventional roller shade (see Figure 3.18), with the difference of 46% deep in the room, proving the advantage of bottom-up shade towards the conventional roller shades, by allowing the natural light to enter from the top section of the façade deep into the room.

Table 3.6: Useful Daylight Illuminance for a bottom-up shade and a roller shade ($\tau_{bottom\text{-}up}=\tau_{roller}=5\%$)

	Bottom-up	**Roller shade**
<100 lx	14.6%	15.0%
100-2000 lx	85.4%	82.6%
> 2000 lx	0.0%	2.4%

In terms of UDI, both shades perform alike (see Table 3.6). The control strategies applied for both cases ensure that the upper threshold is negligible. On the other hand, the lower threshold is caused due to daylight "unavailability" (e.g. sunset hours, overcast days, etc).

Moreover, a comparison was made between the two configurations (bottom-up shade and conventional roller shade), in terms of annual lighting energy consumption (see Figure 3.19), following the previous control strategies. For the case of active on-off control strategy, the bottom-up configuration consumes 21% less energy than the conventional roller shade configuration, a difference that increases to 41% for the case of continuous dimming. Similar to before, the use of dimming control could significantly reduce the energy consumption for artificial lighting.

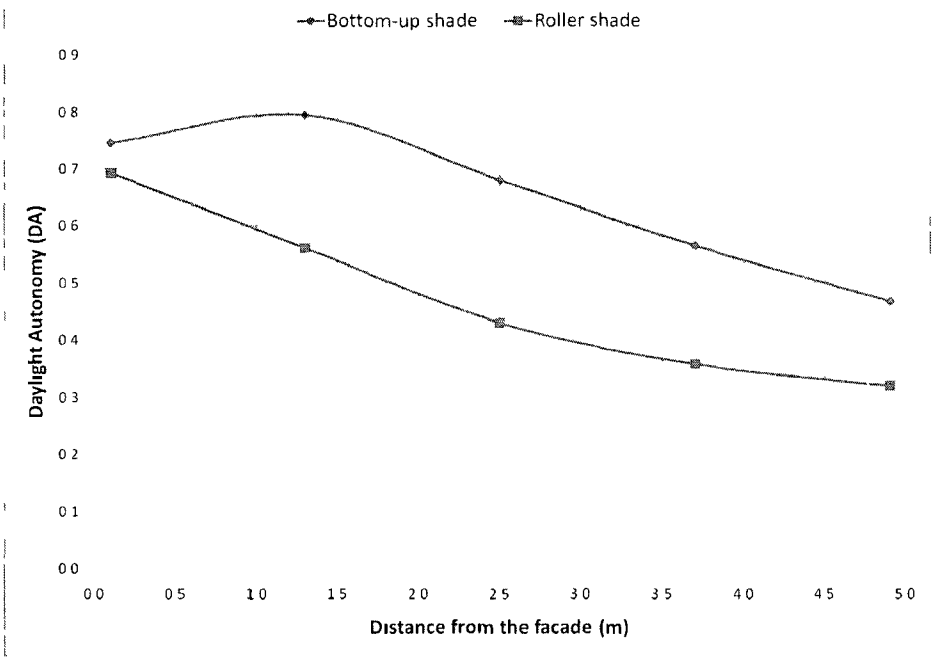

Figure 3.18. : Daylight Autonomy distribution for bottom-up shade and conventional roller shade

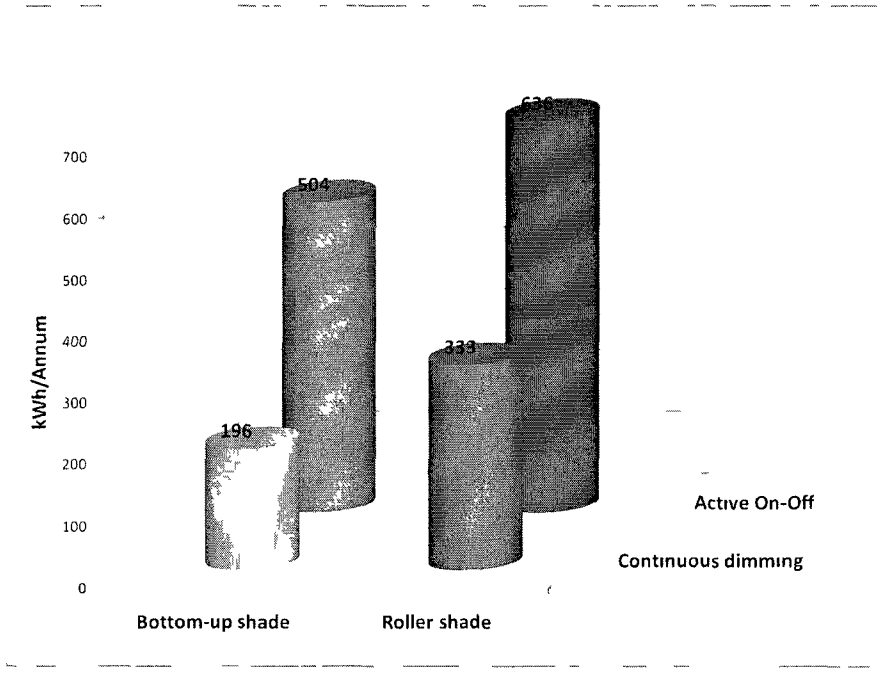

Figure 3.19: Annual lighting energy consumption for bottom-up shade and a conventional roller shade under two different control strategies for artificial lighting: Active On-Off and continuous dimming

3.10.3 Performance under CIE Sky Models

The CIE standard sky models were used to demonstrate the performance of bottom-up shades under extreme case scenarios (Clear Day & Overcast Day). Figure 3.20 and Figure 3.21 present the daily performance of a bottom-up shade of 5% transmittance ($\tau_{bottom\text{-}up}$=5%) for the previous office, for a CIE clear and CIE Overcast day, respectively.

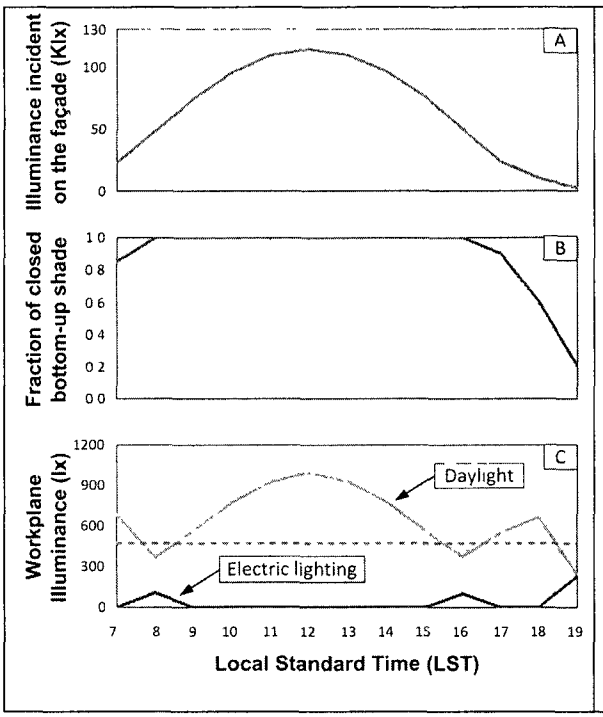

Figure 3.20: Daily performance of a bottom-up shade during a CIE Clear day

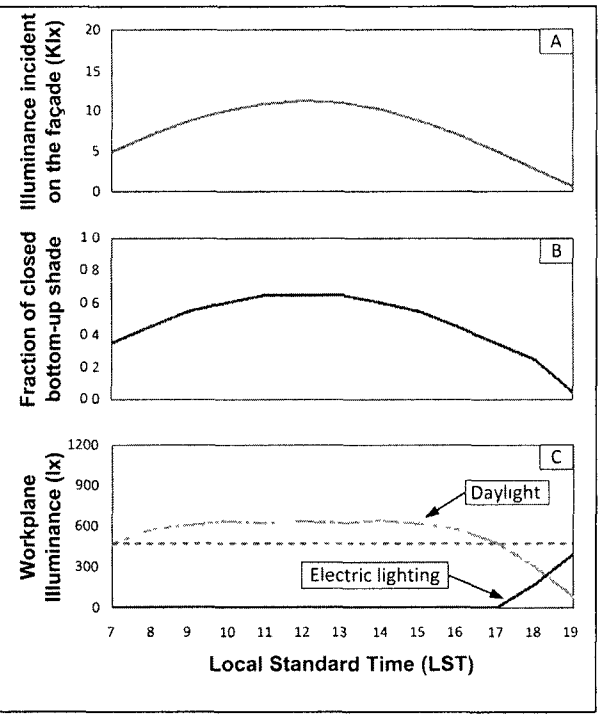

Figure 3.21: Daily performance of a bottom-up shade during a CIE Overcast day

A three-graph set is used for each case. The graph A presents the daily exterior illuminance incident on the façade, the graph B presents the position of the shade due to GFZ and AWI control strategies applied and the graph C presents the average workplane illuminance levels due to daylighting as well as the additional electric lighting needed in order to maintain 500 lx (dashed line) on the workplane.

During the CIE Clear day (see Figure 3.20), the bottom-up shade is mainly closed, due to high exterior illuminance levels, in order to prevent oversupply of daylight and glare. However, even with closed shade, the average workplane illuminance obtains high values, due to shade transmittance. Therefore, the orientation of the VDU's perpendicular to the façade is essential.

On a CIE Overcast day (see Figure 3.21), the position of the bottom-up shade varies from 0%-65% closed, preserving the workplane illuminance in desirable levels. After 17:00 the electric lights are dimmed from 0% to 83% (at 19:00) in order to maintain the minimum workplane illuminance levels at 500 lx. In both cases, the use of electric lighting is minimal, demonstrating the ability of the bottom-up shade to provide sufficient daylight in the space so that the occupants could work by almost daylight alone.

Chapter 4: Experimental Study and Model Verification

4.1 Introduction

A full scale experiment was conducted at the solar lab of Concordia University (see Figure 4.1), Engineering and Visual Arts Building in Montreal, Canada (45° 30' N, 73° 36' W). The experimental objective of this study was twofold:

- Verify the daylighting/lighting numerical model
- Verify the thermal performance of bottom-up shade and compare the results with conventional roller shades

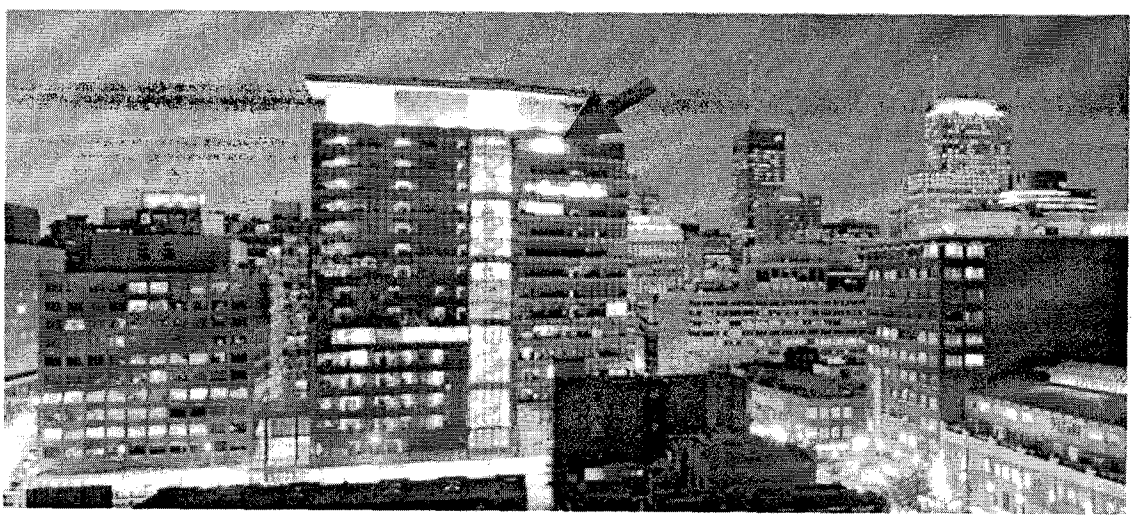

Figure 4.1: Solar lab of Concordia University[1]

4.2 Perimeter Zone

The experiment was carried out at the fenestration section (perimeter zone) of the solar lab. The fenestration surface azimuth is approximately 20^0 west of south and there are no external obstructions.

[1] www.kpmbarchitects.com

The fenestration section consists of six identical façades. Each façade consists of three sections: the spandrel that extends 0.8 m from the floor, the lower "clear glazing" section and the upper "fritted glazing" section (50% grey ceramic frit). Each glazing section is 1.3 m high and 1.5 m wide. The perimeter zone extends 3.2 m inwards from the façade and can be partitioned with floor-to-ceiling white drapes. Two of the six façades were used for the experiments. The first one was equipped with a conventional roller shade and the second one with a bottom-up shade.

4.3 Experimental Set-up

Several sensors were used to record the thermal performance of the two shading devices installed in identical sections. T-thermocouples were used to record surface temperature (interior glazing, frame and shade) and air (exterior, cavity between glazing and shade, and room) temperatures (see Figure 4.2).

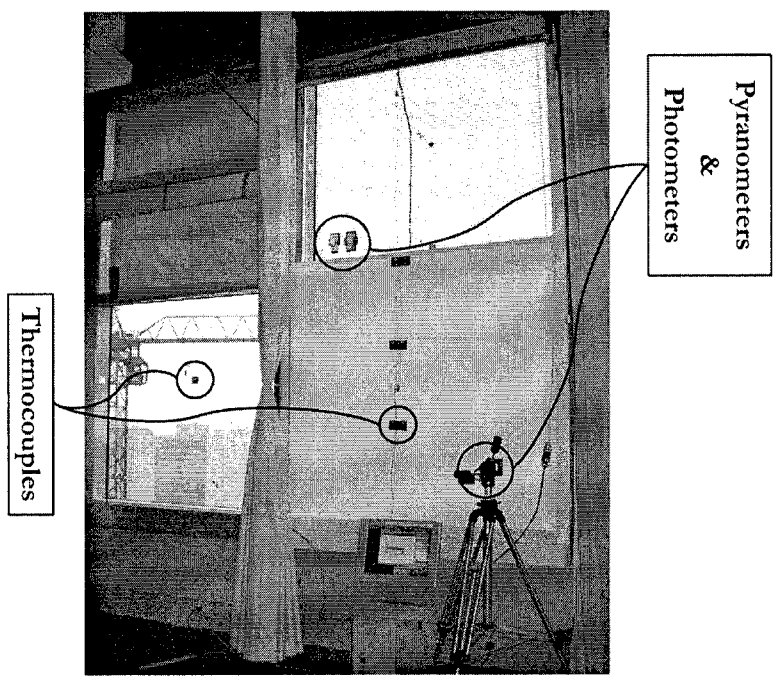

Figure 4.2: Experimental set-up for a conventional roller shade (on the left) and a bottom-up roller shade (on the right)

Li-cor pyranometers were used to record the exterior solar radiation (W/m^2) incident on the façade as well as the solar radiation transmitted through the glazing and the shade. Li-cor photometers were used to record the exterior illuminance (lx) on the façade, the luminous exitance (lx) of the glazing and the shade as well as the workplane illuminance in several points through the depth of the room. A KANOMAX anemometer was used for manual measurements of air velocity (m/s) on site.

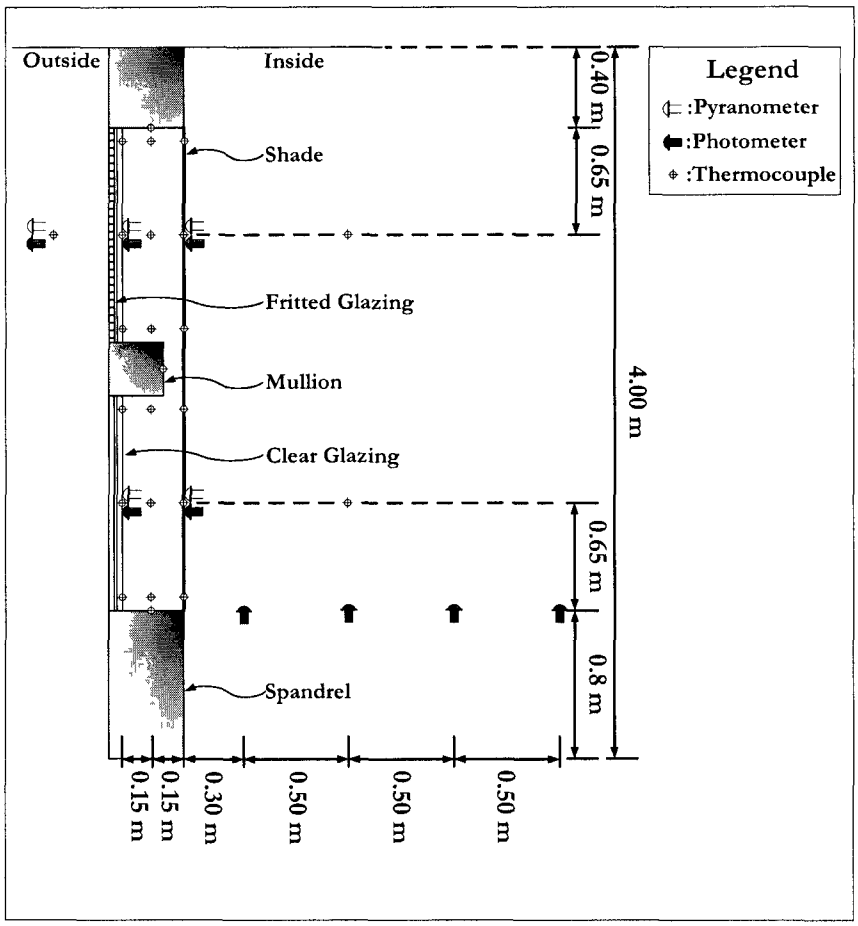

Figure 4.3: Cross section schematic of the experimental set-up

For the interior glazing surface, three thermocouples were used for each glazing section (clear and fritted): one installed on the geometric center of the glazing, one installed 5 cm away from the lower horizontal frame and one installed 5 cm away from the upper

horizontal frame. For the frame surface, one thermocouple was installed on the geometric center of each horizontal and vertical frame (see Figure 4.3).

Finally, the data was recorded in a pc connected with the sensors through an *Agilent 34907A* data acquisition and control unit. The following sections discuss the sensors used.

4.3.1 Thermocouples

Surface and air temperatures were measured using T-type thermocouples (copper–constantan). T-thermocouple is suited for measurements in the −200°C to 350°C range with an absolute error of ±0 5°C between −40°C and 125°C.

4.3.2 Pyranometer Sensor

The solar radiation was measured using Li-cor LI-200 Pyranometer Sensor[2] (see Figure 4.4a). The sensor features a silicon photovoltaic detector calibrated against an Eppley Precision Spectral Pyranometer (PSP) under natural daylight conditions. Relative error under these conditions is ± 3% (within a time stability of less than ± 2%, over a year period). It is cosine corrected up to 80° angle of incidence and its spectral response is from 280-2800 nm, with a linear response up to 3000 W/m^2, for operating temperatures of -40°C to 65°C. Its response time is 10 μs.

4.3.3 Photometer Sensor

The illuminance was measured using Li-cor LI-210 Photometric Sensor[2] (see Figure 4.4b). The sensor features a silicon photodiode that provides a spectral response which matches the CIE Standard Observer Curve (photopic curve) within ± 5% (with a time stability of less than ± 2%, over a year period). It is cosine corrected up to 80° angle of

[2] www licor com

incidence, with a linear response up to 100 klx, for operating temperatures of -20°C to 65°C. Its response time is 10 μs.

4.3.4 Anemometer

The air velocity in the cavity between glazing and shade as well as between cavity and room was measured manually using KANOMAX anemomaster A031[3] (see Figure 4.4c). The sensor features a telescopic straight and articulating probe able to measure air velocities in the range of 0.1 m/s to 30 m/s, within an accuracy of ± 2.0 % of reading and resolution of 0.01 m/s (0 m/s to 9.99 m/s) and 0.1 m/s (10 m/s to 30 m/s).

Figure 4.4: a) A Li-cor pyranometer[2], b) a Li-cor photometer[2] and c) a KANOMAX anemometer[3]

4.4 Fenestration Properties

Because of the thermal experiments conducted, the characterization of the fenestration (glazing, shading devices) is essential. Consequently, the thermal and visual properties of major fenestration components are presented.

[3] kanomax-usa com

4.4.1 Glazing Properties

Both clear and fritted glazing sections of the façade are double-glazed, low-e coated (outer side of interior pane) and argon filled. The clear glazing has a normal total solar transmittance (τ_{solar}) of 39% and a normal total visible transmittance ($\tau_{visible}$) of 69%. The center-of-clear-glazing U-value is 1.6 W/m^{2}K and the SHGC is 0.37 (Bessoudo, 2008).

The fritted glazing has a total solar transmittance to the normal of 27% and a total visible transmittance to the normal of 48%. The center-of-fritted-glazing U-value is 1.6 W/m^{2}K and the SHGC is 0.28.

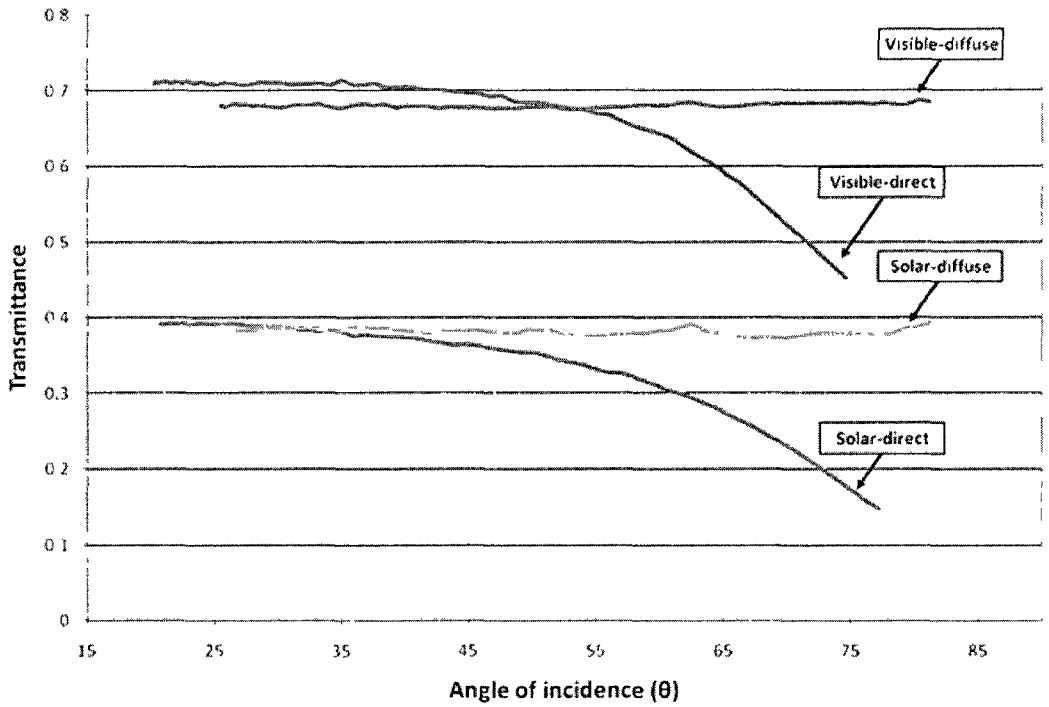

Figure 4.5: Experimental transmittance of clear glazing

The dependence of the glazing transmittance on angle of incidence (θ) was determined using the ratio between the values given from the pyranometer (I_{glass}) and photometer (E_{glass}) installed behind the glazing over the values given from the exterior (I_{ext} and E_{ext}) sensors ($\tau_{solar}(\theta) = \frac{I_{glass}(\theta)}{I_{ext}(\theta)}$ and $\tau_{visible}(\theta) = \frac{E_{glass}(\theta)}{E_{ext}(\theta)}$) (see Figure 4.5 and Figure 4.6).

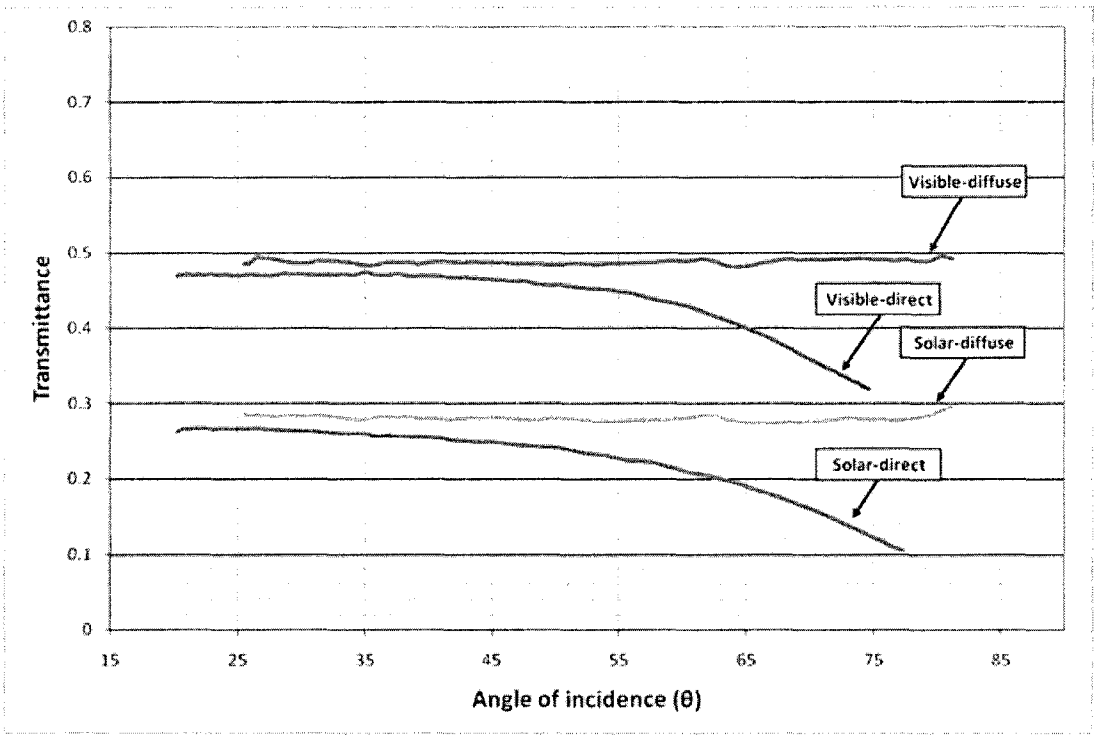

Figure 4.6: Experimental transmittance of fritted glazing

The diffuse transmittance was determined under overcast sky conditions, when the solar radiation incident on the façade was below 120 W/m^2. Then, the direct transmittance was calculated by determining the total transmittance and abstracting the diffuse, under clear sky conditions, when the solar radiation incident on the façade was above 500 W/m^2 and no clouds formed at the sky dome. Lastly, the relative error for the solar transmittances is ± 5% and for the visible transmittances is ± 7%, due to instruments' error.

4.4.2 Shading Devices Properties

Two shading devices were used during the experiments: a bottom-up shade and a conventional roller shade. Somfy Canada Inc[4] donated a prototype bottom-up roller shade to Concordia University to be used for daylighting and thermal experiments. This product operates in reverse (opens from top to bottom) of a typical roller shade, so as to cover the bottom part of the window, providing privacy to the occupants, while allowing daylight to enter from the top section The shade is automated and moves along vertical tracks attached to the window frame, therefore "sealing" the cavity between glazing and shade. It is installed approximately 30 cm away from the window glazing. The fabric is white open weave and its optical and solar properties are: transmittance of $\tau_{bottom-up} = 18\%$, reflectance of $\rho_{bottom-up} = 74\%$, emissivity of $\varepsilon_{bottom-up} = 90\%$ and perforation of $\delta_{bottom-up} = 5\%$.

The roller shade is a conventional roller shade that operates manually and it is installed approximately 30 cm away from the window glazing. The fabric is beige open weave and its optical and solar properties are: $\tau_{roller} = 5\%$, $\rho_{roller} = 55\%$, $\varepsilon_{roller} = 90\%$ and $\delta_{roller} = 3\%$.

For both shades, it was experimentally found that the properties are independent of solar angle of incidence.

4.5 Model Verification

Experiments were conducted to verify the daylighting/lighting numerical model under clear and overcast sky conditions The experiments performed for various angles of incidence (θ) as well as for different shade's positions The luminous exitance of the glazing, as measured by the Li-cor photometers, was used as input to the model. The optical

[4] www somfysystems com

reflectance of the room surfaces used, based on measurements, were: $\rho_{wall} = 70\%$, $\rho_{floor} = 5\%$ and $\rho_{ceiling} = 80\%$. Finally, the simulation workplane illuminance values were compared with the experimental values recorded by the Li-cor photometers installed at the workplane.

The results showed that: on clear days the simulation overestimates the workplane illuminance between 1%-10% (see Figure 4.7), while on overcast days the simulation overestimates the workplane illuminance between 9%-13% (see Figure 4.8). The difference is acceptable for design purposes and it is caused due to the limitation of one-bounce ray tracing applied for the direct sunlight as well as the assumption of Lambertian room surfaces. Moreover, the assumption that the sunlight transmitted through the shade is perfectly diffuse, without taking into consideration possible direct sunlight coming through the fabric perforation, is responsible for the higher error closer to the façade.

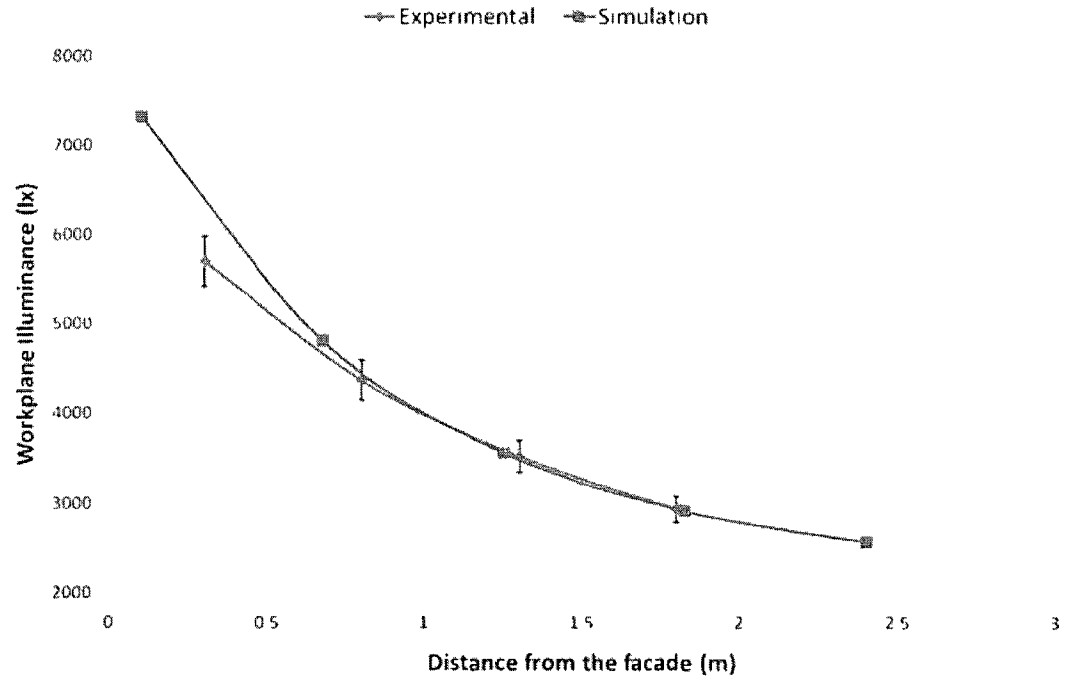

Figure 4.7: Comparison of predicted and measured workplane illuminance for a clear day (50% open)

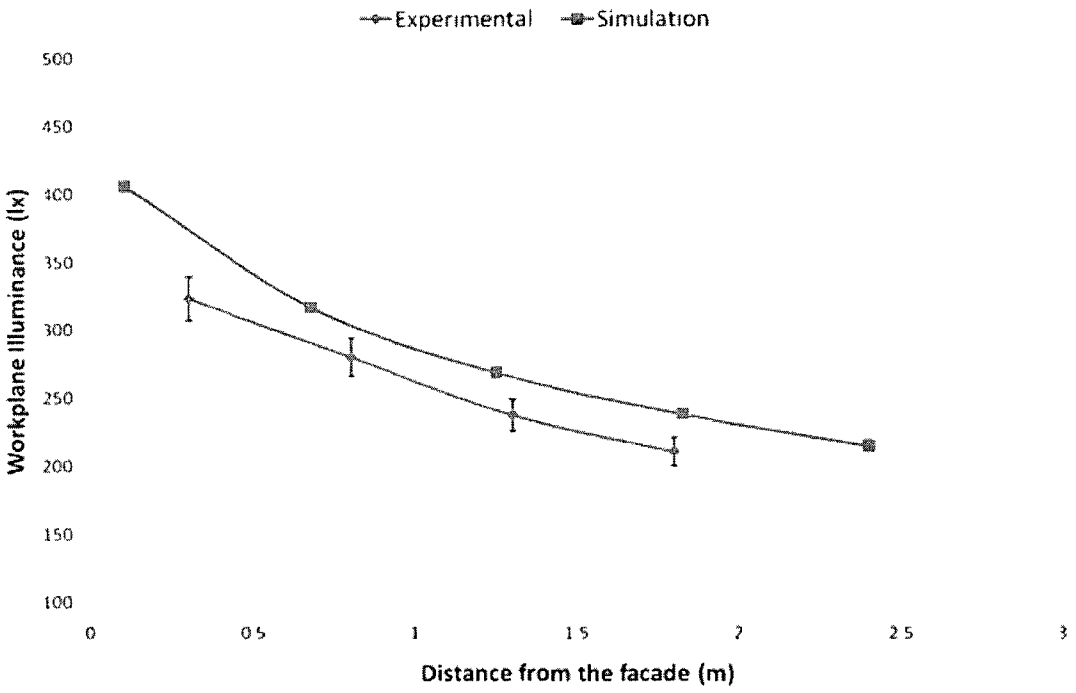

Figure 4.8: Comparison of predicted and measured workplane illuminance for an overcast day (50% open)

4.6 Thermal Measurements

Thermal experiments were conducted to examine possible advantages on the use of bottom-up shade. The existence of a "sealed" cavity (bottom-up shade configuration) could possibly decrease the heat flow through the building fenestration. Therefore, the thermal performance of bottom-up shade was compared with a conventional roller shade under the following design day conditions:

- Clear cold day
- Overcast cold day
- Clear warm day

For a cold clear day (see Figure 4.9A) with an average outdoor temperature of -10°C [(min, max)=(-14°C, -6°C)] and a solar peak at 944 W/m^2, the results showed that during the night, the roller shade configuration (conventional cavity) presents overall higher temperatures than the bottom-up configuration. The average temperature difference ($\Delta T_i = T_{i_{roller\ shade\ conf}} - T_{i_{bottom\ up\ conf}}$, where i=inside glazing, cavity air, shade or room air) for the inside glazing is $\Delta T_{inside\ glazing} \approx 0.3$°C (see Figure 4.9B), for the cavity air is $\Delta T_{cavity\ air} \approx 1.5$°C (see Figure 4.9C) and for the shades is $\Delta T_{shade} \approx 0.5$°C (see Figure 4.9D). Assuming that the two shades have similar thermal resistance, as both are made by conventional fabrics with no particular thermal properties and knowing that both fenestration configurations are exposed in identical outdoor and indoor (see Figure 4.9E) conditions, the reason for the temperature difference is the "sealed" cavity.

The "sealed" cavity is able to trap the cold air film, which is in contact with the cold glazing, inside the cavity between the shade and the glazing, by preventing energy flow through natural convection and eventually decreasing the energy losses to the outside. Therefore, at the "sealed" cavity, the surface and air temperatures are lower than the conventional one. Moreover, the air velocities measured at the open sides of the roller shade's cavity were approximately 0.03 m/s, indicating a downward cold draft from the cavity to the room.

During the day, the ΔT_i, at the solar peak, for the inside glazing is $\Delta T_{inside\ glazing} \approx 1.5$°C (see Figure 4.9B), for the cavity air is $\Delta T_{cavity\ air} \approx -3.3$°C (see Figure 4.9C) and for the shades is $\Delta T_{shade} \approx 5.1$°C (see Figure 4.9D). The high ΔT_{shade} is due to high solar absorbance of the roller shade (five times higher than the bottom-up). Heat transfer through infrared radiation causes a warmer inside glazing for the conventional cavity, due to warmer shade. Therefore,

someone would expect higher air temperatures in the conventional cavity than the "sealed" one, due to warmer cavity surfaces (inside glazing and shade). This is not the case; as the roller shade's cavity is not "sealed", the room air is able to enter the cavity from the sides of the shade and mix with the cavity air, keeping the conventional cavity air at temperatures closer to the room air temperatures. As the "sealed" cavity is not perfectly sealed, due to fabric perforation, this process is present to the "sealed" cavity too, but at lower rate. In addition, the air velocities measured inside the conventional as well as the "sealed" cavity varied from 0.05 m/s (morning and afternoon) to 0.09 m/s (solar noon).

Similar results with the cold clear night are obtained for a cold overcast day (see Figure 4.10), with an average outdoor temperature of -6.5°C [(min, max)=(-7.7°C, -4.1°C)] and a solar peak at 217 W/m^2, where similar temperature differences are observed, not just the night but during the day too, due to lack of solar radiation.

For a warm clear day (see Figure 4.11A) with an average outdoor temperature of 16.6°C [(min, max)=(8.6°C, 26.2°C)] and a solar peak at 627 W/m^2, the results showed that during the night, the conventional cavity presents overall higher temperatures than the "sealed" one. The ΔTi for the inside glazing is $\Delta T_{inside\ glazing} \approx 0.4$°C (see Figure 4.11B), for the cavity air is $\Delta T_{cavity\ air} \approx 0.8$°C (see Figure 4.11C) and for the shades is $\Delta T_{shade} \approx 0.5$°C (see Figure 4.11D), indicating an advantageous thermal performance of the "sealed" cavity, similar to a cold night.

During the day, the ΔTi, at the solar peak, for the inside glazing is $\Delta T_{inside\ glazing} \approx 1.5$°C (see Figure 4.11B), for the cavity air is $\Delta T_{cavity\ air} \approx -3.0$°C (see Figure 4.11C) and for the shades is $\Delta T_{shade} \approx 3.0$°C (see Figure 4 11D). Finally, in both cases (warm night and clear warm day), the air velocities were very similar to a cold clear night and day, respectively.

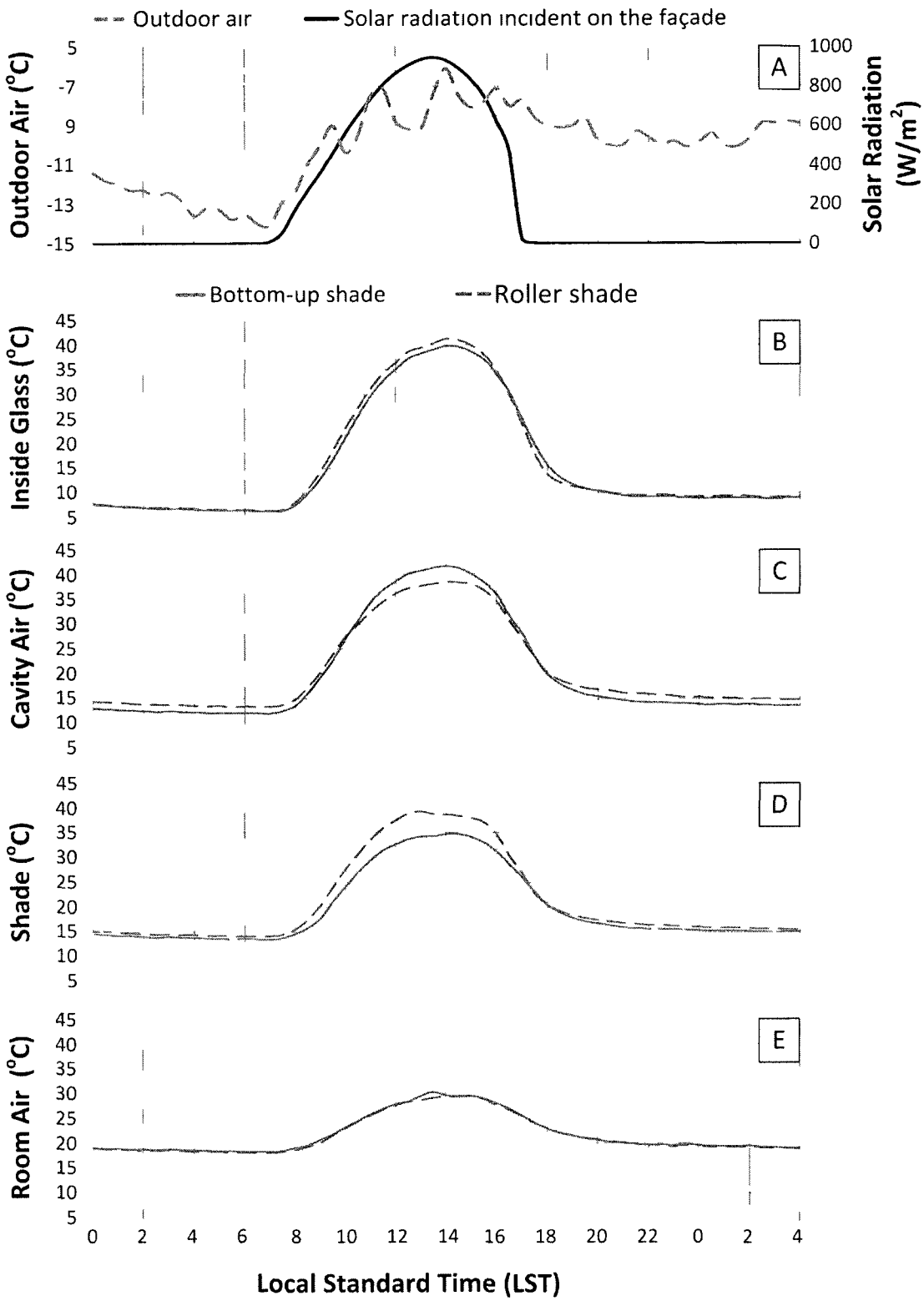

Figure 4 9 Temperatures comparison between a "sealed" (bottom-up shade) cavity and a conventional (roller shade) one for a cold clear day

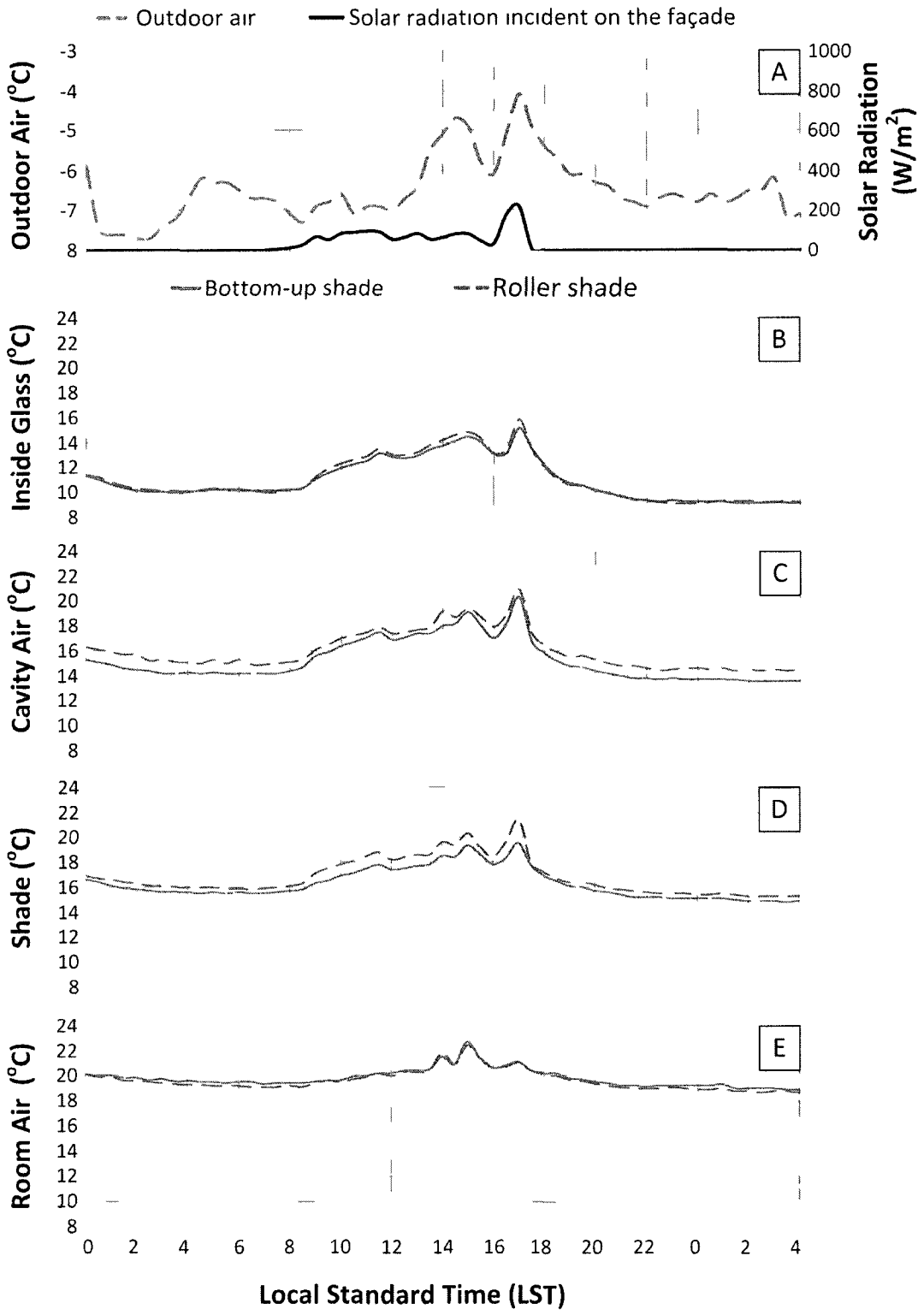

Figure 4 10 Temperatures comparison between a "sealed" (bottom-up shade) cavity and a conventional (roller shade) one for a cold overcast day

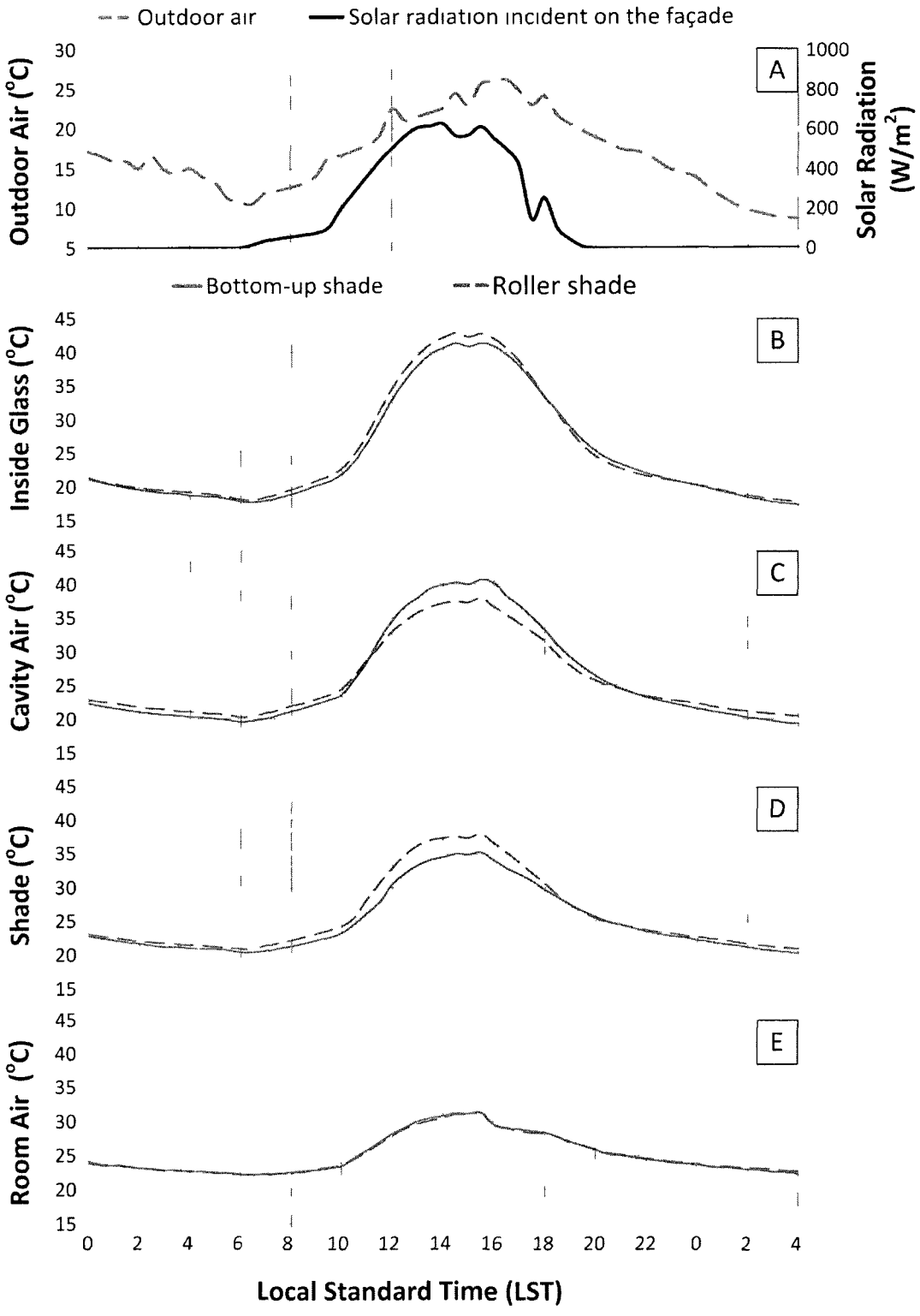

Figure 4 11 Temperatures comparison between a "sealed" (bottom-up shade) cavity and a conventional (roller shade) one for a warm clear day

Finally, through the one year of thermal experiments conducted, no condensation was observed. Furthermore, higher accumulation of dust occurred on the "sealed" cavity configuration compared to the non-sealed cavity; an observation that is unrelated to the thermal performance of bottom-up shade, but it is important to be reported.

To conclude, the potential benefits of a "sealed" cavity on fenestration thermal performance are apparent. However, they have to be quantified. The use of a "sealed" cavity can increase the effective thermal resistance of the fenestration by trapping the air that is in contact with the glazing therefore, reducing the heat transfer through the fenestration, by minimizing heat transfer through natural convection. Moreover, a shade with low emissivity could minimize the heat transfer through radiation too, by decreasing even more the energy flow.

In order to elucidate the potential of closed shades during the non-occupancy hours and adapting this concept to shades' control strategies, the following experiment was contacted. During a cold night with an average outdoor temperature of -6.0°C [(min, max)=(-6.5°C, -5.4°C)] and under thermal equilibrium, the bottom-up shade opened (see Figure 4.12). Surface and air temperatures were monitored during this change, in order to examine the thermal response of the system. The results showed that when the shade was opened, the cavity air temperature increased 4.2°C, from 15.3°C to 19.5°C when the inside glazing increased 3.0°C, from 10.6°C to 13.6°C (3.1°C less that the shade temperature, when the shade was closed). This increase of surface and air temperature illustrates the increase of heat transfer from the room to the fenestration and eventually to the outside. Hence, the knowledge of the effect of shades on the fenestration's effective thermal resistance provides information about how the shades should be controlled during times of non-occupancy. For example, if during a cold night, there is a need for building cooling, the shade could open to

increase energy flow to the outside and help to passively cool the building. If, on the other hand, there is a need of preserving the building temperatures, then the shades could be closed, to decrease the energy losses to the outside. In both cases, energy savings could be achieved by reducing the mechanical cooling or heating required.

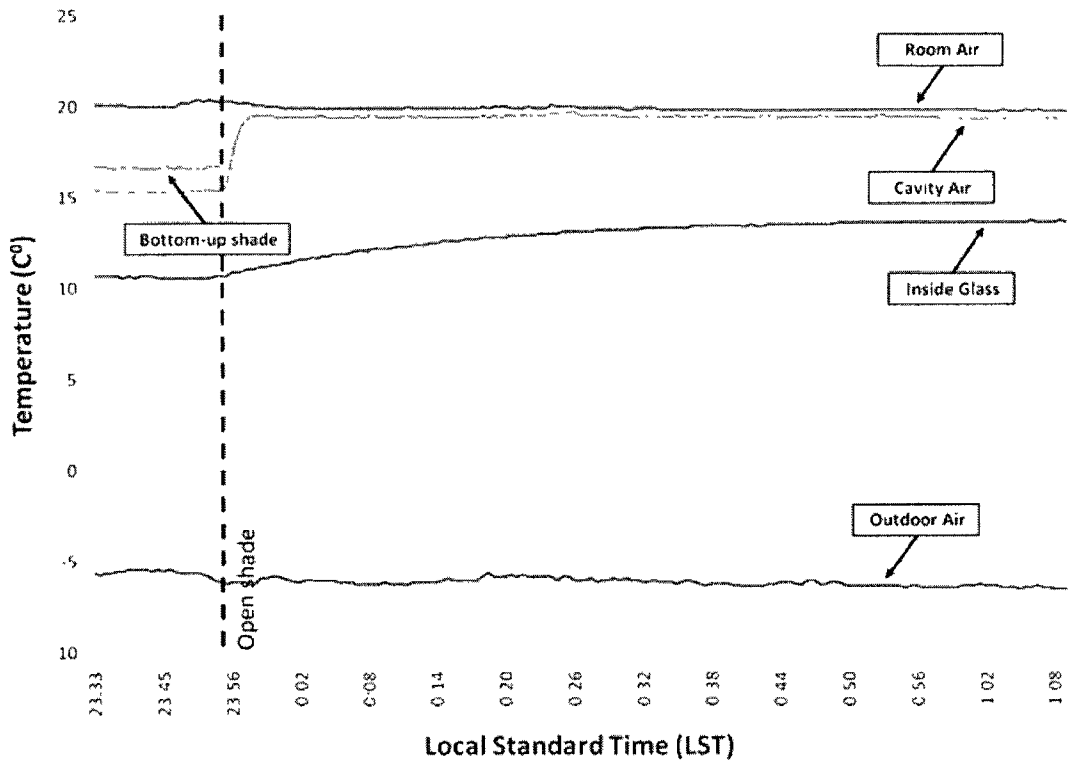

Figure 4.12: Temperature response of the fenestration by opening the bottom-up shade, during a cold night

Chapter 5: Conclusions and Recommendations

5.1 Conclusions

In this study, the daylighting and thermal performance of "bottom-up" shades was presented. The bottom-up is a motorized roller shade that operates in reverse of a conventional roller shade (opens from top to bottom), so as to cover the bottom part of the window, providing privacy to the occupants, while allowing daylight to enter from the top section.

A daylighting numerical model, verified with experimental measurements (1%-13% agreement), was developed based on the radiosity method and one-bounce ray tracing. As inputs, the model uses: (i) the geographic location (latitude, longitude), (ii) the room geometry and orientation, (iii) the visible reflectance of the room elements and (iv) the visible reflectance and transmittance of the façade and the shading device, as a function of solar angle of incidence (θ), to determine the daylighting potential of bottom-up shades on the space's lighting performance and energy savings in artificial lighting.

Two different control strategies were introduced in order to ensure proper lighting conditions for the occupants: the 'Glare-Free Zone' (GFZ) and the Acceptable Workplane Illuminance (AWI). For the GFZ, the shade position is calculated as a function of the solar and room geometry in order to protect seated and/or standing occupants from direct glare, and at the same time allow direct sunlight to penetrate into the office to illuminate the back part of the room. For the AWI, the shade position is calculated in order to maintain the average workplane illuminance at acceptable levels (500 lx) and to simultaneously not exceed the value of 1000 lx at any location on the workplane. Control algorithms were developed based on correlations between the shade position, outdoor illuminance and workplane

illuminance, for various room geometries using the following design days: Equinox, summer and winter Solstice, summer and winter typical clear day, summer and winter typical overcast day. The control algorithms developed for the bottom-up shades are applicable for any location and orientation around the world

A sensitivity analysis of the impact of bottom-up shade optical properties on the daylighting and lighting energy demand was performed. The results showed that the bottom-up shade of visible transmittance equal to $\tau = 10\%$ performs better than $\tau = 0\%$ and $\tau = 5\%$ in terms of daylight and energy consumption for artificial lighting However, when visual display units (VDU) are present, reflected glare may possibly occur during sunny days. Consequently, the combination of unison dimming control for artificial lighting and the bottom-up shade of $\tau = 5\%$, could give similar results in terms of visual performance and artificial lighting energy consumption, minimizing the possibility of reflected glare.

In addition, a bottom-up shade of $\tau = 5\%$ was compared with a conventional roller shade of equal transmittance. Its annual daylight performance was significantly higher, maintaining the minimum workplane illuminance requirements by 8%-58% more of the time than the roller shade configuration. At the back part of the room, away from the façade, where the need for artificial lighting is more apparent, the minimum workplane illuminance requirements were met 46% more, proving the advantage of bottom-up shade towards the conventional roller shades by allowing the natural light to enter from the top section of the façade deep into the room and illuminate the space, reducing the annual energy consumption for artificial lighting by 21%-41%.

Finally, thermal experiments were conducted for a clear and an overcast cold day as well as a clear warm day, to examine the possible advantages of the use of bottom-up shade. The results showed an increased effective thermal resistance of the fenestration, when the shades

are closed, compared with open. The use of a "sealed" cavity can increase the thermal performance of the fenestration by trapping the air that is in contact with the glazing inside, thus minimizing the heat transfer through natural convection. Taking this into consideration, a third control strategy was introduced, applied when the occupants are absent, giving priority to thermal aspects. Therefore, when heat transfer between the indoor and outdoor environment is desired (i e. during a cold night, when there is a need for building cooling, the shade could be left open to increase energy flow to the outside and help to passively cool the building), the shade should be open, otherwise, the shade should be kept closed. This could result in a potential reduction in heating or cooling load for the building.

5.2 Recommendations

As the architectural trend of transparent building envelopes is becoming mainstream, the use of advanced dynamic shading devices to control solar gains and provide visual comfort to the occupants is becoming more and more common, if not essential. Therefore, the need for standard daylight performance metrics on shading devices is crucial. A standard procedure based on comparative studies should be made to guide building designers, owners and users as to the appropriate shading device and control strategy suitable for their specific application.

Moreover, as the visual and thermal comfort of the occupants is vital, occupant response and behavior has to be considered in employing control strategies on shading devices, by considering their wishes and providing a manual override system. Thus, testing the proposed bottom-up shade control algorithms with people, to see any user response factors that need to be included, would be practical.

Furthermore, the potential benefits of a "sealed" cavity on fenestration thermal performance are apparent. However, a more detailed study using CFD modeling is needed to quantify its thermal performance as well as to study the possibility of condensation to occur.

Finally, as advanced dynamic envelope systems begin to be adapted on new office buildings, a bottom-up shade incorporated with a venetian blind on the top part is recommended. This advanced shading system is promising, as it is able to redirect or diffuse the daylight onto the ceiling, minimizing the possibility of glare, while maintaining the workplane illuminance at acceptable levels.

References

ASHRAE. (2005). *ASHRAE Handbook of fundamentals.* American Society of Heating Refrigerating and Air-Conditioning Engineers Inc., Atlanta, GA.

Athienitis AK & Santamouris M. (2002). *Thermal analysis and design of passive solar buildings.* James & James Science Publishers, London.

Athienitis AK & Tzempelikos A. (2002). A methodology for simulation of daylight room illuminance distribution and light dimming for a room with a controlled shading device. *Solar Energy* **72,** 271-281.

Bessoudo M. (2008). Thermal Comfort Conditions Near Glazed Façades: An Experimental and Simulation Study In *BCEE.* Concordia, Montreal.

Bessoudo M, Tzempelikos A, Athienitis AK & Zmeureanu R. (2007). Simulation of thermal comfort conditions in highly-glazed perimeter zones with shading devices. In *2nd Canadian Solar Buildings Conference.* Calgary.

Breitenbach J, Lart S, Langle I & Rosenfeld JLJ. (2001). Optical and thermal performance of glazing with integral venetian blinds. *Energy & Buildings* **33,** 433-442.

Carmody J, Selkowitz S, Lee E, Arasteh D & Willmert T. (2004). *Window systems for high-performance buildings.* W.W. Norton, New York.

Dubois MC. (2001). Impact of Shading Devices on Daylight Quality in Offices: Simulations with Radiance. In *Dept of Building Science.* Lund Institute of Technology, Lund.

Duffie J & Beckmann W. (2006). *Solar engineering of thermal processes.* Whiley, New York, NY.

Edwards L, Torcellini PA & National Renewable Energy L. (2002). *A literature review of the effects of natural light on building occupants.* National Renewable Energy Laboratory.

Fisekis K, Davies M, Kolokotroni M & Langford P. (2003). Prediction of discomfort glare from windows. *Lighting Research and Technology* **35,** 360-369.

Galasiu AD, Atif MR & MacDonald RA. (2004). Impact of window blinds on daylight-linked dimming and automatic on/off lighting controls. *Solar Energy* **76,** 523-544.

Ge H & Fazio P. (2004). Experimental investigation of cold draft induced by two different types of glazing panels in metal curtain walls. *Building and Environment* **39,** 115-125.

Glassner AS. (1989). *Introduction to ray tracing.* Academic press, London.

Guillemin A & Molteni S. (2002). An energy-efficient controller for shading devices self-adapting to the user wishes. *Building and Environment* **37,** 1091-1097.

Guillemin A & Morel N. (2002). Experimental results of a self-adaptive integrated control system in buildings: a pilot study. *Solar Energy* **72,** 397-403.

Heschong L. (2002). Daylighting and human performance. *ASHRAE journal* **44,** 65-67.

Hodder SG & Parsons K. (2007). The effects of solar radiation on thermal comfort. *International journal of biometeorology* **51,** 233-250.

Huizenga C, Zhang HUI, Mattelaer P, Yu T, Arens E & Lyons P. (2006). Window Performance for Human Thermal Comfort. Center for the Built Environment, Califirnia.

Hunt DRG. (1979). The use of artificial lighting in relation to daylight levels and occupancy. *Building and Environment* **14,** 21-33.

Kapsis K, Tzempelikos A, Athienitis AK & Zmeureanu R. (2008) Daylighting & Thermal Performance of Bottom-up Shade. In *3rd Canadian Solar Building Conference.* Fredericton, NB.

Kapsis K, Tzempelikos A, Athienitis AK & Zmeureanu R. (2009). A Control Algorithm for Bottom-up Roller Shade. In *4th Canadian Solar Building Conference.* Toronto, ON.

Kim W, Ahn HT & Kim JT. (2008). A first approach to discomfort glare in the presence of non-uniform luminance. *Building and Environment* **43,** 1953-1960.

Klems JH. (2000). Solar Heat Gain Through Fenestration Systems Containing Shading: Procedures for Estimating Performance from Minimal Data. *Lawrence Berkeley National Laboratory.*

Kuhn TE. (2006). Solar control: A general evaluation method for facades with venetian blinds or other solar control systems. *Energy & Buildings* **38,** 648-660.

Kuhn TE, Buhler C & Platzer WJ. (2001). Evaluation of overheating protection with sun-shading systems. *Solar Energy* **69,** 59-74.

Lang KR. (2001). *The Cambridge encyclopedia of the sun.* Cambridge University Press, Cambridge.

Lee ES, DiBartolomeo DL & Selkowitz SE. (1998). Thermal and daylighting performance of an automated venetian blind and lighting system in a full-scale private office. *Energy and buildings* **29,** 47-63.

Lee ES & Selkowitz SE. (2006). The New York Times Headquarters daylighting mockup: Monitored performance of the daylighting control system. *Energy & Buildings* **38,** 914-929.

Lee JS & Kim BS. (2007). Development of the nomo-graph for evaluation on discomfort glare of windows. *Solar Energy* **81,** 799-808.

Leslie RP. (2003). Capturing the daylight dividend in buildings: why and how? *Building and Environment* **38,** 381-385.

Lyons PR, Arasteh D & Huizenga C. (2000). Window performance for human thermal comfort. *Transactions-American Society of Heating Refrigerating and Air-Conditioning Engineers Inc*
106, 594-604.

Murdoch JB. (2003) *Illuminating Engineering, for Edison's lamp to the LED.* Visions Communications, New York, NY.

Nabil A & Mardaljevic J. (2006). Useful daylight illuminances: A replacement for daylight factors. *Energy and Buildings* **38,** 905-913.

Nazzal AA. (2001) A new daylight glare evaluation method: Introduction of the monitoring protocol and calculation method. *Energy and Buildings* **33,** 257-265.

Newsham GR. (2009). The role of dimmable lighting in demand-responsive buildings. *Lighting design & application (LD+A)* **4,** 30-32, 34, 36.

NRCan. (2007). National Energy Use Database, 1990 to 2005, Comprehensive Energy Use Database, Commercial/Institutional Sector.

O'Neill B. (2008). Model - based control of venetian blinds. In *BCEE.* Concordia University, Montreal.

Osterhaus WKE. (2005). Discomfort glare assessment and prevention for daylight applications in office environments. *Solar Energy* **79,** 140-158.

Osterhaus WKE & Bailey IL. (1992). Large area glare sources and their effect on visual discomfort and visual performance at computer workstations. In *Industry Applications Society Annual Meeting, 1992, Conference Record of the 1992 IEEE*, pp. 1825-1829

Park K-W & Athienitis AK. (2003). Workplane illuminance prediction method for daylighting control systems. *Solar Energy* **75,** 277-284.

Park K-W, O'Neill B, Karava P, Mouriki E & Athienitis AK. (2008). A control algorithm for motorized roller blinds in an atrium integrated with a hybrid ventilation system. In *3rd Canadian Solar Buildings Conference.* Fredericton, Canada.

Perez R, Ineichen P, Seals R, Michalsky J & Stewart R. (1990). Modeling daylight availability and irradiance components from direct and global irradiance. *Solar Energy* **44,** 271-289.

Rea MS. (2000). *The IESNA lighting handbook: reference & application.* Illuminating Engineering Society of North America, New York, NY.

Reinhart C, Mardaljevic J & Rogers Z. (2006). Dynamic daylight performance metrics for sustainable building design. *Leukos* **3,** 1-25.

Reinhart CF & Walkenhorst O. (2001). Validation of dynamic RADIANCE-based daylight simulations for a test office with external blinds. *Energy and Buildings* **33,** 683-697.

Roche L. (2002). Summertime performance of an automated lighting and blinds control system. *Lighting Research & Technology* **34,** 11.

Rosenfeld AH & Selkowitz SE. (1977). Beam Daylighting: an Alternative Illumination Technique." *Energy and Buildings* **1,** 43-50.

Sen Z. (2008). *Solar Energy Fundamentals and Modeling Techniques: Atmosphere, Environment, Climate Change and Renewable Energy*, vol. 1st edition. Springer Verlag, London.

Sezgen O & Koomey JG. (2000). Interactions between lighting and space conditioning energy use in US commercial buildings. *Energy* **25,** 793-805.

Shahid H & Naylor D. (2005). Energy performance assessment of a window with a horizontal Venetian blind. *Energy & Buildings* **37,** 836-843.

Sutter Y, Dumortier D & Fontoynont M. (2006). The use of shading systems in VDU task offices: A pilot study. *Energy & Buildings* **38,** 780-789.

Tzempelikos A & Athienitis AK. (2007). The impact of shading design and control on building cooling and lighting demand. *Solar Energy* **81,** 369-382.

Tzempelikos A, Athienitis AK & Karava P. (2007). Simulation of façade and envelope design options for a new institutional building. *Solar Energy* **81,** 1088-1103.

Veitch JA. (2006). Lighting for well-being: a revolution in lighting? In *2nd CIE Expert Symposium on Lighting and Health*, pp. 56-61. Vienna.

Veitch JA & McColl SL. (1995). Modulation of fluorescent light: Flicker rate and light source effects on visual performance and visual comfort. *Lighting Research and technology* **27,** 243-254.

Veitch JA & Newsham GR. (1998). Determinants of lighting quality I: State of the science. *Journal of the Illuminating Engineering Society* **27,** 92-106.

Velds M. (2002). User acceptance studies to evaluate discomfort glare in daylit rooms. *Solar Energy* **73,** 95-103.

Waide P & Tanishima S. (2006). *Light's Labour's Lost: Policies for Energy-efficient Lighting.* OECD.

Webb AR. (2006). Considerations for lighting in the built environment: non-visual effects of light. *Energy & Buildings* **38,** 721-727.

Williams G. (2008). *Linear algebra with applications.* Jones and Bartlett Publishers, Sudbury, MA.

Zmeureanu R & Peragine C. (1999). Evaluation of interactions between lighting and HVAC systems in a large commercial building. *Energy Conversion and Management* **40,** 1229.

Appendix A:

Daylighting/Lighting Model Input Parameters

Input parameters

Define Input parameters

$\psi := 0 \cdot deg$ ...window surface azimuth

$W_{rm} := 4 \cdot m$ ...width of room (along facade)

$D_{rm} := 5 \cdot m$ ...depth of room

$H_{rm} := 4 \cdot m$ ...height of room

$D_{fr} := 30cm$ ...depth of the fenestration frame

$\tau_{shade} := 0.05$ ...shade transmittance

$H_{setpoint} := 1.8m$ ...height of the GFZ
(1.50m for seated and 1.80m for standing occupants)

Select day of the year

$n := 123$

Select time of the day

$t := 7, 8 .. 19$

Typical Meteorological Weather Data for the selected day and time frame

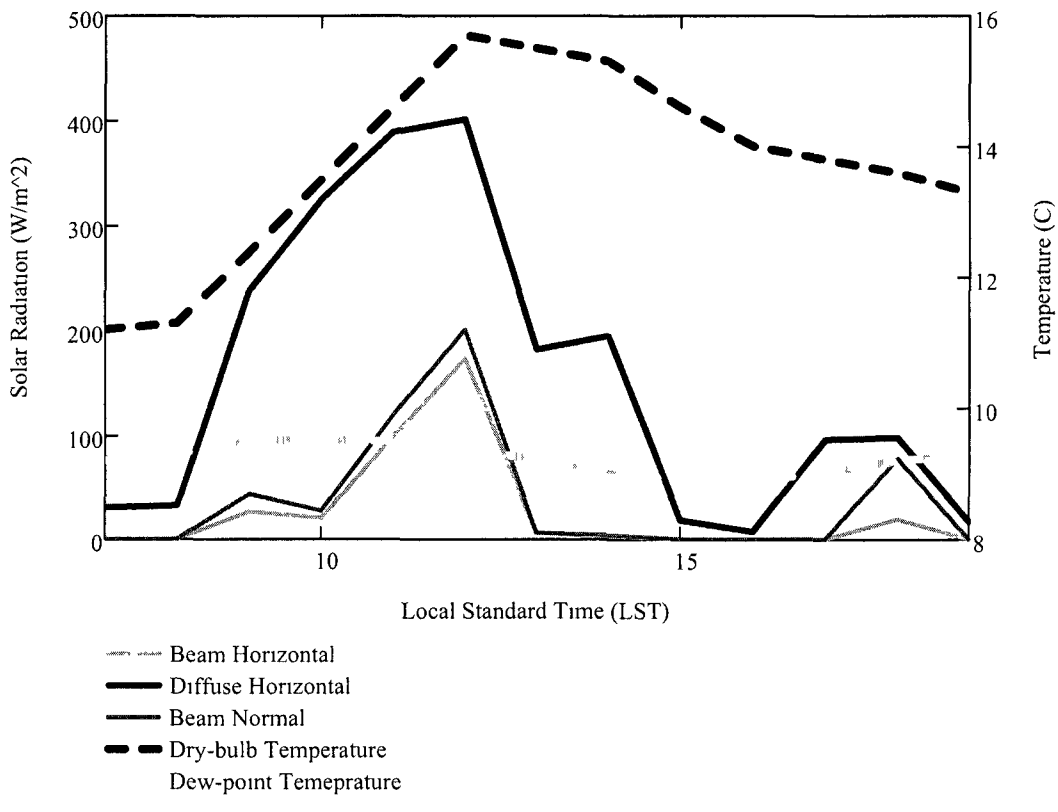

Input parameters for an office space in Montreal

L_w = 45 5 deg	Latitude
LNG = 74 deg	Longitude
STM = 75 deg	Local standard time meridian

H_{sp} = 0 8m	height of spandrel
$H_{workplane}$ = 0 8m	height of the workplane from the floor
β_w = 90 deg	surface (fenestration) tilt angle

$H_{facade} = H_{rm} - H_{sp} - 0\ 1m = 3\ 1\ m$	height of the fenestration
$W_{facade} = W_{rm} - 0\ 2m = 3\ 8\ m$	width of the fenestration
$A_{facade} = H_{facade}\ W_{facade} = 11\ 78\ m^2$	area of the fenestration

$\rho_{shadeout}$ = 0 7	exterior shade reflectance
$\rho_{shadein}$ = 0 7	interior shade reflectance
ρ_{floor} = 0 30	floor reflectance
$\rho_{ceiling}$ = 0 8	ceiling reflectance
ρ_{wall} = 0 70	wall reflectance
ρ_{facade} = 0 1	interior glass reflectance

Appendix B:

Determination of Solar Geometry

Solar geometry

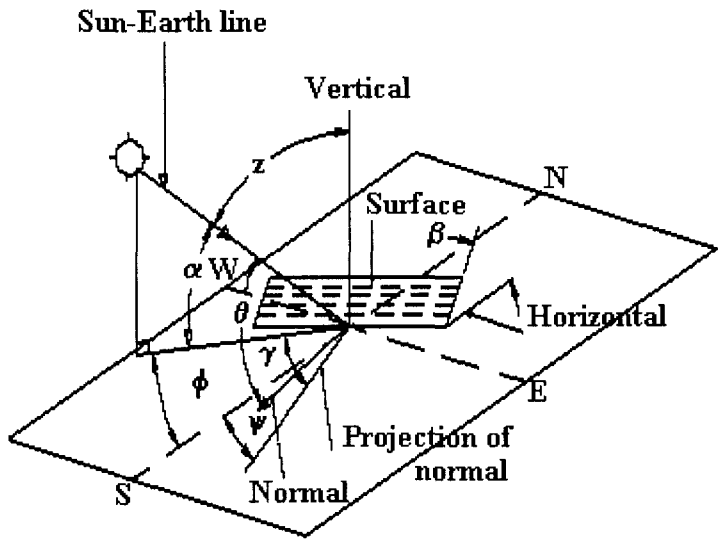

Figure A 1 Solar geometry (Athienitis, 1993)

Equation of time (ET)

$$ET(n) = \left(9.87 \sin\left(4\pi \frac{n-81}{364}\right) - 7.53 \cos\left(2\pi \frac{n-81}{364}\right) - 1.5 \sin\left(2\pi \frac{n-81}{364}\right)\right) \text{min}$$

Apparent Solar Time (AST)

$$AST(n,t) = t\ \text{hr} + ET(n) + \frac{(STM - LNG)\ \text{hr}}{15\ \text{deg}}$$

Solar declination

$$\delta(n) = 23.45\ \text{deg} \sin\left(360 \frac{284+n}{365}\ \text{deg}\right)$$

Hour angle (H)

$$H(n,t) = (AST(n,t) - 12\ \text{hr})\left(15 \frac{\text{deg}}{\text{hr}}\right)$$

Sunset hour angle (h_s)

$$h_s(n) = (\text{acos}(-\tan(L)\ \tan(\delta(n))))$$

Sunset time (t_s)

$$t_s(n) = h_s(n) \frac{\text{hr}}{15\ \text{deg}}$$

Surface sunset time (t_{ss})

$$t_{ss}(n) = \text{min}\left(\left(h_s(n)\ \ \text{acos}\left(-\tan\left(L - \beta_w\right)\ \tan(\delta(n))\right)\right)\right) \frac{\text{hr}}{15\ \text{deg}}$$

Solar altitude (α_s):

$$\alpha_s(n,t) := \begin{cases} \operatorname{asin}\left[\begin{array}{l}(\cos(L))\cdot\cos(\delta(n))\cdot\cos(H(n,t)) \ldots \\ +(\sin(L))\cdot\sin(\delta(n))\end{array}\right] & \text{if } \operatorname{asin}\left[\begin{array}{l}(\cos(L))\cdot\cos(\delta(n))\cdot\cos(H(n,t)) \ldots \\ +\sin(L)\cdot\sin(\delta(n))\end{array}\right] > 0\cdot \\ 0\cdot\text{deg} \quad \text{otherwise} \end{cases}$$

Solar azimuth (f):

$$\phi(n,t) := \operatorname{acos}\left(\frac{\sin(\alpha_s(n,t))\cdot\sin(L) - \sin(\delta(n))}{\cos(\alpha_s(n,t))\cdot\cos(L)}\right)\cdot\frac{H(n,t)}{|H(n,t)|}$$

Surface solar azimuth (g):

$$\gamma(n,t) := \phi(n,t) - \psi$$

Zenith angle (Z):

$$Z(n,t) := \operatorname{acos}((\cos(L)\cdot\cos(\delta(n))\cdot\cos(H(n,t)) + \sin(L)\cdot\sin(\delta(n))))$$

Angle of incidence (θ):

$$\theta\theta(n,t) := \cos(\alpha_s(n,t))\cdot\cos(|\gamma(n,t)|)\cdot\sin(\beta_w) + \sin(\alpha_s(n,t))\cdot\cos(\beta_w)$$

$$\theta(n,t) := \operatorname{acos}\left(\frac{\theta\theta(n,t) + |\theta\theta(n,t)|}{2}\right)$$

Profile angle (d):

$$d(n,t) := \operatorname{atan}\left(\frac{\tan(\alpha_s(n,t))}{\cos(\gamma(n,t))}\right)$$

Major Solar Angles

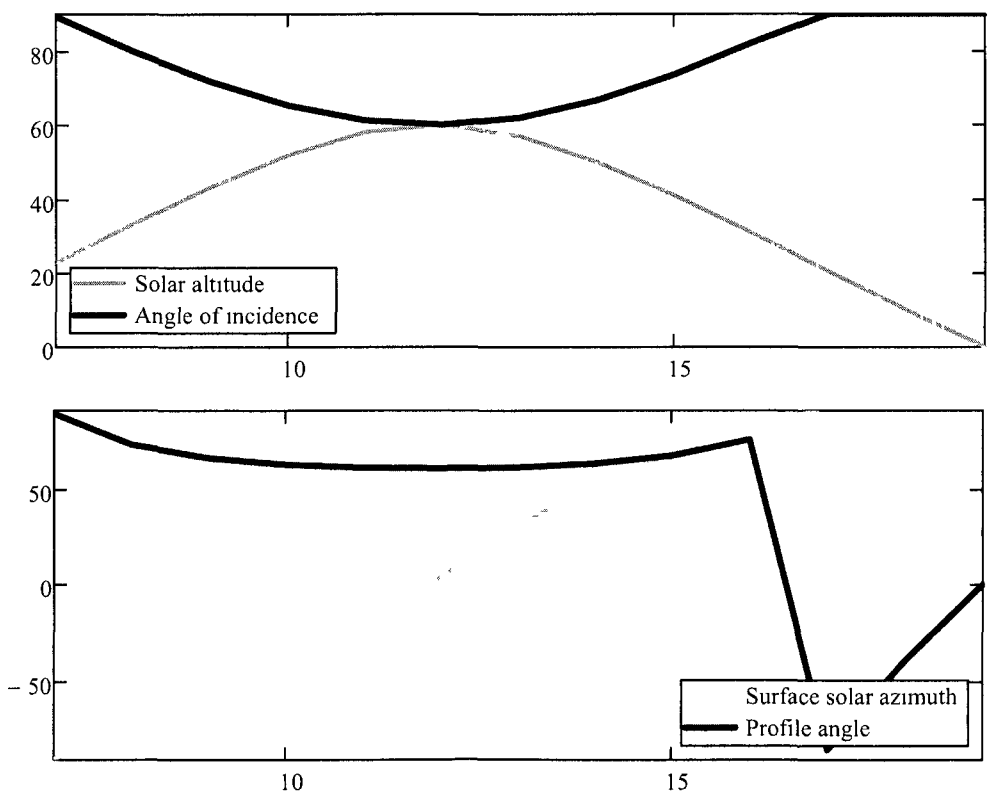

Appendix C:

Perez "All-Weather" Sky Model

Perez Irradiance model (programmed by Dr. A.Tzempelikos)

Ground reflectance $\rho_g(n,t) = \begin{cases} 0.6 & \text{if } T_o(n,t) \le 3 \wedge (120 > n \vee n > 243) \\ 0.2 & \text{otherwise} \end{cases}$

Extraterrestrial solar radiation (outside the atmosphere)

Solar constant $I_{sc} = 1367 \frac{W}{m^2}$

Normal extraterrestrial solar radiation $I_{exn}(n) = I_{sc}\left(1 + 0.033 \cos\left(\frac{360\ n}{365}\ \text{deg}\right)\right)$

Global horizontal irradiance

$I_h(n,t) = I_{bh}(n,t) + I_{dh}(n,t)$

Incident beam radiation on an inclined surface

$I_b(n,t) = \left(I_{bn}(n,t)\cos(\theta(n,t))\right)$

Perez diffuse irradiance model:

Diffuse radiation consists of three components

1 Isotropic part, received uniformly from all the sky dome
2 Circumsolar diffuse, resulting from forward scattering of solar radiation and concentrated in the part of the sky around the sun
3 Horizon brightening, concentrated near the horizon, most pronounced in clear skies

Horizon brightness coefficients

$a_P(n,t) = \max(0, \cos(\theta(n,t)))$ $\quad b_P(n,t) = \max\left(\cos(85\ \text{deg}), \sin\left(\alpha_s(n,t)\right)\right)$

Relative optical air mass

$$m_{opt}(n,t) = \frac{1}{\sin\left(\alpha_s(n,t)\right) + 0.15\left(\alpha_s(n,t)\frac{\pi}{180\ \text{deg}} + 3.885\right)^{-1.253}}$$

Sky brightness

$\Delta(n,t) = m_{opt}(n,t)\frac{I_{dh}(n,t)}{I_{exn}(n)}$

Sky clearness

$$\varepsilon(n,t) = \begin{cases} \dfrac{\frac{I_{dh}(n,t) + I_{bn}(n,t)}{I_{dh}(n,t)} + 5.535\ 10^{-6}\left(90\ \text{deg} - \alpha_s(n,t)\right)^3}{1 + 5.535\ 10^{-6}\left(90\ \text{deg} - \alpha_s(n,t)\right)^3} & \text{if } I_{dh}(n,t) > 0\ \frac{W}{m^2} \\ 0 & \text{otherwise} \end{cases}$$

Statistically derived irradiance coefficients for Perez model

$$f_{11}(n,t) = \begin{cases} -0.008 & \text{if } \varepsilon(n,t) \le 1.065 \\ 0.130 & \text{if } 1.065 < \varepsilon(n,t) \le 1.23 \\ 0.330 & \text{if } 1.23 < \varepsilon(n,t) \le 1.5 \\ 0.568 & \text{if } 1.5 < \varepsilon(n,t) \le 1.95 \\ 0.873 & \text{if } 1.95 < \varepsilon(n,t) \le 2.8 \\ 1.132 & \text{if } 2.8 < \varepsilon(n,t) \le 4.5 \\ 1.060 & \text{if } 4.5 < \varepsilon(n,t) \le 6.2 \\ 0.678 & \text{otherwise} \end{cases} \qquad f_{12}(n,t) = \begin{cases} 0.588 & \text{if } \varepsilon(n,t) \le 1.065 \\ 0.683 & \text{if } 1.065 < \varepsilon(n,t) \le 1.23 \\ 0.487 & \text{if } 1.23 < \varepsilon(n,t) \le 1.5 \\ 0.187 & \text{if } 1.5 < \varepsilon(n,t) \le 1.95 \\ -0.392 & \text{if } 1.95 < \varepsilon(n,t) \le 2.8 \\ -1.237 & \text{if } 2.8 < \varepsilon(n,t) \le 4.5 \\ -1.600 & \text{if } 4.5 < \varepsilon(n,t) \le 6.2 \\ -0.327 & \text{otherwise} \end{cases}$$

$$f_{13}(n,t) = \begin{cases} -0.062 & \text{if } \varepsilon(n,t) \le 1.065 \\ -0.151 & \text{if } 1.065 < \varepsilon(n,t) \le 1.2 \\ -0.221 & \text{if } 1.23 < \varepsilon(n,t) \le 1.5 \\ -0.295 & \text{if } 1.5 < \varepsilon(n,t) \le 1.95 \\ -0.362 & \text{if } 1.95 < \varepsilon(n,t) \le 2.8 \\ -0.412 & \text{if } 2.8 < \varepsilon(n,t) \le 4.5 \\ -0.359 & \text{if } 4.5 < \varepsilon(n,t) \le 6.2 \\ -0.25 & \text{otherwise} \end{cases} \qquad f_{21}(n,t) = \begin{cases} -0.060 & \text{if } \varepsilon(n,t) \le 1.065 \\ -0.019 & \text{if } 1.065 < \varepsilon(n,t) \le 1.23 \\ 0.055 & \text{if } 1.23 < \varepsilon(n,t) \le 1.5 \\ 0.109 & \text{if } 1.5 < \varepsilon(n,t) \le 1.95 \\ 0.226 & \text{if } 1.95 < \varepsilon(n,t) \le 2.8 \\ 0.288 & \text{if } 2.8 < \varepsilon(n,t) \le 4.5 \\ 0.264 & \text{if } 4.5 < \varepsilon(n,t) \le 6.2 \\ 0.156 & \text{otherwise} \end{cases}$$

$$f_{22}(n,t) = \begin{cases} 0.072 & \text{if } \varepsilon(n,t) \le 1.065 \\ 0.066 & \text{if } 1.065 < \varepsilon(n,t) \le 1.23 \\ -0.064 & \text{if } 1.23 < \varepsilon(n,t) \le 1.5 \\ -0.152 & \text{if } 1.5 < \varepsilon(n,t) \le 1.95 \\ -0.462 & \text{if } 1.95 < \varepsilon(n,t) \le 2.8 \\ -0.823 & \text{if } 2.8 < \varepsilon(n,t) \le 4.5 \\ -1.127 & \text{if } 4.5 < \varepsilon(n,t) \le 6.2 \\ -1.377 & \text{otherwise} \end{cases} \qquad f_{23}(n,t) = \begin{cases} -0.022 & \text{if } \varepsilon(n,t) \le 1.065 \\ -0.029 & \text{if } 1.065 < \varepsilon(n,t) \le 1.23 \\ -0.026 & \text{if } 1.23 < \varepsilon(n,t) \le 1.5 \\ -0.014 & \text{if } 1.5 < \varepsilon(n,t) \le 1.95 \\ -0.001 & \text{if } 1.95 < \varepsilon(n,t) \le 2.8 \\ 0.056 & \text{if } 2.8 < \varepsilon(n,t) \le 4.5 \\ 0.131 & \text{if } 4.5 < \varepsilon(n,t) \le 6.2 \\ 0.251 & \text{otherwise} \end{cases}$$

Brightness coefficients

$$F_1(n,t) = \max\left[0, f_{11}(n,t) + f_{12}(n,t)\,\Delta(n,t) + \pi\,\frac{\left(90\ \text{deg} - \alpha_s(n,t)\right)}{180\ \text{deg}}\,f_{13}(n,t)\right]$$

$$F_2(n,t) = \max\left[0, f_{21}(n,t) + f_{22}(n,t)\,\Delta(n,t) + \pi\,\frac{\left(90\ \text{deg} - \alpha_s(n,t)\right)}{180\ \text{deg}}\,f_{23}(n,t)\right]$$

Sky diffuse radiation on a tilted surface:

$$I_{ds}(n,t) := I_{dh}(n,t)\cdot\left[\left(1 - F_1(n,t)\right)\cdot\left(\frac{1 + \cos\left(\beta_w\right)}{2}\right) + F_1(n,t)\cdot\frac{a_P(n,t)}{b_P(n,t)} + F_2(n,t)\cdot\sin\left(\beta_w\right)\right]$$

Ground-reflected radiation on a tilted surface:

$$I_{dg}(n,t) := I_h(n,t)\cdot\rho_g(n,t)\cdot\frac{1 - \cos\left(\beta_w\right)}{2}$$

Total diffuse radiation on a tilted surface:

$$I_d(n,t) := I_{ds}(n,t) + I_{dg}(n,t)$$

The total incident solar radiation on a tilted surface:

$$I(n,t) := I_b(n,t) + I_{ds}(n,t) + I_{dg}(n,t)$$

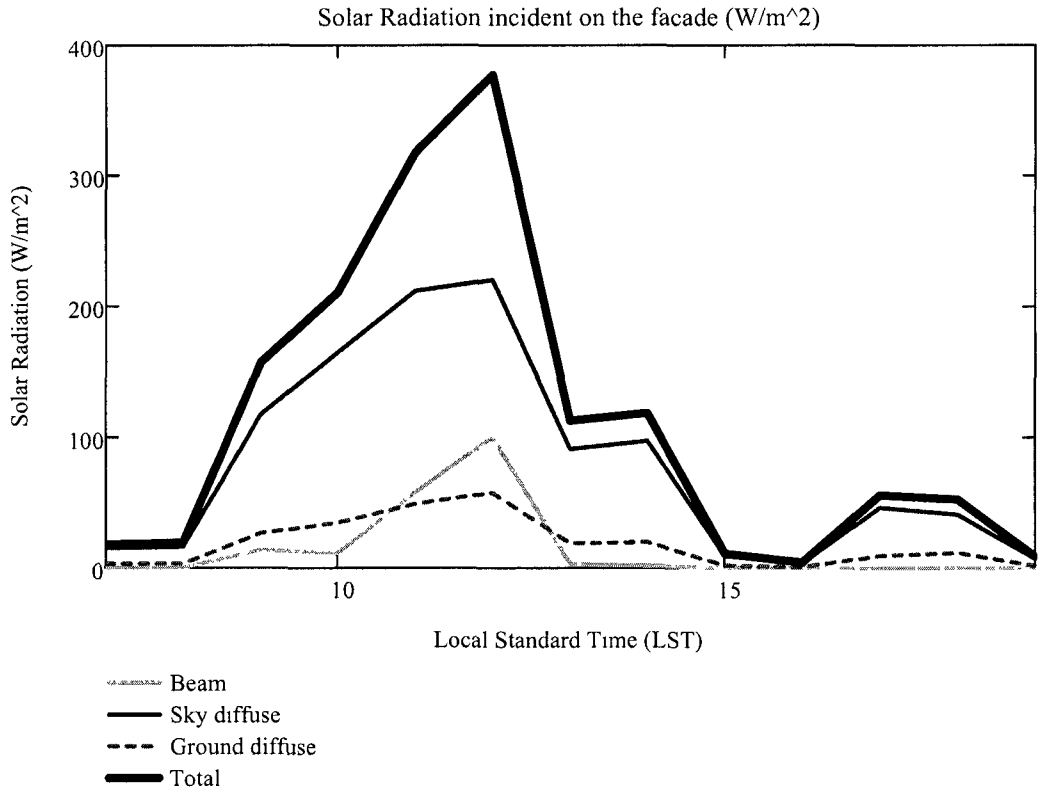

Switch from function of time to time array:

Solar Radiation:

$I_{ba_t} := I_b(n,t)$ $I_{da_t} := I_d(n,t)$

$I_{dsa_t} := I_{ds}(n,t)$ $I_{a_t} := I(n,t)$

$I_{dga_t} := I_{dg}(n,t)$

Outside temperature:

$T_{oa_t} := T_o(n,t)$

Perez Illuminance model

Luminous efficacy coefficients

Direct luminous efficacy

$$ab(n,t) = \begin{cases} 57\,20 & \text{if } \varepsilon(n,t) \le 1\,065 \\ 98\,99 & \text{if } 1\,065 < \varepsilon(n,t) \le 1\,23 \\ 109\,83 & \text{if } 1\,23 < \varepsilon(n,t) \le 1\,5 \\ 110\,34 & \text{if } 1\,5 < \varepsilon(n,t) \le 1\,95 \\ 106\,36 & \text{if } 1\,95 < \varepsilon(n,t) \le 2\,8 \\ 107\,19 & \text{if } 2\,8 < \varepsilon(n,t) \le 4\,5 \\ 105\,75 & \text{if } 4\,5 < \varepsilon(n,t) \le 6\,2 \\ 101\,18 & \text{otherwise} \end{cases} \qquad bb(n,t) = \begin{cases} -4\,55 & \text{if } \varepsilon(n,t) \le 1\,065 \\ -3\,46 & \text{if } 1\,065 < \varepsilon(n,t) \le 1\,23 \\ -4\,90 & \text{if } 1\,23 < \varepsilon(n,t) \le 1\,5 \\ -5\,84 & \text{if } 1\,5 < \varepsilon(n,t) \le 1\,95 \\ -3\,97 & \text{if } 1\,95 < \varepsilon(n,t) \le 2\,8 \\ -1\,25 & \text{if } 2\,8 < \varepsilon(n,t) \le 4\,5 \\ 0\,77 & \text{if } 4\,5 < \varepsilon(n,t) \le 6\,2 \\ 1\,58 & \text{otherwise} \end{cases}$$

$$cb(n,t) = \begin{cases} -2\,98 & \text{if } \varepsilon(n,t) \le 1\,065 \\ -1\,21 & \text{if } 1\,065 < \varepsilon(n,t) \le 1\,23 \\ -1\,71 & \text{if } 1\,23 < \varepsilon(n,t) \le 1\,5 \\ -1\,99 & \text{if } 1\,5 < \varepsilon(n,t) \le 1\,95 \\ -1\,75 & \text{if } 1\,95 < \varepsilon(n,t) \le 2\,8 \\ -1\,51 & \text{if } 2\,8 < \varepsilon(n,t) \le 4\,5 \\ -1\,26 & \text{if } 4\,5 < \varepsilon(n,t) \le 6\,2 \\ -1\,10 & \text{otherwise} \end{cases} \qquad db(n,t) = \begin{cases} 117\,12 & \text{if } \varepsilon(n,t) \le 1\,065 \\ 12\,38 & \text{if } 1\,065 < \varepsilon(n,t) \le 1\,23 \\ -8\,81 & \text{if } 1\,23 < \varepsilon(n,t) \le 1\,5 \\ -4\,56 & \text{if } 1\,5 < \varepsilon(n,t) \le 1\,95 \\ -6\,16 & \text{if } 1\,95 < \varepsilon(n,t) \le 2\,8 \\ -26\,73 & \text{if } 2\,8 < \varepsilon(n,t) \le 4\,5 \\ -34\,44 & \text{if } 4\,5 < \varepsilon(n,t) \le 6\,2 \\ -8\,29 & \text{otherwise} \end{cases}$$

Diffuse luminous efficacy:

$$ad(n,t) = \begin{cases} 97\,24 & \text{if } \varepsilon(n,t) \le 1\,065 \\ 107\,22 & \text{if } 1\,065 < \varepsilon(n,t) \le 1\,23 \\ 104\,97 & \text{if } 1\,23 < \varepsilon(n,t) \le 1\,5 \\ 102\,39 & \text{if } 1\,5 < \varepsilon(n,t) \le 1\,95 \\ 100\,71 & \text{if } 1\,95 < \varepsilon(n,t) \le 2\,8 \\ 106\,42 & \text{if } 2\,8 < \varepsilon(n,t) \le 4\,5 \\ 141\,88 & \text{if } 4\,5 < \varepsilon(n,t) \le 6\,2 \\ 152\,23 & \text{otherwise} \end{cases} \qquad bd(n,t) = \begin{cases} -0\,46 & \text{if } \varepsilon(n,t) \le 1\,065 \\ 1\,15 & \text{if } 1\,065 < \varepsilon(n,t) \le 1\,23 \\ 2\,96 & \text{if } 1\,23 < \varepsilon(n,t) \le 1\,5 \\ 5\,59 & \text{if } 1\,5 < \varepsilon(n,t) \le 1\,95 \\ 5\,94 & \text{if } 1\,95 < \varepsilon(n,t) \le 2\,8 \\ 3\,83 & \text{if } 2\,8 < \varepsilon(n,t) \le 4\,5 \\ 1\,90 & \text{if } 4\,5 < \varepsilon(n,t) \le 6\,2 \\ 0\,35 & \text{otherwise} \end{cases}$$

$$cd(n,t) = \begin{cases} 12\,00 & \text{if } \varepsilon(n,t) \le 1\,065 \\ 0\,59 & \text{if } 1\,065 < \varepsilon(n,t) \le 1\,23 \\ -5\,53 & \text{if } 1\,23 < \varepsilon(n,t) \le 1\,5 \\ -13\,95 & \text{if } 1\,5 < \varepsilon(n,t) \le 1\,95 \\ -22\,75 & \text{if } 1\,95 < \varepsilon(n,t) \le 2\,8 \\ -36\,15 & \text{if } 2\,8 < \varepsilon(n,t) \le 4\,5 \\ -53\,24 & \text{if } 4\,5 < \varepsilon(n,t) \le 6\,2 \\ -45\,27 & \text{otherwise} \end{cases} \qquad dd(n,t) = \begin{cases} -8\,91 & \text{if } \varepsilon(n,t) \le 1\,065 \\ -3\,95 & \text{if } 1\,065 < \varepsilon(n,t) \le 1\,23 \\ -8\,77 & \text{if } 1\,23 < \varepsilon(n,t) \le 1\,5 \\ -13\,90 & \text{if } 1\,5 < \varepsilon(n,t) \le 1\,95 \\ -23\,74 & \text{if } 1\,95 < \varepsilon(n,t) \le 2\,8 \\ -28\,83 & \text{if } 2\,8 < \varepsilon(n,t) \le 4\,5 \\ -14\,03 & \text{if } 4\,5 < \varepsilon(n,t) \le 6\,2 \\ -7\,98 & \text{otherwise} \end{cases}$$

Precipitable water content

$$WC(n,t) = e^{0.07\,T_{dp}(n,t) - 0.075}$$

Diffuse horizontal illuminance

$$E_{dh}(n,t) = I_{dh}(n,t)\left(\begin{array}{l} ad(n,t) + bd(n,t)\,WC(n,t) + cd(n,t)\,\sin\left(\alpha_s(n,t)\right) \\ + dd(n,t)\,\ln\left(\Delta(n,t) + 10^{-10}\right) \end{array}\right) \text{ lx } \frac{m^2}{W}$$

Direct normal illuminance

$$E_{bn}(n,t) = \max\left[0, I_{bn}(n,t)\left[\begin{array}{l} ab(n,t) + bb(n,t)\,WC(n,t) \\ + cb(n,t)\,e^{5.73\left(90\,\text{deg} - \alpha_s(n,t)\right)\frac{\pi}{180\,\text{deg}} - 5} + db(n,t)\,\Delta(n,t) \end{array}\right]\right] \text{ lx } \frac{m}{W}$$

Direct horizontal illuminance

$$E_{bh}(n,t) = E_{bn}(n,t)\,\sin\left(\alpha_s(n,t)\right)$$

Global horizontal illuminance

$$E_h(n,t) = E_{bh}(n,t) + E_{dh}(n,t)$$

Beam illuminance on a tilted surface

$$E_b(n,t) = \left(E_{bn}(n,t)\,\cos(\theta(n,t))\right)$$

Statistically derived illuminance coefficients for Perez model

$$f_{11}(n,t) = \begin{cases} 0.011 & \text{if } \varepsilon(n,t) \le 1.065 \\ 0.429 & \text{if } 1.065 < \varepsilon(n,t) \le 1.23 \\ 0.809 & \text{if } 1.23 < \varepsilon(n,t) \le 1.5 \\ 1.014 & \text{if } 1.5 < \varepsilon(n,t) \le 1.95 \\ 1.282 & \text{if } 1.95 < \varepsilon(n,t) \le 2.8 \\ 1.426 & \text{if } 2.8 < \varepsilon(n,t) \le 4.5 \\ 1.485 & \text{if } 4.5 < \varepsilon(n,t) \le 6.2 \\ 1.170 & \text{otherwise} \end{cases} \qquad f_{12}(n,t) = \begin{cases} 0.570 & \text{if } \varepsilon(n,t) \le 1.065 \\ 0.363 & \text{if } 1.065 < \varepsilon(n,t) \le 1.23 \\ -0.054 & \text{if } 1.23 < \varepsilon(n,t) \le 1.5 \\ -0.252 & \text{if } 1.5 < \varepsilon(n,t) \le 1.95 \\ -0.420 & \text{if } 1.95 < \varepsilon(n,t) \le 2.8 \\ -0.653 & \text{if } 2.8 < \varepsilon(n,t) \le 4.5 \\ -1.214 & \text{if } 4.5 < \varepsilon(n,t) \le 6.2 \\ -0.300 & \text{otherwise} \end{cases}$$

$$f_{13}(n,t) = \begin{cases} -0.081 & \text{if } \varepsilon(n,t) \le 1.065 \\ -0.307 & \text{if } 1.065 < \varepsilon(n,t) \le 1.23 \\ -0.442 & \text{if } 1.23 < \varepsilon(n,t) \le 1.5 \\ -0.531 & \text{if } 1.5 < \varepsilon(n,t) \le 1.95 \\ -0.689 & \text{if } 1.95 < \varepsilon(n,t) \le 2.8 \\ -0.779 & \text{if } 2.8 < \varepsilon(n,t) \le 4.5 \\ -0.784 & \text{if } 4.5 < \varepsilon(n,t) \le 6.2 \\ -0.615 & \text{otherwise} \end{cases} \qquad f_{21}(n,t) = \begin{cases} -0.095 & \text{if } \varepsilon(n,t) \le 1.065 \\ 0.050 & \text{if } 1.065 < \varepsilon(n,t) \le 1.23 \\ 0.181 & \text{if } 1.23 < \varepsilon(n,t) \le 1.5 \\ 0.275 & \text{if } 1.5 < \varepsilon(n,t) \le 1.95 \\ 0.380 & \text{if } 1.95 < \varepsilon(n,t) \le 2.8 \\ 0.425 & \text{if } 2.8 < \varepsilon(n,t) \le 4.5 \\ 0.411 & \text{if } 4.5 < \varepsilon(n,t) \le 6.2 \\ 0.518 & \text{otherwise} \end{cases}$$

$$f_{22}(n,t) = \begin{cases} 0.158 & \text{if } \varepsilon(n,t) \le 1.065 \\ 0.008 & \text{if } 1.065 < \varepsilon(n,t) \le 1.23 \\ -0.169 & \text{if } 1.23 < \varepsilon(n,t) \le 1.5 \\ -0.35 & \text{if } 1.5 < \varepsilon(n,t) \le 1.95 \\ -0.559 & \text{if } 1.95 < \varepsilon(n,t) \le 2.8 \\ -0.785 & \text{if } 2.8 < \varepsilon(n,t) \le 4.5 \\ -0.629 & \text{if } 4.5 < \varepsilon(n,t) \le 6.2 \\ -1.892 & \text{otherwise} \end{cases} \qquad f_{23}(n,t) = \begin{cases} -0.018 & \text{if } \varepsilon(n,t) \le 1.065 \\ -0.065 & \text{if } 1.065 < \varepsilon(n,t) \le 1.23 \\ -0.092 & \text{if } 1.23 < \varepsilon(n,t) \le 1.5 \\ -0.096 & \text{if } 1.5 < \varepsilon(n,t) \le 1.95 \\ -0.114 & \text{if } 1.95 < \varepsilon(n,t) \le 2.8 \\ -0.097 & \text{if } 2.8 < \varepsilon(n,t) \le 4.5 \\ -0.082 & \text{if } 4.5 < \varepsilon(n,t) \le 6.2 \\ -0.055 & \text{otherwise} \end{cases}$$

Brightness coefficients

$$F_1(n,t) = \max\left[0, f_{11}(n,t) + f_{12}(n,t)\,\Delta(n,t) + \pi\,\frac{(90\text{ deg} - \alpha_s(n,t))}{180\text{ deg}}\,f_{13}(n,t)\right]$$

$$F_2(n,t) = \max\left[0, f_{21}(n,t) + f_{22}(n,t)\,\Delta(n,t) + \pi\,\frac{(90\text{ deg} - \alpha_s(n,t))}{180\text{ deg}}\,f_{23}(n,t)\right]$$

Sky diffuse illuminance on a tilted surface

$$E_{ds}(n,t) = E_{dh}(n,t)\left[\left(1 - F_1(n,t)\right)\left(\frac{1 + \cos(\beta_w)}{2}\right) + F_1(n,t)\,\frac{a_P(n,t)}{b_P(n,t)} + F_2(n,t)\,\sin(\beta_w)\right]$$

Ground-reflected illuminance on a tilted surface

$$E_{dg}(n,t) = E_h(n,t)\,\rho_g(n,t)\,\frac{1 - \cos(\beta_w)}{2}$$

Total diffuse illuminance on a tilted surface

$$E_d(n,t) = E_{ds}(n,t) + E_{dg}(n,t)$$

The total incident illuminance on a tilted surface

$$E(n,t) = E_b(n,t) + E_{ds}(n,t) + E_{dg}(n,t)$$

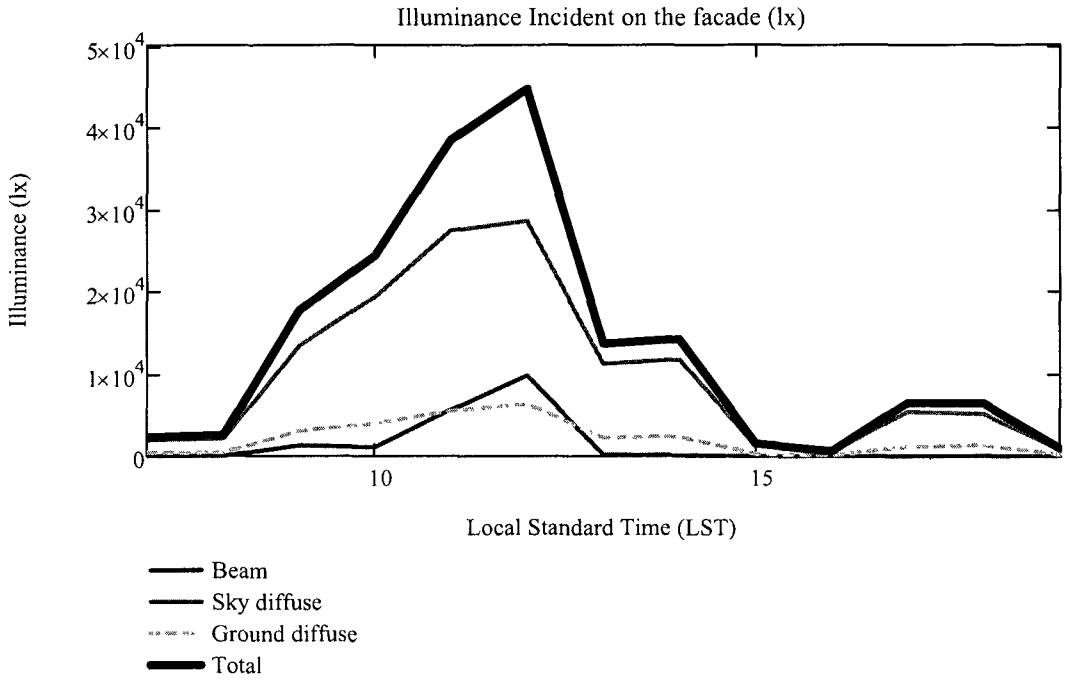

Switch from function of time to time array:

Solar Illuminance:

$E_{b_t} := E_b(n,t)$

$E_{ds_t} := E_{ds}(n,t)$

$E_{dg_t} := E_{dg}(n,t)$

$E_{d_t} := E_d(n,t)$

$E_t := E(n,t)$

Appendix D:

Bottom-up Shade Control Strategies

Control strategy of the bottom-up shade

Visible transmittance of a double glazing window

Note ASHRAE 17a LE CLR (3mm, Low-e Double Glazing, e = 0 2 on surface 2)

$\theta'(n,t) = \theta(n,t)\,\frac{180}{\pi}$ transformation from radians to degrees

Direct

$$\tau_{b_t} = \begin{cases} \dfrac{\left(\begin{array}{l} -0\ 0015\ \theta'(n,t)^3 \\ +0\ 0654\ \theta'(n,t)^2 - 0\ 7247\ \theta'(n,t) + 589\ 11 \end{array}\right)}{10^3} & \text{if } \theta'(n,t) \le 90 \\ 0 \quad \text{otherwise} \end{cases}$$

Diffuse

$\tau_{d_t} = 0\ 5$

Luminous exitance of the facade

$$E_{facadeb_t} = \begin{cases} 0 \text{lx} \quad \text{if } I_t \le 120\ \frac{W}{m^2} \\ \tau_{b_t}\, E_{b_t} \quad \text{if } I_t > 120\ \frac{W}{m^2} \end{cases}$$ direct component

$$E_{facaded_t} = \begin{cases} \tau_{b_t}\, E_{b_t} + \tau_{d_t}\, E_{d_t} \quad \text{if } I_t \le 120\ \frac{W}{m^2} \\ \tau_{d_t}\, E_{d_t} \quad \text{if } I_t > 120\ \frac{W}{m^2} \end{cases}$$ diffuse component

$E_{incident_t} = E_{facadeb_t} + E_{facaded_t}$

Irradiation exitance of the facade

$$I_{facadeb_t} = \begin{cases} 0 \text{lx} \quad \text{if } I_t \le 120\ \frac{W}{m^2} \\ \tau_{b_t}\, I_{b_t} \quad \text{if } I_t > 120\ \frac{W}{m^2} \end{cases}$$ direct component

$$I_{facaded_t} = \begin{cases} \tau_{b_t}\, I_{b_t} + \tau_{d_t}\, I_{d_t} \quad \text{if } I_t \le 120\ \frac{W}{m^2} \\ \tau_{d_t}\, I_{d_t} \quad \text{if } I_t > 120\ \frac{W}{m^2} \end{cases}$$ diffuse component

$I_{incident_t} = I_{facadeb_t} + I_{facaded_t}$

Position of the shade to reduce glare

$$X_t = \begin{cases} (D_{rm} - 1.00m)\tan(d(n,t)) - H_{sp} + H_{setpoint} & \text{if } d(n,t) > 0 \\ H_{facade} - 10^{-3}m & \text{otherwise} \end{cases}$$

$$\Psi'_{shade_t} = \begin{cases} X_t & \text{if } 0 < X_t < H_{facade} \\ H_{facade} - 10^{-3}m & \text{otherwise} \end{cases}$$

$$\Psi_{shade_t} = \begin{cases} H_{facade} - 10^{-3}m & \text{if } t \geq 21 \vee t \leq 6 \\ \Psi'_{shade_t} & \text{otherwise} \end{cases}$$

Correction factor due to frame shading

$$Y''_{frame_t} = \begin{cases} D_{fr}\tan(d(n,t)) & \text{if } d(n,t) > 0 \\ 10^{-3}m & \text{otherwise} \end{cases}$$

$$Y'_{frame_t} = \begin{cases} Y''_{frame_t} & \text{if } \left(0 < Y''_{frame_t} < H_{facade}\right) \\ 10^{-3}m & \text{if } \left(Y''_{frame_t} \leq 0\right) \\ H_{facade} - 10^{-3}m & \text{otherwise} \end{cases}$$

$$Y_{frame_t} = H_{facade} - Y'_{frame_t}$$

height of the sunlit part of the facade due to frame shading

$$H_{FGZshade_t} = \begin{cases} \min\left(\Psi_{shade_t}, Y_{frame_t}\right) & \text{if } I_t > 120\ \frac{W}{m^2} \\ 10^{-3}m & \text{otherwise} \end{cases}$$

minimum position of the bottom-up shade to reduce glare

$$H_{AWIshade_t} = 0.97\left(1 - \exp\left(\frac{-I_{incident_t}}{50\ \frac{W}{m^2}}\right)\right)H_{facade}$$

position of the bottom-up shade due to acceptable workplane illuminance

$$H_{shade_t} = \max\left(H_{FGZshade_t}, H_{AWIshade_t}\right)$$

$$H_{shade_t} = \begin{cases} 10^{-3}\,m & \text{if } H_{shade_t} \le 0.01\,H_{facade} \\ 0.05\,H_{facade} & \text{if } 0.01\,H_{facade} < H_{shade_t} \le 0.05\,H_{facade} \\ 0.10\,H_{facade} & \text{if } 0.05\,H_{facade} < H_{shade_t} \le 0.10\,H_{facade} \\ 0.15\,H_{facade} & \text{if } 0.10\,H_{facade} < H_{shade_t} \le 0.15\,H_{facade} \\ 0.20\,H_{facade} & \text{if } 0.15\,H_{facade} < H_{shade_t} \le 0.20\,H_{facade} \\ 0.25\,H_{facade} & \text{if } 0.20\,H_{facade} < H_{shade_t} \le 0.25\,H_{facade} \\ 0.30\,H_{facade} & \text{if } 0.25\,H_{facade} < H_{shade_t} \le 0.30\,H_{facade} \\ 0.35\,H_{facade} & \text{if } 0.30\,H_{facade} < H_{shade_t} \le 0.35\,H_{facade} \\ 0.40\,H_{facade} & \text{if } 0.35\,H_{facade} < H_{shade_t} \le 0.40\,H_{facade} \\ 0.45\,H_{facade} & \text{if } 0.40\,H_{facade} < H_{shade_t} \le 0.45\,H_{facade} \\ 0.50\,H_{facade} & \text{if } 0.45\,H_{facade} < H_{shade_t} \le 0.50\,H_{facade} \\ 0.55\,H_{facade} & \text{if } 0.50\,H_{facade} < H_{shade_t} \le 0.55\,H_{facade} \\ 0.60\,H_{facade} & \text{if } 0.55\,H_{facade} < H_{shade_t} \le 0.60\,H_{facade} \\ 0.65\,H_{facade} & \text{if } 0.60\,H_{facade} < H_{shade_t} \le 0.65\,H_{facade} \\ 0.70\,H_{facade} & \text{if } 0.65\,H_{facade} < H_{shade_t} \le 0.70\,H_{facade} \\ 0.75\,H_{facade} & \text{if } 0.70\,H_{facade} < H_{shade_t} \le 0.75\,H_{facade} \\ 0.80\,H_{facade} & \text{if } 0.75\,H_{facade} < H_{shade_t} \le 0.80\,H_{facade} \\ 0.85\,H_{facade} & \text{if } 0.80\,H_{facade} < H_{shade_t} \le 0.85\,H_{facade} \\ 0.90\,H_{facade} & \text{if } 0.85\,H_{facade} < H_{shade_t} \le 0.90\,H_{facade} \\ 0.95\,H_{facade} & \text{if } 0.90\,H_{facade} < H_{shade_t} \le 0.95\,H_{facade} \\ H_{facade} - 10^{-3}\,m & \text{if } H_{shade_t} > 0.95\,H_{facade} \end{cases}$$

Distance of the unshaded part of the bottom-up shade from the horizontal frames

Note The distance is taken from 1) The eastern horizontal frame for $H(n,t)<0$
2) The western horizontal frame for $H(n,t)>0$

$$X'_{frame_t} = \begin{cases} \left| D_{fr} \tan(\gamma(n,t)) \right| & \text{if } d(n,t) > 0 \\ 0 & \text{otherwise} \end{cases}$$

$$X_{frame_t} = \begin{cases} X'_{frame_t} & \text{if } 0 \le X'_{frame_t} \le W_{facade} \\ W_{facade} & \text{otherwise} \end{cases}$$

$$W_{unshaded_t} := W_{facade} - X_{frame_t}$$ ...width of the sunlit part of the facade due to frame shading

Luminous exitance of the shade (correction due to frame shading):

Sunlit part of the shade:

$$A_{sunlitshade_t} := if\left(H_{shade_t} > Y_{frame_t}, Y_{frame_t} \cdot W_{unshaded_t}, H_{shade_t} \cdot W_{unshaded_t}\right)$$

Shaded part of the shade:

$$A_{shadedshade_t} := H_{shade_t} \cdot W_{facade} - A_{sunlitshade_t}$$

$$E_{shade_t} := \frac{\left[\tau_{shade} \cdot \left[\frac{A_{sunlitshade_t} \cdot \left(E_{facaded_t} + E_{facadeb_t}\right) + A_{shadedshade_t} \cdot E_{facaded_t}}{\left(H_{shade_t} \cdot W_{facade}\right)}\right]\right]}{1 - \rho_{facade} \cdot \rho_{shadeout}}$$

Appendix E:

Determination of Room View Factors

Room View Factors

$D_{facadetop} := H_{rm} - H_{facade} - H_{sp}$ ...distance from top of the facade to ceiling

$D_{shadetop_t} := H_{rm} - H_{sp} - H_{shade_t}$ ...distance from top of the shade to ceiling

View Factors Between Internal Surfaces

The view factors for the room below are determined after calculating first the view factors between two rectangular finite surfaces inclined at 90 degrees to each other with one common surface as follows:

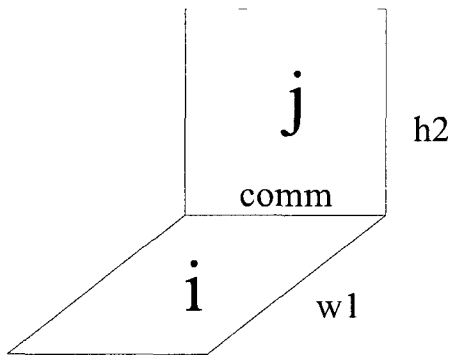

Define the following intermediate variables for calculating view factor from surface i to surface j:

$w = \frac{w1}{comm}$ $h = \frac{h2}{comm}$

$A(h,w) := h^2 + w^2$ $B(w) := 1 + w^2$

$C(h) := 1 + h^2$ $D(h,w) := 1 + \left(h^2 + w^2\right)$

$E(w) := w^2$ $G(h) := h^2$

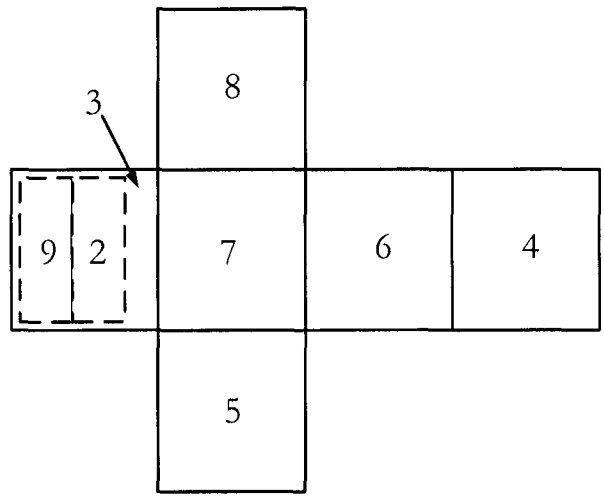

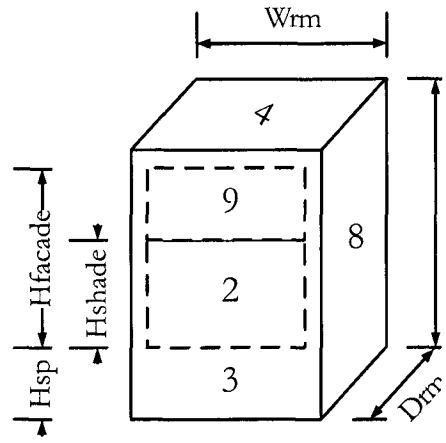

Legend

1 South fenestration (2+3+9)
2 Shading device
3 South Wall
4 Ceiling
5 East Wall
6 North Wall
7 Floor
8 East Wall
9 Unshaded facade

View factor F_{ij} from i to j

$$F_{ij}(w,h) = \frac{\left(w \operatorname{atan}\left(\frac{1}{w}\right) + h \operatorname{atan}\left(\frac{1}{h}\right)\right) - \sqrt{A(h,w)} \operatorname{atan}\left(\frac{1}{\sqrt{A(h,w)}}\right) + 0.25 \ln\left[\left(\frac{E(w)\, D(h,w)}{B(w)\, A(h,w)}\right)^{E(w)} \left(\frac{G(h)\, D(h,w)}{C(h)\, A(h,w)}\right)^{G(h)} \frac{B(w)\, C(h)}{D(h,w)}\right]}{\pi\, w}$$

The other view factors between the room surfaces are calculated by applying the following principles

1. Reciprocity $A_i F_{i,j} = A_j F_{j,i}$

2. Symmetry, e g $F_{7,5} = F_{7,8}$

3. Energy conservation $\sum_j F_{i,j} = 1$ (for any surface i)

Area of room surfaces

$A_1 = W_{rm} H_{rm}$ $A_5 = D_{rm} H_{rm}$ $A_8 = A_5$

$A_{2_t} = W_{facade} H_{shade_t}$ $A_6 = A_1$ $A_{9_t} = W_{facade}\left(H_{facade} - H_{shade_t}\right)$

$A_4 = W_{rm} D_{rm}$ $A_7 = A_4$ $A_{3_t} = A_1 - A_{2_t} - A_{9_t}$

Calculate view factors

$w1 = H_{rm}$ $\quad h2 = D_{rm}$ $\quad comm = W_{rm}$

$w = \frac{w1}{comm}$ $\quad h = \frac{h2}{comm}$

$F_{67} = F_{IJ}(w,h)$ $\quad F_{76} = A_6 \frac{F_{67}}{A_7}$

$F_{64} = F_{67}$ $\quad F_{46} = F_{76}$ $\quad F_{41} = F_{46}$

$F_{14} = F_{67}$ $\quad F_{17} = F_{67}$ $\quad F_{71} = F_{46}$

$w1 = W_{rm}$ $\quad h2 = D_{rm}$ $\quad comm = H_{rm}$

$w = \frac{w1}{comm}$ $\quad h = \frac{h2}{comm}$

$F_{65} = F_{IJ}(w,h)$ $\quad F_{56} = A_6 \frac{F_{65}}{A_5}$ $\quad F_{68} = F_{65}$

$F_{86} = F_{56}$ $\quad F_{15} = F_{68}$ $\quad F_{51} = F_{86}$

$F_{18} = F_{68}$ $\quad F_{81} = F_{86}$

$w1 = H_{rm}$ $\quad h2 = W_{rm}$ $\quad comm = D_{rm}$

$w = \frac{w1}{comm}$ $\quad h = \frac{h2}{comm}$

$F_{87} = F_{IJ}(w,h)$ $\quad F_{78} = A_8 \frac{F_{87}}{A_7}$ $\quad F_{57} = F_{87}$

$F_{75} = F_{78}$ $\quad F_{45} = F_{78}$ $\quad F_{54} = F_{87}$

$F_{84} = F_{87}$ $\quad F_{48} = F_{78}$

$F_{16} = 1 - 2\,F_{18} - 2\,F_{14}$ $\quad F_{61} = F_{16}$

$F_{58} = 1 - 2\,F_{54} - 2\,F_{56}$ $\quad F_{85} = F_{58}$

$F_{47} = 1 - 2\,F_{48} - 2\,F_{46}$ $\quad F_{74} = F_{47}$

View factors between surfaces 2, 9 and surface 7.

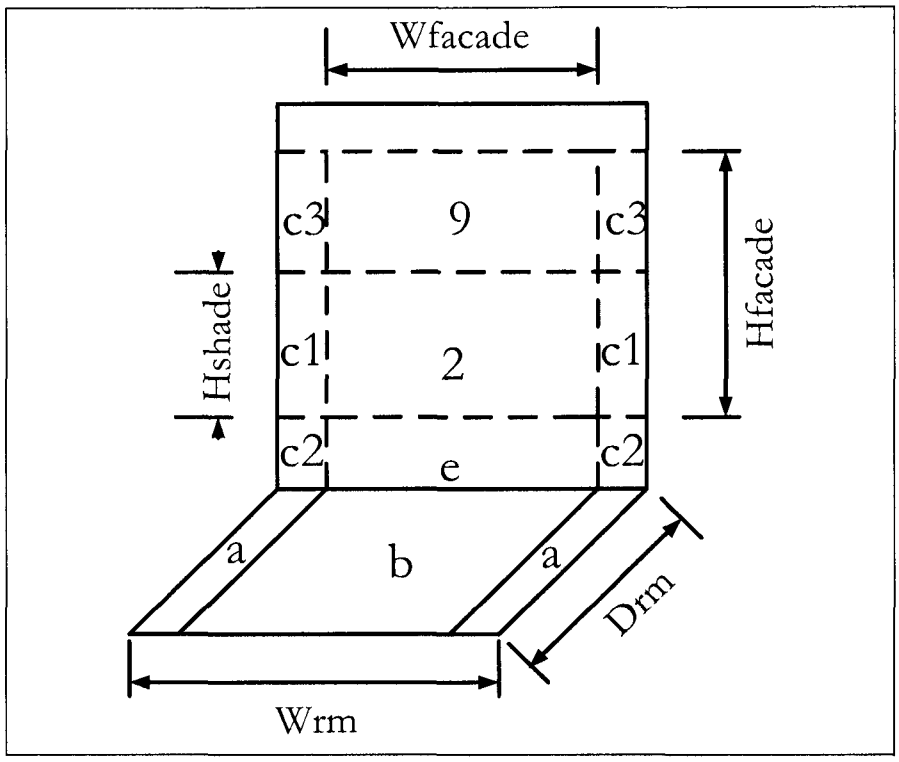

$Ab = W_{facade}\, D_{rm}$ $\qquad DIS = \dfrac{W_{rm} - W_{facade}}{2}$

$Aa = DIS\, D_{rm}$ $\qquad Aab = D_{rm}\left(DIS + W_{facade}\right)$

$w1 = D_{rm}$ $\qquad h2 = H_{sp}$ $\qquad comm = W_{facade}$

$w = \dfrac{w1}{comm}$ $\qquad h = \dfrac{h2}{comm}$

$Fb\_e = F_{IJ}(w,h)$

$w1 = D_{rm}$ $\qquad h2_t = H_{shade_t} + H_{sp}$ $\qquad comm = W_{facade}$

$w = \dfrac{w1}{comm}$ $\qquad h_t = \dfrac{h2_t}{comm}$

$Fb\_2e_t = F_{IJ}\left(w, h_t\right)$

$w1 = D_{rm}$ $\qquad h2_t = H_{facade} + H_{sp}$ $\qquad comm = W_{facade}$

$w = \dfrac{w1}{comm}$ $\qquad h_t = \dfrac{h2_t}{comm}$

$Fb\_29e_t = F_{IJ}\left(w, h_t\right)$

$w1 = D_{rm}$ $\quad h2 = H_{sp}$ $\quad comm = DIS$

$$w = \frac{w1}{comm} \qquad h = \frac{h2}{comm}$$

$Fa\_c2 = F_{IJ}(w,h)$

$w1 = D_{rm}$ $\quad h2_t = H_{shade_t} + H_{sp}$ $\quad comm = DIS$

$$w = \frac{w1}{comm} \qquad h_t = \frac{h2_t}{comm}$$

$Fa\_c1c2_t = F_{IJ}(w,h_t)$

$w1 = D_{rm}$ $\quad h2 = H_{facade} + H_{sp}$ $\quad comm = DIS$

$$w = \frac{w1}{comm} \qquad h = \frac{h2}{comm}$$

$Fa\_c1c2c3 = F_{IJ}(w,h)$

$w1 = D_{rm}$ $\quad h2 = H_{sp}$ $\quad comm = W_{facade} + DIS$

$$w = \frac{w1}{comm} \qquad h = \frac{h2}{comm}$$

$Fab\_c2e = F_{IJ}(w,h)$

$w1 = D_{rm}$ $\quad h2_t = H_{shade_t} + H_{sp}$ $\quad comm = W_{facade} + DIS$

$$w = \frac{w1}{comm} \qquad h_t = \frac{h2_t}{comm}$$

$Fab\_c1c2e2_t = F_{IJ}(w,h_t)$

$w1 = D_{rm}$ $\quad h2 = H_{facade} + H_{sp}$ $\quad comm = W_{facade} + DIS$

$$w = \frac{w1}{comm} \qquad h = \frac{h2}{comm}$$

$Fab\_c1c2c3e29 = F_{IJ}(w,h)$

$$F2\_b_t = \left(Fb\_2e_t - Fb\_e\right)\frac{Ab}{A2_t}$$

$$F9\_b_t = \left(Fb\_29e_t - Fb\_2e_t\right)\frac{Ab}{A9_t}$$

$$Fa\_2e_t = \frac{Aab\ Fab\_c1c2e2_t - Aa\ Fa\_c1c2_t - Ab\ Fb\_2e_t}{2\ Aa}$$

$$Fa\_29e_t = \frac{Aab\ Fab\_c1c2c3e29 - Aa\ Fa\_c1c2c3 - Ab\ Fb\_29e_t}{2\ Aa}$$

$$Fa\_e_t = \frac{Aab\ Fab\_c2e - Aa\ Fa\_c2 - Ab\ Fb\_e}{2\ Aa}$$

$$F2\_a_t = \left(Fa\_2e_t - Fa\_e_t\right)\frac{Aa}{A2_t}$$

$$F9\_a_t = \left(Fa\_29e_t - Fa\_2e_t\right)\frac{Aa}{A9_t}$$

$$F27_t = 2\ F2\_a_t + F2\_b_t \qquad F72_t = A2_t\frac{F27_t}{A7}$$

$$F97_t = 2\ F9\_a_t + F9\_b_t \qquad F79_t = A9_t\frac{F97_t}{A7}$$

View factors between surfaces 2, 9 and surface 4.

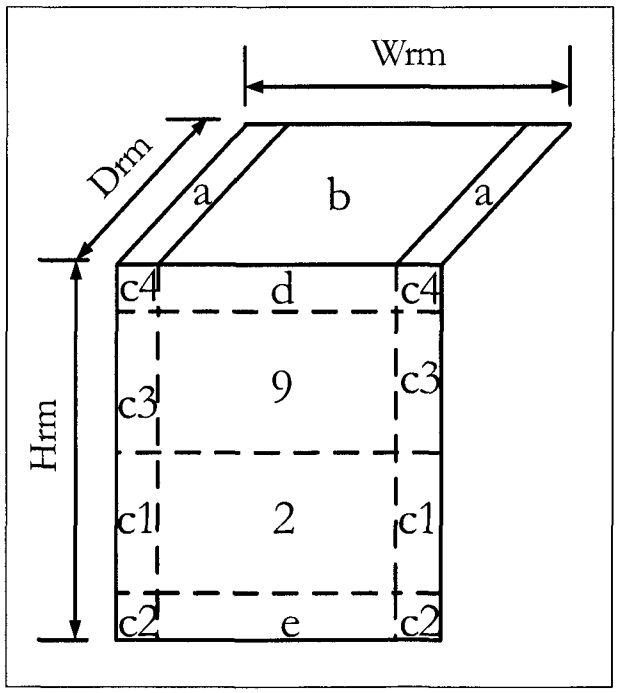

$w1 = D_{rm}$ $\quad h2 = D_{facadetop}$ $\quad comm = W_{facade}$

$$w = \frac{w1}{comm} \qquad h = \frac{h2}{comm}$$

$Fb\_d = F_{IJ}(w, h)$

$w1 = D_{rm}$ $\quad h2_t = D_{shadetop_t}$ $\quad comm = W_{facade}$

$$w = \frac{w1}{comm} \qquad h_t = \frac{h2_t}{comm}$$

$Fb\_9d_t = F_{IJ}(w, h_t)$

$w1 = D_{rm}$ $\quad h2_t = H_{shade_t} + D_{shadetop_t}$ $\quad comm = W_{facade}$

$$w = \frac{w1}{comm} \qquad h_t = \frac{h2_t}{comm}$$

$Fb\_29d_t = F_{IJ}(w, h_t)$

$w1 = D_{rm}$ $\quad h2 = D_{facadetop}$ $\quad comm = DIS$

$$w = \frac{w1}{comm} \qquad h = \frac{h2}{comm}$$

$Fa\_c4 = F_{IJ}(w, h)$

$w1 = D_{rm}$ $\quad h2_t = D_{shadetop_t}$ $\quad comm = DIS$

$$w = \frac{w1}{comm} \qquad h_t = \frac{h2_t}{comm}$$

$Fa\_c3c4_t = F_{IJ}(w, h_t)$

$w1 = D_{rm}$ $\quad h2_t = H_{shade_t} + D_{shadetop_t}$ $\quad comm = DIS$

$$w = \frac{w1}{comm} \qquad h_t = \frac{h2_t}{comm}$$

$Fa\_c1c3c4_t = F_{IJ}(w, h_t)$

$wl = D_{rm}$ $\quad h2 = D_{facadetop}$ $\quad comm = W_{facade} + DIS$

$$w = \frac{wl}{comm} \qquad h = \frac{h2}{comm}$$

$$Fab\_c4d = F_{IJ}(w,h)$$

$wl = D_{rm}$ $\quad h2_t = D_{shadetop_t}$ $\quad comm = W_{facade} + DIS$

$$w = \frac{wl}{comm} \qquad h_t = \frac{h2_t}{comm}$$

$$Fab\_9c3c4d_t = F_{IJ}(w,h_t)$$

$wl = D_{rm}$ $\quad h2_t = H_{shade_t} + D_{shadetop_t}$ $\quad comm = W_{facade} + DIS$

$$w = \frac{wl}{comm} \qquad h_t = \frac{h2_t}{comm}$$

$$Fab\_29c1c3c4d_t = F_{IJ}(w,h_t)$$

$$F9\_b_t = (Fb\_9d_t - Fb\_d)\frac{Ab}{A9_t}$$

$$F2\_b_t = (Fb\_29d_t - Fb\_9d_t)\frac{Ab}{A2_t}$$

$$Fa\_9d_t = \frac{Aab\ Fab\_9c3c4d_t - Aa\ Fa\_c3c4_t - Ab\ Fb\_9d_t}{2\ Aa}$$

$$Fa\_29d_t = \frac{Aab\ Fab\_29c1c3c4d_t - Aa\ Fa\_c1c3c4_t - Ab\ Fb\_29d_t}{2\ Aa}$$

$$Fa\_d = \frac{Aab\ Fab\_c4d - Aa\ Fa\_c4 - Ab\ Fb\_d}{2\ Aa}$$

$$F9\_a_t = (Fa\_9d_t - Fa\_d)\frac{Aa}{A9_t}$$

$$F2\_a_t = (Fa\_29d_t - Fa\_9d_t)\frac{Aa}{A2_t}$$

$F_{24_t} := 2 \cdot F2\_a_t + F2\_b_t$ $\quad F_{42_t} := A_{2_t} \cdot \frac{F_{24_t}}{A_4}$

$F_{94_t} := 2 \cdot F9\_a_t + F9\_b_t$ $\quad F_{49_t} := A_{9_t} \cdot \frac{F_{94_t}}{A_4}$

View factors between surfaces 2, 9 and surfaces 5, 8.

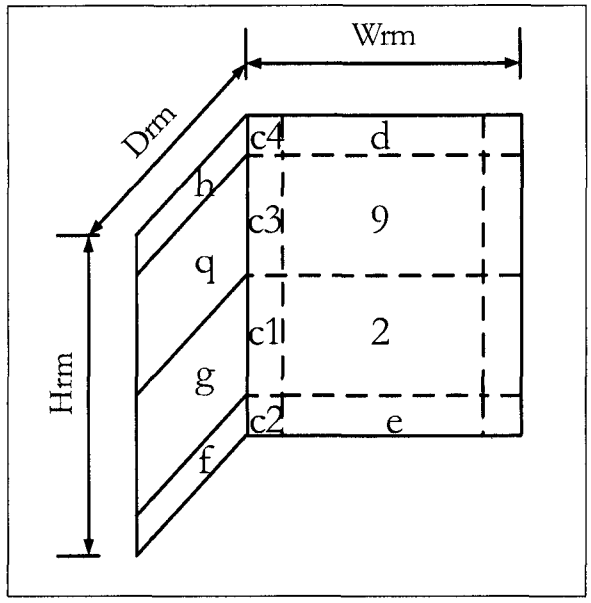

$Ad := W_{facade} \cdot D_{facadetop}$ $\quad Ae := W_{facade} \cdot H_{sp}$ $\quad Ag_t := D_{rm} \cdot H_{shade_t}$

$Af := H_{sp} \cdot D_{rm}$ $\quad Ac1_t := H_{shade_t} \cdot DIS$ $\quad Ac2 := H_{sp} \cdot DIS$

$Ah := D_{facadetop} \cdot D_{rm}$ $\quad Ac3_t := DIS \cdot \left(H_{facade} - H_{shade_t}\right)$

$Agf_t := Ag_t + Af$ $\quad Aq_t := D_{rm} \cdot \left(H_{facade} - H_{shade_t}\right)$ $\quad Aqh_t := Aq_t + Ah$

$Aqgh_t := Aq_t + Ag_t + Ah$ $\quad Aqgf_t := Ag_t + Af + Aq_t$ $\quad Aqg_t := Ag_t + Aq_t$

$w1 := D_{rm}$ $\quad h2 := W_{facade} + DIS$ $\quad comm_t := H_{shade_t}$

$w_t := \frac{w1}{comm_t}$ $\quad h_t := \frac{h2}{comm_t}$

$Fg\_2c1_t := Fij\left(w_t, h_t\right)$

$w1 := D_{rm}$ $h2 := W_{facade} + DIS$ $comm_t := H_{facade} - H_{shade_t}$

$w_t := \frac{w1}{comm_t}$ $h_t := \frac{h2}{comm_t}$

$Fq\_9c3_t := Fij(w_t, h_t)$

$w1 := D_{rm}$ $h2 := DIS$ $comm_t := H_{shade_t}$

$w_t := \frac{w1}{comm_t}$ $h_t := \frac{h2}{comm_t}$

$Fg\_c1_t := Fij(w_t, h_t)$

$w1 := D_{rm}$ $h2 := DIS$ $comm_t := H_{facade} - H_{shade_t}$

$w_t := \frac{w1}{comm_t}$ $h_t := \frac{h2}{comm_t}$

$Fq\_c3_t := Fij(w_t, h_t)$

$w1 := D_{rm}$ $h2 := DIS$ $comm := D_{facadetop}$

$w := \frac{w1}{comm}$ $h := \frac{h2}{comm}$

$Fh\_c4 := Fij(w, h)$

$w1 := D_{rm}$ $h2 := W_{facade} + DIS$ $comm := D_{facadetop}$

$w := \frac{w1}{comm}$ $h := \frac{h2}{comm}$

$Fh\_dc4 := Fij(w, h)$

$w1 := D_{rm}$ $h2 := W_{facade} + DIS$ $comm_t := H_{facade} - H_{shade_t} + D_{facadetop}$

$w_t := \frac{w1}{comm_t}$ $h_t := \frac{h2}{comm_t}$

$Fqh\_c3c4d9_t := Fij(w_t, h_t)$

$w1 = D_{rm}$ $\quad h2 = W_{facade} + DIS$ $\quad comm = H_{facade} + D_{facadetop}$

$$w = \frac{w1}{comm} \qquad h = \frac{h2}{comm}$$

Fqgh_c1c3c4d29 = Fij(w,h)

$w1 = D_{rm}$ $\quad h2 = DIS$ $\quad comm_t = H_{facade} - H_{shade_t} + D_{facadetop}$

$$w_t = \frac{w1}{comm_t} \qquad h_t = \frac{h2}{comm_t}$$

$$Fqh\_c3c4_t = Fij(w_t, h_t)$$

$w1 = D_{rm}$ $\quad h2 = DIS$ $\quad comm = H_{facade} + D_{facadetop}$

$$w = \frac{w1}{comm} \qquad h = \frac{h2}{comm}$$

Fqhg_c1c3c4 = Fij(w,h)

$w1 = D_{rm}$ $\quad h2 = W_{facade} + DIS$ $\quad comm = H_{facade}$

$$w = \frac{w1}{comm} \qquad h = \frac{h2}{comm}$$

Fqg_29c1c3 = Fij(w,h) $\qquad$ Fqg_29c1c3 = 0 153

$w1 = D_{rm}$ $\quad h2 = DIS$ $\quad comm_t = H_{shade_t}$

$$w_t = \frac{w1}{comm_t} \qquad h_t = \frac{h2}{comm_t}$$

$$Fg\_c1_t = Fij(w_t, h_t)$$

$$F2\_g_t = \left(Fg\_2c1_t - Fg\_c1_t\right) \frac{Ag_t}{A2_t}$$

$$F9\_q_t = \left(Fq\_9c3_t - Fq\_c3_t\right) \frac{Aq_t}{A9_t}$$

$$Fh\_9c3_t = \frac{Aqh_t\ Fqh\_c3c4d9_t - Ah\ Fh\_dc4 - Aq_t\ Fq\_9c3_t}{2\ Ah}$$

$$Fh\_c3_t = \frac{Aqh_t\ Fqh\_c3c4_t - Ah\ Fh\_c4 - Aq_t\ Fq\_c3_t}{2\ Ah}$$

$$Fhq\_2c1_t = \frac{Aqgh_t\ Fqgh\_c1c3c4d29 - Aqh_t\ Fqh\_c3c4d9_t - Ag_t\ Fg\_2c1_t}{2\ Aqh_t}$$

$$Fqh\_c1_t = \frac{Aqgh_t\ Fqhg\_c1c3c4 - Aqh_t\ Fqh\_c3c4_t - Ag_t\ Fg\_c1_t}{2\ Aqh_t}$$

$$F9\_h_t = \left(Fh\_9c3_t - Fh\_c3_t\right) \frac{Ah}{A9_t}$$

$$F2\_qh_t = \left(Fhq\_2c1_t - Fqh\_c1_t\right) \frac{Aqh_t}{A2_t}$$

$w1 = D_{rm}$ $\quad$ $h2 = DIS$ $\quad$ $comm = H_{sp}$

$$w = \frac{w1}{comm} \qquad h = \frac{h2}{comm}$$

$Ff\_c2 = F_{IJ}(w,h)$

$w1 = D_{rm}$ $\quad$ $h2 = W_{facade} + DIS$ $\quad$ $comm = H_{sp}$

$$w = \frac{w1}{comm} \qquad h = \frac{h2}{comm}$$

$Ff\_ec2 = F_{IJ}(w,h)$

$w1 = D_{rm}$ $\quad$ $h2 = W_{facade} + DIS$ $\quad$ $comm_t = H_{shade_t} + H_{sp}$

$$w_t = \frac{w1}{comm_t} \qquad h_t = \frac{h2}{comm_t}$$

$Fgf\_c1c2e2_t = F_{IJ}(w_t, h_t)$

$w1 = D_{rm}$ $\quad h2 = W_{facade} + DIS$ $\quad comm = H_{facade} + H_{sp}$

$$w = \frac{w1}{comm} \qquad h = \frac{h2}{comm}$$

$Fqgf\_c1c2c3e29 = F_{IJ}(w,h)$

$w1 = D_{rm}$ $\quad h2 = DIS$ $\quad comm_t = H_{shade_t} + H_{sp}$

$$w_t = \frac{w1}{comm_t} \qquad h_t = \frac{h2}{comm_t}$$

$Fgf\_c1c2_t = F_{IJ}(w_t, h_t)$

$w1 = D_{rm}$ $\quad h2 = DIS$ $\quad comm = H_{facade} + H_{sp}$

$$w = \frac{w1}{comm} \qquad h = \frac{h2}{comm}$$

$Fqgf\_c1c2c3 = F_{IJ}(w,h)$

$$Ff\_2c1_t = \frac{Agf_t\, Fgf\_c1c2e2_t - Af\, Ff\_ec2 - Ag_t\, Fg\_2c1_t}{2\, Af}$$

$$Ff\_c1_t = \frac{Agf_t\, Fgf\_c1c2_t - Af\, Ff\_c2 - Ag_t\, Fg\_c1_t}{2\, Af}$$

$$F2\_f_t = \left(Ff\_2c1_t - Ff\_c1_t\right)\frac{Af}{A_{2_t}}$$

$$Ffg\_9c3_t = \frac{Aqgf_t\, Fqgf\_c1c2c3e29 - Agf_t\, Fgf\_c1c2e2_t - Aq_t\, Fq\_9c3_t}{2\, Agf_t}$$

$$Ffg\_c3_t = \frac{Aqgf_t\, Fqgf\_c1c2c3 - Agf_t\, Fgf\_c1c2_t - Aq_t\, Fq\_c3_t}{2\, Agf_t}$$

$$F9\_fg_t = \left(Ffg\_9c3_t - Ffg\_c3_t\right)\frac{Agf_t}{A_{9_t}}$$

$$F_{25_t} = F2\_qh_t + F2\_g_t + F2\_f_t \qquad F_{52_t} = A_{2_t} \frac{F_{25_t}}{A_5}$$

$$F_{28_t} = F_{25_t} \qquad F_{82_t} = F_{52_t}$$

$$F_{26_t} = 1 - 2\,F_{25_t} - F_{27_t} - F_{24_t} \qquad F_{62_t} = F_{26_t} \frac{A_{2_t}}{A_6}$$

$$F_{95_t} = F9\_h_t + F9\_q_t + F9\_fg_t \qquad F_{59_t} = F_{95_t} \frac{A_{9_t}}{A_5}$$

$$F_{98_t} = F_{95_t} \qquad F_{89_t} = F_{59_t}$$

$$F_{96_t} = 1 - 2\,F_{95_t} - F_{97_t} - F_{94_t} \qquad F_{69_t} = F_{96_t} \frac{A_{9_t}}{A_6}$$

$$F_{43_t} = F_{41} - F_{42_t} - F_{49_t} \qquad F_{73_t} = F_{71} - F_{72_t} - F_{79_t}$$

$$F_{53_t} = F_{51} - F_{52_t} - F_{59_t} \qquad F_{83_t} = F_{81} - F_{82_t} - F_{89_t}$$

$$F_{63_t} = F_{61} - F_{62_t} - F_{69_t} \qquad F_{93_t} = 0$$

$$F_{34_t} = A_4 \frac{F_{43_t}}{A_{3_t}} \qquad F_{36_t} = A_6 \frac{F_{63_t}}{A_{3_t}} \qquad F_{38_t} = A_8 \frac{F_{83_t}}{A_{3_t}}$$

$$F_{35_t} = A_5 \frac{F_{53_t}}{A_{3_t}} \qquad F_{37_t} = A_7 \frac{F_{73_t}}{A_{3_t}} \qquad F_{39_t} = A_{9_t} \frac{F_{93_t}}{A_{3_t}}$$

More on View factors

$$F_{11} = 0 \qquad F_{44} = 0 \qquad F_{77} = 0 \qquad F_{19} = 0$$

$$F_{22} = 0 \qquad F_{55} = 0 \qquad F_{88} = 0 \qquad F_{91} = 0$$

$$F_{33} = 0 \qquad F_{66} = 0 \qquad F_{99} = 0 \qquad F_{29} = 0$$

$$F_{12} = 0 \qquad F_{21} = 0 \qquad F_{31} = 0 \qquad F_{92} = 0$$

$$F_{13} = 0 \qquad F_{23} = 0 \qquad F_{32} = 0$$

$$F_{\sim\sim t} := \begin{pmatrix} F_{22} & F_{23} & F_{24_t} & F_{25_t} & F_{26_t} & F_{27_t} & F_{28_t} & F_{29} \\ F_{32} & F_{33} & F_{34_t} & F_{35_t} & F_{36_t} & F_{37_t} & F_{38_t} & F_{39_t} \\ F_{42_t} & F_{43_t} & F_{44} & F_{45} & F_{46} & F_{47} & F_{48} & F_{49_t} \\ F_{52_t} & F_{53_t} & F_{54} & F_{55} & F_{56} & F_{57} & F_{58} & F_{59_t} \\ F_{62_t} & F_{63_t} & F_{64} & F_{65} & F_{66} & F_{67} & F_{68} & F_{69_t} \\ F_{72_t} & F_{73_t} & F_{74} & F_{75} & F_{76} & F_{77} & F_{78} & F_{79_t} \\ F_{82_t} & F_{83_t} & F_{84} & F_{85} & F_{86} & F_{87} & F_{88} & F_{89_t} \\ F_{92} & F_{93_t} & F_{94_t} & F_{95_t} & F_{96_t} & F_{97_t} & F_{98_t} & F_{99} \end{pmatrix}$$

Appendix F:

Flux-Transfer Analysis

Flux-transfer analysis within an enclosed room

i) For diffuse daylighting

Initial luminous exitance of each room surface

$$M_{o_t} = \begin{pmatrix} E_{shade_t} \\ 0 \\ 0 \\ 0 \\ 0 \\ 0 \\ 0 \\ E_{facaded_t} \end{pmatrix}$$

Reflectance of each room surface

$$\rho = \begin{pmatrix} \rho_{shadein} & 0 & 0 & 0 & 0 & 0 & 0 & 0 \\ 0 & \rho_{wall} & 0 & 0 & 0 & 0 & 0 & 0 \\ 0 & 0 & \rho_{ceiling} & 0 & 0 & 0 & 0 & 0 \\ 0 & 0 & 0 & \rho_{wall} & 0 & 0 & 0 & 0 \\ 0 & 0 & 0 & 0 & \rho_{wall} & 0 & 0 & 0 \\ 0 & 0 & 0 & 0 & 0 & \rho_{floor} & 0 & 0 \\ 0 & 0 & 0 & 0 & 0 & 0 & \rho_{wall} & 0 \\ 0 & 0 & 0 & 0 & 0 & 0 & 0 & \rho_{facade} \end{pmatrix}$$

"Final" luminous exitance of each room surface

$$i = 8 \qquad I = identity(8) = \begin{pmatrix} 1 & 0 & 0 & 0 & 0 & 0 & 0 & 0 \\ 0 & 1 & 0 & 0 & 0 & 0 & 0 & 0 \\ 0 & 0 & 1 & 0 & 0 & 0 & 0 & 0 \\ 0 & 0 & 0 & 1 & 0 & 0 & 0 & 0 \\ 0 & 0 & 0 & 0 & 1 & 0 & 0 & 0 \\ 0 & 0 & 0 & 0 & 0 & 1 & 0 & 0 \\ 0 & 0 & 0 & 0 & 0 & 0 & 1 & 0 \\ 0 & 0 & 0 & 0 & 0 & 0 & 0 & 1 \end{pmatrix} \qquad M_{1_t} = \left(I - \rho F_t\right)^{-1} M_{o_t}$$

Configuration factors between room surfaces and workplane

Configuration factors for points positioned to a plane parallel to the source plane

$$C_{parallel}(z,y,w) = \frac{1}{2\pi}\left(\frac{z}{\sqrt{z^2+y^2}}\,\mathrm{atan}\left(\frac{w}{\sqrt{z^2+y^2}}\right) + \frac{w}{\sqrt{w^2+y^2}}\,\mathrm{atan}\left(\frac{z}{\sqrt{w^2+y^2}}\right)\right)$$

Configuration factors for points positioned to a plane perpendicular to the source plane

$$C_{perpendicular}(z,y,w) = \frac{1}{2\pi}\left(\mathrm{atan}\left(\frac{w}{y}\right) - \frac{y}{\sqrt{z^2+y^2}}\,\mathrm{atan}\left(\frac{w}{\sqrt{z^2+y^2}}\right)\right)$$

$j = 1,2 \ldots 25$ number of selected points

South wall and facade (surface 1)

$z_{j,t} = H_{rm} - H_{workplane}$

$$y_{j,t} = \begin{cases} 0.1\text{m} & \text{if } 1 \le j \le 5 \\ \frac{D_{rm} - 0.2\text{m}}{4} + 0.1\text{m} & \text{if } 6 \le j \le 10 \\ \frac{2\,(D_{rm} - 0.2\text{m})}{4} + 0.1\text{m} & \text{if } 11 \le j \le 15 \\ \frac{3\,(D_{rm} - 0.2\text{m})}{4} + 0.1\text{m} & \text{if } 16 \le j \le 20 \\ D_{rm} - 0.1\text{m} & \text{otherwise} \end{cases}$$

$$w_{j,t} = \begin{cases} 0.1\text{m} & \text{if } j = 1 \vee j = 6 \vee j = 11 \vee j = 16 \vee j = 21 \\ \frac{W_{rm} - 0.2\text{m}}{4} + 0.1\text{m} & \text{if } j = 2 \vee j = 7 \vee j = 12 \vee j = 17 \vee j = 22 \\ \frac{2\,(W_{rm} - 0.2\text{m})}{4} + 0.1\text{m} & \text{if } j = 3 \vee j = 8 \vee j = 13 \vee j = 18 \vee j = 23 \\ \frac{3\,(W_{rm} - 0.2\text{m})}{4} + 0.1\text{m} & \text{if } j = 4 \vee j = 9 \vee j = 14 \vee j = 19 \vee j = 24 \\ W_{rm} - 0.1\text{m} & \text{otherwise} \end{cases}$$

$C_{south1_{j,t}} = C_{perpendicular}(z_{j,t}, y_{j,t}, w_{j,t})$

$$w_{J,t} = \begin{cases} 0\,1m \text{ if } J = 5 \vee J = 10 \vee J = 15 \vee J = 20 \vee J = 25 \\ \frac{W_{rm} - 0\,2m}{4} + 0\,1m \text{ if } J = 4 \vee J = 9 \vee J = 14 \vee J = 19 \vee J = 24 \\ \frac{2\left(W_{rm} - 0\,2m\right)}{4} + 0\,1m \text{ if } J = 3 \vee J = 8 \vee J = 13 \vee J = 18 \vee J = 23 \\ \frac{3\left(W_{rm} - 0\,2m\right)}{4} + 0\,1m \text{ if } J = 2 \vee J = 7 \vee J = 12 \vee J = 17 \vee J = 22 \\ W_{rm} - 0\,1m \text{ otherwise} \end{cases}$$

$$C_{south2_{J,t}} = C_{perpendicular}\left(z_{J,t}, y_{J,t}, w_{J,t}\right)$$

$$C_{south_{J,t}} = C_{south1_{J,t}} + C_{south2_{J,t}}$$

Spandrel

$$z_{J,t} = if\left[\left(H_{sp} - H_{workplane}\right) > 0m, H_{sp} - H_{workplane}, 0\ m\right]$$

$$w_{J,t} = \begin{cases} 0m \text{ if } J = 1 \vee J = 6 \vee J = 11 \vee J = 16 \vee J = 21 \\ \frac{W_{rm} - 0\,2m}{4} \text{ if } J = 2 \vee J = 7 \vee J = 12 \vee J = 17 \vee J = 22 \\ \frac{2\left(W_{rm} - 0\,2m\right)}{4} \text{ if } J = 3 \vee J = 8 \vee J = 13 \vee J = 18 \vee J = 23 \\ \frac{3\left(W_{rm} - 0\,2m\right)}{4} \text{ if } J = 4 \vee J = 9 \vee J = 14 \vee J = 19 \vee J = 24 \\ W_{rm} - 0\,2m \text{ otherwise} \end{cases}$$

$$C_{spandrel1_{J,t}} = C_{perpendicular}\left(z_{J,t}, y_{J,t}, w_{J,t}\right)$$

$$w_{J,t} = \begin{cases} 0m \text{ if } J = 5 \vee J = 10 \vee J = 15 \vee J = 20 \vee J = 25 \\ \frac{W_{rm} - 0\,2m}{4} \text{ if } J = 4 \vee J = 9 \vee J = 14 \vee J = 19 \vee J = 24 \\ \frac{2\left(W_{rm} - 0\,2m\right)}{4} \text{ if } J = 3 \vee J = 8 \vee J = 13 \vee J = 18 \vee J = 23 \\ \frac{3\left(W_{rm} - 0\,2m\right)}{4} \text{ if } J = 2 \vee J = 7 \vee J = 12 \vee J = 17 \vee J = 22 \\ W_{rm} - 0\,2m \text{ otherwise} \end{cases}$$

$$C_{spandrel2_{J,t}} = C_{perpendicular}\left(z_{J,t}, y_{J,t}, w_{J,t}\right)$$

$$C_{spandrel_{J,t}} = C_{spandrel1_{J,t}} + C_{spandrel2_{J,t}}$$

Shaded facade (surface 2)

$$z_{j,t} = \begin{cases} H_{shade_t} + H_{sp} - H_{workplane} & \text{if } H_{shade_t} + H_{sp} > H_{workplane} \\ 0 & \text{otherwise} \end{cases}$$

$$w_{j,t} = \begin{cases} 0m & \text{if } j = 1 \vee j = 6 \vee j = 11 \vee j = 16 \vee j = 21 \\ \frac{W_{rm} - 0.2m}{4} & \text{if } j = 2 \vee j = 7 \vee j = 12 \vee j = 17 \vee j = 22 \\ \frac{2\left(W_{rm} - 0.2m\right)}{4} & \text{if } j = 3 \vee j = 8 \vee j = 13 \vee j = 18 \vee j = 23 \\ \frac{3\left(W_{rm} - 0.2m\right)}{4} & \text{if } j = 4 \vee j = 9 \vee j = 14 \vee j = 19 \vee j = 24 \\ W_{rm} - 0.2m & \text{otherwise} \end{cases}$$

$$C_{shaded1_{j,t}} = C_{perpendicular}\left(z_{j,t}, y_{j,t}, w_{j,t}\right)$$

$$w_{j,t} = \begin{cases} 0m & \text{if } j = 5 \vee j = 10 \vee j = 15 \vee j = 20 \vee j = 25 \\ \frac{W_{rm} - 0.2m}{4} & \text{if } j = 4 \vee j = 9 \vee j = 14 \vee j = 19 \vee j = 24 \\ \frac{2\left(W_{rm} - 0.2m\right)}{4} & \text{if } j = 3 \vee j = 8 \vee j = 13 \vee j = 18 \vee j = 23 \\ \frac{3\left(W_{rm} - 0.2m\right)}{4} & \text{if } j = 2 \vee j = 7 \vee j = 12 \vee j = 17 \vee j = 22 \\ W_{rm} - 0.2m & \text{otherwise} \end{cases}$$

$$C_{shaded2_{j,t}} = C_{perpendicular}\left(z_{j,t}, y_{j,t}, w_{j,t}\right)$$

$$C_{shaded_{j,t}} = \left(C_{shaded1_{j,t}} + C_{shaded2_{j,t}}\right) - C_{spandrel_{j,t}}$$

Unshaded facade (surface 9)

$$z_{j,t} = H_{sp} + H_{facade} - H_{workplane}$$

$$w_{j,t} = \begin{cases} 0m & \text{if } j = 1 \vee j = 6 \vee j = 11 \vee j = 16 \vee j = 21 \\ \frac{W_{rm} - 0.2m}{4} & \text{if } j = 2 \vee j = 7 \vee j = 12 \vee j = 17 \vee j = 22 \\ \frac{2\left(W_{rm} - 0.2m\right)}{4} & \text{if } j = 3 \vee j = 8 \vee j = 13 \vee j = 18 \vee j = 23 \\ \frac{3\left(W_{rm} - 0.2m\right)}{4} & \text{if } j = 4 \vee j = 9 \vee j = 14 \vee j = 19 \vee j = 24 \\ W_{rm} - 0.2m & \text{otherwise} \end{cases}$$

$$C_{unshaded1_{j,t}} = C_{perpendicular}\left(z_{j,t}, y_{j,t}, w_{j,t}\right)$$

$$w_{j,t} = \begin{cases} 0m \text{ if } j = 5 \vee j = 10 \vee j = 15 \vee j = 20 \vee j = 25 \\ \frac{W_{rm} - 0.2m}{4} \text{ if } j = 4 \vee j = 9 \vee j = 14 \vee j = 19 \vee j = 24 \\ \frac{2\left(W_{rm} - 0.2m\right)}{4} \text{ if } j = 3 \vee j = 8 \vee j = 13 \vee j = 18 \vee j = 23 \\ \frac{3\left(W_{rm} - 0.2m\right)}{4} \text{ if } j = 2 \vee j = 7 \vee j = 12 \vee j = 17 \vee j = 22 \\ W_{rm} - 0.2m \text{ otherwise} \end{cases}$$

$$C_{unshaded2_{j,t}} = C_{perpendicular}\left(z_{j,t}, y_{j,t}, w_{j,t}\right)$$

$$C_{unshaded_{j,t}} = \left(C_{unshaded1_{j,t}} + C_{unshaded2_{j,t}}\right) - C_{spandrel_{j,t}} - C_{shaded_{j,t}}$$

South wall (surface 3)

$$C_{southwall_{j,t}} = C_{south_{j,t}} - C_{unshaded_{j,t}} - C_{shaded_{j,t}}$$

North wall (surface 6)

$$z_{j,t} = H_{rm} - H_{workplane}$$

$$y_{j,t} = \begin{cases} 0.1m \text{ if } 21 \le j \le 25 \\ \frac{D_{rm} - 0.2m}{4} + 0.1m \text{ if } 16 \le j \le 20 \\ \frac{2\left(D_{rm} - 0.2m\right)}{4} + 0.1m \text{ if } 11 \le j \le 15 \\ \frac{3\left(D_{rm} - 0.2m\right)}{4} + 0.1m \text{ if } 6 \le j \le 10 \\ D_{rm} - 0.1m \text{ otherwise} \end{cases}$$

$$w_{j,t} = \begin{cases} 0.1m \text{ if } j = 1 \vee j = 6 \vee j = 11 \vee j = 16 \vee j = 21 \\ \frac{W_{rm} - 0.2m}{4} + 0.1\,m \text{ if } j = 2 \vee j = 7 \vee j = 12 \vee j = 17 \vee j = 22 \\ \frac{2\left(W_{rm} - 0.2m\right)}{4} + 0.1m \text{ if } j = 3 \vee j = 8 \vee j = 13 \vee j = 18 \vee j = 23 \\ \frac{3\left(W_{rm} - 0.2m\right)}{4} + 0.1m \text{ if } j = 4 \vee j = 9 \vee j = 14 \vee j = 19 \vee j = 24 \\ W_{rm} - 0.1m \text{ otherwise} \end{cases}$$

$$C_{north1_{j,t}} = C_{perpendicular}\left(z_{j,t}, y_{j,t}, w_{j,t}\right)$$

$$w_{j,t} = \begin{cases} 0.1m \text{ if } j = 5 \vee j = 10 \vee j = 15 \vee j = 20 \vee j = 25 \\ \frac{W_{rm} - 0.2m}{4} + 0.1m \text{ if } j = 4 \vee j = 9 \vee j = 14 \vee j = 19 \vee j = 24 \\ \frac{2\left(W_{rm} - 0.2m\right)}{4} + 0.1m \text{ if } j = 3 \vee j = 8 \vee j = 13 \vee j = 18 \vee j = 23 \\ \frac{3\left(W_{rm} - 0.2m\right)}{4} + 0.1m \text{ if } j = 2 \vee j = 7 \vee j = 12 \vee j = 17 \vee j = 22 \\ W_{rm} - 0.1m \text{ otherwise} \end{cases}$$

$$C_{north2_{j,t}} = C_{perpendicular}\left(z_{j,t}, y_{j,t}, w_{j,t}\right)$$

$$C_{north_{j,t}} = C_{north1_{j,t}} + C_{north2_{j,t}}$$

East wall (surface 8)

$$z_{j,t} = H_{rm} - H_{workplane}$$

$$y_{j,t} = \begin{cases} 0.1m \text{ if } j = 1 \vee j = 6 \vee j = 11 \vee j = 16 \vee j = 21 \\ \frac{W_{rm} - 0.2m}{4} + 0.1m \text{ if } j = 2 \vee j = 7 \vee j = 12 \vee j = 17 \vee j = 22 \\ \frac{2\left(W_{rm} - 0.2m\right)}{4} + 0.1m \text{ if } j = 3 \vee j = 8 \vee j = 13 \vee j = 18 \vee j = 23 \\ \frac{3\left(W_{rm} - 0.2m\right)}{4} + 0.1m \text{ if } j = 4 \vee j = 9 \vee j = 14 \vee j = 19 \vee j = 24 \\ W_{rm} - 0.1m \text{ otherwise} \end{cases}$$

$$w_{j,t} = \begin{cases} 0.1m \text{ if } 1 \le j \le 5 \\ \frac{D_{rm} - 0.2m}{4} + 0.1 m \text{ if } 6 \le j \le 10 \\ \frac{2\left(D_{rm} - 0.2m\right)}{4} + 0.1m \text{ if } 11 \le j \le 15 \\ \frac{3\left(D_{rm} - 0.2m\right)}{4} + 0.1m \text{ if } 16 \le j \le 20 \\ D_{rm} - 0.1m \text{ otherwise} \end{cases}$$

$$C_{east1_{j,t}} = C_{perpendicular}\left(z_{j,t}, y_{j,t}, w_{j,t}\right)$$

$$w_{j,t} = \begin{cases} 0.1\text{m} \text{ if } 21 \le j \le 25 \\ \frac{D_{rm} - 0.2\text{m}}{4} + 0.1\text{ m} \text{ if } 16 \le j \le 20 \\ \frac{2\left(D_{rm} - 0.2\text{m}\right)}{4} + 0.1\text{m} \text{ if } 11 \le j \le 15 \\ \frac{3\left(D_{rm} - 0.2\text{m}\right)}{4} + 0.1\text{m} \text{ if } 6 \le j \le 10 \\ D_{rm} - 0.1\text{m} \text{ otherwise} \end{cases}$$

$$C_{east2_{j,t}} = C_{perpendicular}\left(z_{j,t}, y_{j,t}, w_{j,t}\right)$$

$$C_{east_{j,t}} = C_{east1_{j,t}} + C_{east2_{j,t}}$$

West wall (surface 5)

$$z_{j,t} = H_{rm} - H_{workplane}$$

$$y_{j,t} = \begin{cases} 0.1\text{m} \text{ if } j = 5 \vee j = 10 \vee j = 15 \vee j = 20 \vee j = 25 \\ \frac{W_{rm} - 0.2\text{m}}{4} + 0.1\text{m} \text{ if } j = 4 \vee j = 9 \vee j = 14 \vee j = 19 \vee j = 24 \\ \frac{2\left(W_{rm} - 0.2\text{m}\right)}{4} + 0.1\text{m} \text{ if } j = 3 \vee j = 8 \vee j = 13 \vee j = 18 \vee j = 23 \\ \frac{3\left(W_{rm} - 0.2\text{m}\right)}{4} + 0.1\text{m} \text{ if } j = 2 \vee j = 7 \vee j = 12 \vee j = 17 \vee j = 22 \\ W_{rm} - 0.1\text{m} \text{ otherwise} \end{cases}$$

$$w_{j,t} = \begin{cases} 0.1\text{m} \text{ if } 1 \le j \le 5 \\ \frac{D_{rm} - 0.2\text{m}}{4} + 0.1\text{ m} \text{ if } 6 \le j \le 10 \\ \frac{2\left(D_{rm} - 0.2\text{m}\right)}{4} + 0.1\text{m} \text{ if } 11 \le j \le 15 \\ \frac{3\left(D_{rm} - 0.2\text{m}\right)}{4} + 0.1\text{m} \text{ if } 16 \le j \le 20 \\ D_{rm} - 0.1\text{m} \text{ otherwise} \end{cases}$$

$$C_{west1_{j,t}} = C_{perpendicular}\left(z_{j,t}, y_{j,t}, w_{j,t}\right)$$

$$w_{j,t} = \begin{cases} 0.1\text{m} & \text{if } 21 \le j \le 25 \\ \frac{D_{rm} - 0.2\text{m}}{4} + 0.1\text{ m} & \text{if } 16 \le j \le 20 \\ \frac{2\left(D_{rm} - 0.2\text{m}\right)}{4} + 0.1\text{m} & \text{if } 11 \le j \le 15 \\ \frac{3\left(D_{rm} - 0.2\text{m}\right)}{4} + 0.1\text{m} & \text{if } 6 \le j \le 10 \\ D_{rm} - 0.1\text{m} & \text{otherwise} \end{cases}$$

$$C_{west2_{j,t}} = C_{perpendicular}\left(z_{j,t}, y_{j,t}, w_{j,t}\right)$$

$$C_{west_{j,t}} = C_{west1_{j,t}} + C_{west2_{j,t}}$$

Ceiling (surface 4)

$$C_{ceiling_{j,t}} = 1 - C_{south_{j,t}} - C_{north_{j,t}} - C_{east_{j,t}} - C_{west_{j,t}}$$

$$C_{room_{j,t}} = \left(C_{shaded_{j,t}}\ C_{southwall_{j,t}}\ C_{ceiling_{j,t}}\ C_{west_{j,t}}\ C_{north_{j,t}}\ 0\ C_{east_{j,t}}\ C_{unshaded_{j,t}}\right.$$

Workplane Illuminance due to diffuse daylighting

$E_{workplane_{j,t}} = C_{room_{j,t}} M1_t$ workplane illuminace due to diffuse daylighting transmitted through the fenestration

$$E_{wpd_t} = \begin{pmatrix} E_{workplane_{1,t}} & E_{workplane_{2,t}} & E_{workplane_{3,t}} & E_{workplane_{4,t}} & E_{workplane_{5,t}} \\ E_{workplane_{6,t}} & E_{workplane_{7,t}} & E_{workplane_{8,t}} & E_{workplane_{9,t}} & E_{workplane_{10,t}} \\ E_{workplane_{11,t}} & E_{workplane_{12,t}} & E_{workplane_{13,t}} & E_{workplane_{14,t}} & E_{workplane_{15,t}} \\ E_{workplane_{16,t}} & E_{workplane_{17,t}} & E_{workplane_{18,t}} & E_{workplane_{19,t}} & E_{workplane_{20,t}} \\ E_{workplane_{21,t}} & E_{workplane_{22,t}} & E_{workplane_{23,t}} & E_{workplane_{24,t}} & E_{workplane_{25,t}} \end{pmatrix}$$

Appendix G:

One Bounce Ray-Tracing Analysis

Ray tracing analysis within an enclosed room

i) For direct daylighting

A position vector parallel to window vectors is:

$$\left(X_{o_t}\ Y_{o_t}\ Z_{o_t}\right) := \left(1\ \ \tan(\gamma(n,t))\ \ -\tan\left(\alpha_s(n,t)\right)\cdot\sqrt{1+\tan(\gamma(n,t))^2}\right)$$

Coordinates of the four window corners (initial points of the window vectors):

$$\left(X_{A_t}\ Y_{A_t}\ Z_{A_t}\right) := \left(0\ \ 0.1\ \ \frac{H_{sp}+H_{shade_t}}{m}\right)$$

$$\left(X_{B_t}\ Y_{B_t}\ Z_{B_t}\right) := \left(0\ \ 0.1\ \ \frac{H_{sp}+Y_{frame_t}}{m}\right)$$

$$\left(X_{C_t}\ Y_{C_t}\ Z_{C_t}\right) := \left(0\ \ \frac{0.1m+W_{facade}}{m}\ \ \frac{H_{sp}+Y_{frame_t}}{m}\right)$$

$$\left(X_{D_t}\ Y_{D_t}\ Z_{D_t}\right) := \left(0\ \ \frac{0.1m+W_{facade}}{m}\ \ \frac{H_{sp}+H_{shade_t}}{m}\right)$$

Terminal points of the window vectors:

$$\left(X_{A'_t}\ Y_{A'_t}\ Z_{A'_t}\right) := \left(X_{o_t}+X_{A_t}\ \ Y_{o_t}+Y_{A_t}\ \ Z_{o_t}+Z_{A_t}\right)$$

$$\left(X_{B'_t}\ Y_{B'_t}\ Z_{B'_t}\right) := \left(X_{o_t}+X_{B_t}\ \ Y_{o_t}+Y_{B_t}\ \ Z_{o_t}+Z_{B_t}\right)$$

$$\left(X_{C'_t}\ Y_{C'_t}\ Z_{C'_t}\right) := \left(X_{o_t}+X_{C_t}\ \ Y_{o_t}+Y_{C_t}\ \ Z_{o_t}+Z_{C_t}\right)$$

$$\left(X_{D'_t}\ Y_{D'_t}\ Z_{D'_t}\right) := \left(X_{o_t}+X_{D_t}\ \ Y_{o_t}+Y_{D_t}\ \ Z_{o_t}+Z_{D_t}\right)$$

Define three random points of each interior wall planes (East, West and North wall):

$$\left(X_{E1_t}\ Y_{E1_t}\ Z_{E1_t}\right) := \left(\frac{D_{rm}}{2m}\ \ \frac{W_{rm}}{m}\ \ \frac{H_{rm}}{4m}\right)$$

$$\left(X_{E2_t}\ Y_{E2_t}\ Z_{E2_t}\right) := \left(\frac{D_{rm}}{m}\ \ \frac{W_{rm}}{m}\ \ \frac{H_{rm}}{2m}\right)$$ ...for East wall

$$\left(X_{E3_t}\ Y_{E3_t}\ Z_{E3_t}\right) := \left(\frac{D_{rm}}{6m}\ \ \frac{W_{rm}}{m}\ \ \frac{H_{rm}}{m}\right)$$

$$\left(X_{W1_t}\ Y_{W1_t}\ Z_{W1_t}\right) = \left(\frac{D_{rm}}{2m}\ 0\ \frac{H_{rm}}{4m}\right)$$

$$\left(X_{W2_t}\ Y_{W2_t}\ Z_{W2_t}\right) = \left(\frac{D_{rm}}{m}\ 0\ \frac{H_{rm}}{2m}\right) \qquad \text{for West wall}$$

$$\left(X_{W3_t}\ Y_{W3_t}\ Z_{W3_t}\right) = \left(\frac{D_{rm}}{6m}\ 0\ \frac{H_{rm}}{m}\right)$$

$$\left(X_{N1_t}\ Y_{N1_t}\ Z_{N1_t}\right) = \left(\frac{D_{rm}}{m}\ \frac{W_{rm}}{m}\ \frac{H_{rm}}{4m}\right)$$

$$\left(X_{N2_t}\ Y_{N2_t}\ Z_{N2_t}\right) = \left(\frac{D_{rm}}{m}\ \frac{W_{rm}}{2m}\ \frac{H_{rm}}{m}\right) \qquad \text{for North wall}$$

$$\left(X_{N3_t}\ Y_{N3_t}\ Z_{N3_t}\right) = \left(\frac{D_{rm}}{m}\ \frac{W_{rm}}{6m}\ \frac{H_{rm}}{2m}\right)$$

The point at which a window vector intersects a wall plane is described by setting the window vector equal to the plane in a parametric equation which can be expressed in matrix form as

$$\begin{pmatrix} T_{EA_t} \\ U_{EA_t} \\ V_{EA_t} \end{pmatrix} = \begin{pmatrix} X_{A_t} - X_{A'_t} & X_{E2_t} - X_{E1_t} & X_{E3_t} - X_{E1_t} \\ Y_{A_t} - Y_{A'_t} & Y_{E2_t} - Y_{E1_t} & Y_{E3_t} - Y_{E1_t} \\ Z_{A_t} - Z_{A'_t} & Z_{E2_t} - Z_{E1_t} & Z_{E3_t} - Z_{E1_t} \end{pmatrix}^{-1} \begin{pmatrix} X_{A_t} - X_{E1_t} \\ Y_{A_t} - Y_{E1_t} \\ Z_{A_t} - Z_{E1_t} \end{pmatrix} \qquad \text{for East wall}$$

$$\begin{pmatrix} T_{EB_t} \\ U_{EB_t} \\ V_{EB_t} \end{pmatrix} = \begin{pmatrix} X_{B_t} - X_{B'_t} & X_{E2_t} - X_{E1_t} & X_{E3_t} - X_{E1_t} \\ Y_{B_t} - Y_{B'_t} & Y_{E2_t} - Y_{E1_t} & Y_{E3_t} - Y_{E1_t} \\ Z_{B_t} - Z_{B'_t} & Z_{E2_t} - Z_{E1_t} & Z_{E3_t} - Z_{E1_t} \end{pmatrix}^{-1} \begin{pmatrix} X_{B_t} - X_{E1_t} \\ Y_{B_t} - Y_{E1_t} \\ Z_{B_t} - Z_{E1_t} \end{pmatrix}$$

$$\begin{pmatrix} T_{EC_t} \\ U_{EC_t} \\ V_{EC_t} \end{pmatrix} = \begin{pmatrix} X_{C_t} - X_{C'_t} & X_{E2_t} - X_{E1_t} & X_{E3_t} - X_{E1_t} \\ Y_{C_t} - Y_{C'_t} & Y_{E2_t} - Y_{E1_t} & Y_{E3_t} - Y_{E1_t} \\ Z_{C_t} - Z_{C'_t} & Z_{E2_t} - Z_{E1_t} & Z_{E3_t} - Z_{E1_t} \end{pmatrix}^{-1} \begin{pmatrix} X_{C_t} - X_{E1_t} \\ Y_{C_t} - Y_{E1_t} \\ Z_{C_t} - Z_{E1_t} \end{pmatrix}$$

$$\begin{pmatrix} T_{ED_t} \\ U_{ED_t} \\ V_{ED_t} \end{pmatrix} = \begin{pmatrix} X_{D_t} - X_{D'_t} & X_{E2_t} - X_{E1_t} & X_{E3_t} - X_{E1_t} \\ Y_{D_t} - Y_{D'_t} & Y_{E2_t} - Y_{E1_t} & Y_{E3_t} - Y_{E1_t} \\ Z_{D_t} - Z_{D'_t} & Z_{E2_t} - Z_{E1_t} & Z_{E3_t} - Z_{E1_t} \end{pmatrix}^{-1} \begin{pmatrix} X_{D_t} - X_{E1_t} \\ Y_{D_t} - Y_{E1_t} \\ Z_{D_t} - Z_{E1_t} \end{pmatrix}$$

$$\begin{pmatrix} T_{WA_t} \\ U_{WA_t} \\ V_{WA_t} \end{pmatrix} := \begin{pmatrix} X_{A_t} - X_{A'_t} & X_{W2_t} - X_{W1_t} & X_{W3_t} - X_{W1_t} \\ Y_{A_t} - Y_{A'_t} & Y_{W2_t} - Y_{W1_t} & Y_{W3_t} - Y_{W1_t} \\ Z_{A_t} - Z_{A'_t} & Z_{W2_t} - Z_{W1_t} & Z_{W3_t} - Z_{W1_t} \end{pmatrix}^{-1} \cdot \begin{pmatrix} X_{A_t} - X_{W1_t} \\ Y_{A_t} - Y_{W1_t} \\ Z_{A_t} - Z_{W1_t} \end{pmatrix}$$ ...for West wal

$$\begin{pmatrix} T_{WB_t} \\ U_{WB_t} \\ V_{WB_t} \end{pmatrix} := \begin{pmatrix} X_{B_t} - X_{B'_t} & X_{W2_t} - X_{W1_t} & X_{W3_t} - X_{W1_t} \\ Y_{B_t} - Y_{B'_t} & Y_{W2_t} - Y_{W1_t} & Y_{W3_t} - Y_{W1_t} \\ Z_{B_t} - Z_{B'_t} & Z_{W2_t} - Z_{W1_t} & Z_{W3_t} - Z_{W1_t} \end{pmatrix}^{-1} \cdot \begin{pmatrix} X_{B_t} - X_{W1_t} \\ Y_{B_t} - Y_{W1_t} \\ Z_{B_t} - Z_{W1_t} \end{pmatrix}$$

$$\begin{pmatrix} T_{WC_t} \\ U_{WC_t} \\ V_{WC_t} \end{pmatrix} := \begin{pmatrix} X_{C_t} - X_{C'_t} & X_{W2_t} - X_{W1_t} & X_{W3_t} - X_{W1_t} \\ Y_{C_t} - Y_{C'_t} & Y_{W2_t} - Y_{W1_t} & Y_{W3_t} - Y_{W1_t} \\ Z_{C_t} - Z_{C'_t} & Z_{W2_t} - Z_{W1_t} & Z_{W3_t} - Z_{W1_t} \end{pmatrix}^{-1} \cdot \begin{pmatrix} X_{C_t} - X_{W1_t} \\ Y_{C_t} - Y_{W1_t} \\ Z_{C_t} - Z_{W1_t} \end{pmatrix}$$

$$\begin{pmatrix} T_{WD_t} \\ U_{WD_t} \\ V_{WD_t} \end{pmatrix} := \begin{pmatrix} X_{D_t} - X_{D'_t} & X_{W2_t} - X_{W1_t} & X_{W3_t} - X_{W1_t} \\ Y_{D_t} - Y_{D'_t} & Y_{W2_t} - Y_{W1_t} & Y_{W3_t} - Y_{W1_t} \\ Z_{D_t} - Z_{D'_t} & Z_{W2_t} - Z_{W1_t} & Z_{W3_t} - Z_{W1_t} \end{pmatrix}^{-1} \cdot \begin{pmatrix} X_{D_t} - X_{W1_t} \\ Y_{D_t} - Y_{W1_t} \\ Z_{D_t} - Z_{W1_t} \end{pmatrix}$$

$$\begin{pmatrix} T_{NA_t} \\ U_{NA_t} \\ V_{NA_t} \end{pmatrix} := \begin{pmatrix} X_{A_t} - X_{A'_t} & X_{N2_t} - X_{N1_t} & X_{N3_t} - X_{N1_t} \\ Y_{A_t} - Y_{A'_t} & Y_{N2_t} - Y_{N1_t} & Y_{N3_t} - Y_{N1_t} \\ Z_{A_t} - Z_{A'_t} & Z_{N2_t} - Z_{N1_t} & Z_{N3_t} - Z_{N1_t} \end{pmatrix}^{-1} \cdot \begin{pmatrix} X_{A_t} - X_{N1_t} \\ Y_{A_t} - Y_{N1_t} \\ Z_{A_t} - Z_{N1_t} \end{pmatrix}$$ ...for North wall

$$\begin{pmatrix} T_{NB_t} \\ U_{NB_t} \\ V_{NB_t} \end{pmatrix} := \begin{pmatrix} X_{B_t} - X_{B'_t} & X_{N2_t} - X_{N1_t} & X_{N3_t} - X_{N1_t} \\ Y_{B_t} - Y_{B'_t} & Y_{N2_t} - Y_{N1_t} & Y_{N3_t} - Y_{N1_t} \\ Z_{B_t} - Z_{B'_t} & Z_{N2_t} - Z_{N1_t} & Z_{N3_t} - Z_{N1_t} \end{pmatrix}^{-1} \cdot \begin{pmatrix} X_{B_t} - X_{N1_t} \\ Y_{B_t} - Y_{N1_t} \\ Z_{B_t} - Z_{N1_t} \end{pmatrix}$$

$$\begin{pmatrix} T_{NC_t} \\ U_{NC_t} \\ V_{NC_t} \end{pmatrix} := \begin{pmatrix} X_{C_t} - X_{C'_t} & X_{N2_t} - X_{N1_t} & X_{N3_t} - X_{N1_t} \\ Y_{C_t} - Y_{C'_t} & Y_{N2_t} - Y_{N1_t} & Y_{N3_t} - Y_{N1_t} \\ Z_{C_t} - Z_{C'_t} & Z_{N2_t} - Z_{N1_t} & Z_{N3_t} - Z_{N1_t} \end{pmatrix}^{-1} \cdot \begin{pmatrix} X_{C_t} - X_{N1_t} \\ Y_{C_t} - Y_{N1_t} \\ Z_{C_t} - Z_{N1_t} \end{pmatrix}$$

$$\begin{pmatrix} T_{ND_t} \\ U_{ND_t} \\ V_{ND_t} \end{pmatrix} := \begin{pmatrix} X_{D_t} - X_{D'_t} & X_{N2_t} - X_{N1_t} & X_{N3_t} - X_{N1_t} \\ Y_{D_t} - Y_{D'_t} & Y_{N2_t} - Y_{N1_t} & Y_{N3_t} - Y_{N1_t} \\ Z_{D_t} - Z_{D'_t} & Z_{N2_t} - Z_{N1_t} & Z_{N3_t} - Z_{N1_t} \end{pmatrix}^{-1} \cdot \begin{pmatrix} X_{D_t} - X_{N1_t} \\ Y_{D_t} - Y_{N1_t} \\ Z_{D_t} - Z_{N1_t} \end{pmatrix}$$

So, the intersection points are

$$\begin{pmatrix} X_{EA_t} \\ Y_{EA_t} \\ Z_{EA_t} \end{pmatrix} = \begin{bmatrix} X_{A_t} + \left(X_{A'_t} - X_{A_t}\right) T_{EA_t} \\ Y_{A_t} + \left(Y_{A'_t} - Y_{A_t}\right) T_{EA_t} \\ Z_{A_t} + \left(Z_{A'_t} - Z_{A_t}\right) T_{EA_t} \end{bmatrix}$$

between window vector $\overrightarrow{AA'}$ and east wall

$$\begin{pmatrix} X_{WA_t} \\ Y_{WA_t} \\ Z_{WA_t} \end{pmatrix} = \begin{bmatrix} X_{A_t} + \left(X_{A'_t} - X_{A_t}\right) T_{WA_t} \\ Y_{A_t} + \left(Y_{A'_t} - Y_{A_t}\right) T_{WA_t} \\ Z_{A_t} + \left(Z_{A'_t} - Z_{A_t}\right) T_{WA_t} \end{bmatrix}$$

between window vector $\overrightarrow{AA'}$ and west wall

$$\begin{pmatrix} X_{NA_t} \\ Y_{NA_t} \\ Z_{NA_t} \end{pmatrix} = \begin{bmatrix} X_{A_t} + \left(X_{A'_t} - X_{A_t}\right) T_{NA_t} \\ Y_{A_t} + \left(Y_{A'_t} - Y_{A_t}\right) T_{NA_t} \\ Z_{A_t} + \left(Z_{A'_t} - Z_{A_t}\right) T_{NA_t} \end{bmatrix}$$

between window vector $\overrightarrow{AA'}$ and north wall

$$\begin{pmatrix} X_{EB_t} \\ Y_{EB_t} \\ Z_{EB_t} \end{pmatrix} = \begin{bmatrix} X_{B_t} + \left(X_{B'_t} - X_{B_t}\right) T_{EB_t} \\ Y_{B_t} + \left(Y_{B'_t} - Y_{B_t}\right) T_{EB_t} \\ Z_{B_t} + \left(Z_{B'_t} - Z_{B_t}\right) T_{EB_t} \end{bmatrix}$$

between window vector $\overrightarrow{BB'}$ and east wall

$$\begin{pmatrix} X_{WB_t} \\ Y_{WB_t} \\ Z_{WB_t} \end{pmatrix} = \begin{bmatrix} X_{B_t} + \left(X_{B'_t} - X_{B_t}\right) T_{WB_t} \\ Y_{B_t} + \left(Y_{B'_t} - Y_{B_t}\right) T_{WB_t} \\ Z_{B_t} + \left(Z_{B'_t} - Z_{B_t}\right) T_{WB_t} \end{bmatrix}$$

between window vector $\overrightarrow{BB'}$ and west wall

$$\begin{pmatrix} X_{NB_t} \\ Y_{NB_t} \\ Z_{NB_t} \end{pmatrix} = \begin{bmatrix} X_{B_t} + \left(X_{B'_t} - X_{B_t}\right) T_{NB_t} \\ Y_{B_t} + \left(Y_{B'_t} - Y_{B_t}\right) T_{NB_t} \\ Z_{B_t} + \left(Z_{B'_t} - Z_{B_t}\right) T_{NB_t} \end{bmatrix}$$

between window vector $\overrightarrow{BB'}$ and north wall

$$\begin{pmatrix} X_{EC_t} \\ Y_{EC_t} \\ Z_{EC_t} \end{pmatrix} = \begin{bmatrix} X_{C_t} + \left(X_{C'_t} - X_{C_t}\right) T_{EC_t} \\ Y_{C_t} + \left(Y_{C'_t} - Y_{C_t}\right) T_{EC_t} \\ Z_{C_t} + \left(Z_{C'_t} - Z_{C_t}\right) T_{EC_t} \end{bmatrix}$$

between window vector $\overrightarrow{CC'}$ and east wall

$$\begin{pmatrix} X_{WC_t} \\ Y_{WC_t} \\ Z_{WC_t} \end{pmatrix} = \begin{bmatrix} X_{C_t} + \left(X_{C'_t} - X_{C_t}\right) T_{WC_t} \\ Y_{C_t} + \left(Y_{C'_t} - Y_{C_t}\right) T_{WC_t} \\ Z_{C_t} + \left(Z_{C'_t} - Z_{C_t}\right) T_{WC_t} \end{bmatrix}$$

between window vector $\overrightarrow{CC'}$ and west wall

$$\begin{pmatrix} X_{NC_t} \\ Y_{NC_t} \\ Z_{NC_t} \end{pmatrix} = \begin{bmatrix} X_{C_t} + \left(X_{C'_t} - X_{C_t}\right) T_{NC_t} \\ Y_{C_t} + \left(Y_{C'_t} - Y_{C_t}\right) T_{NC_t} \\ Z_{C_t} + \left(Z_{C'_t} - Z_{C_t}\right) T_{NC_t} \end{bmatrix}$$

between window vector $\overrightarrow{CC'}$ and north wall

$$\begin{pmatrix} X_{ED_t} \\ Y_{ED_t} \\ Z_{ED_t} \end{pmatrix} = \begin{bmatrix} X_{D_t} + \left(X_{D'_t} - X_{D_t}\right) T_{ED_t} \\ Y_{D_t} + \left(Y_{D'_t} - Y_{D_t}\right) T_{ED_t} \\ Z_{D_t} + \left(Z_{D'_t} - Z_{D_t}\right) T_{ED_t} \end{bmatrix}$$

between window vector $\overrightarrow{DD'}$ and east wall

$$\begin{pmatrix} X_{WD_t} \\ Y_{WD_t} \\ Z_{WD_t} \end{pmatrix} = \begin{bmatrix} X_{D_t} + \left(X_{D'_t} - X_{D_t}\right) T_{WD_t} \\ Y_{D_t} + \left(Y_{D'_t} - Y_{D_t}\right) T_{WD_t} \\ Z_{D_t} + \left(Z_{D'_t} - Z_{D_t}\right) T_{WD_t} \end{bmatrix}$$

between window vector $\overrightarrow{DD'}$ and west wall

$$\begin{pmatrix} X_{ND_t} \\ Y_{ND_t} \\ Z_{ND_t} \end{pmatrix} = \begin{bmatrix} X_{D_t} + \left(X_{D'_t} - X_{D_t}\right) T_{ND_t} \\ Y_{D_t} + \left(Y_{D'_t} - Y_{D_t}\right) T_{ND_t} \\ Z_{D_t} + \left(Z_{D'_t} - Z_{D_t}\right) T_{ND_t} \end{bmatrix}$$

between window vector $\overrightarrow{DD'}$ and north wall

Trace the sun patch on the walls

Between window vector $\overrightarrow{AA'}$ and interior walls

$$\begin{pmatrix} x_{EA_t} \\ y_{EA_t} \\ z_{EA_t} \end{pmatrix} = \begin{cases} \begin{pmatrix} X_{EA_t} \\ Y_{EA_t} \\ Z_{EA_t} - \dfrac{H_{workplane}}{m} \end{pmatrix} & \text{if } 0 \le X_{EA_t} \le \dfrac{D_{rm}}{m} \\ \begin{pmatrix} 0 \\ 0 \\ 0 \end{pmatrix} & \text{otherwise} \end{cases}$$

for East wall

$$\begin{pmatrix} x_{NA_t} \\ y_{NA_t} \\ z_{NA_t} \end{pmatrix} := \begin{cases} \begin{pmatrix} X_{NA_t} \\ Y_{NA_t} \\ Z_{NA_t} - \frac{H_{workplane}}{m} \end{pmatrix} & \text{if } 0 \le Y_{NA_t} \le \frac{W_{rm}}{m} \\ \begin{pmatrix} 0 \\ 0 \\ 0 \end{pmatrix} & \text{otherwise} \end{cases}$$

...for North wall

$$\begin{pmatrix} x_{WA_t} \\ y_{WA_t} \\ z_{WA_t} \end{pmatrix} := \begin{cases} \begin{pmatrix} X_{WA_t} \\ Y_{WA_t} \\ Z_{WA_t} - \frac{H_{workplane}}{m} \end{pmatrix} & \text{if } 0 \le X_{WA_t} \le \frac{D_{rm}}{m} \\ \begin{pmatrix} 0 \\ 0 \\ 0 \end{pmatrix} & \text{otherwise} \end{cases}$$

...for West wall

Between window vector $\overrightarrow{BB'}$ and interior walls

$$\begin{pmatrix} x_{EB_t} \\ y_{EB_t} \\ z_{EB_t} \end{pmatrix} := \begin{cases} \begin{pmatrix} X_{EB_t} \\ Y_{EB_t} \\ Z_{EB_t} - \frac{H_{workplane}}{m} \end{pmatrix} & \text{if } 0 \le X_{EB_t} \le \frac{D_{rm}}{m} \\ \begin{pmatrix} 0 \\ 0 \\ 0 \end{pmatrix} & \text{otherwise} \end{cases}$$

...for East wall

$$\begin{pmatrix} x_{NB_t} \\ y_{NB_t} \\ z_{NB_t} \end{pmatrix} := \begin{cases} \begin{pmatrix} X_{NB_t} \\ Y_{NB_t} \\ Z_{NB_t} - \frac{H_{workplane}}{m} \end{pmatrix} & \text{if } 0 \le Y_{NB_t} \le \frac{W_{rm}}{m} \\ \begin{pmatrix} 0 \\ 0 \\ 0 \end{pmatrix} & \text{otherwise} \end{cases}$$

...for North wall

$$\begin{pmatrix} x_{WB_t} \\ y_{WB_t} \\ z_{WB_t} \end{pmatrix} = \begin{cases} \begin{pmatrix} X_{WB_t} \\ Y_{WB_t} \\ Z_{WB_t} - \frac{H_{workplane}}{m} \end{pmatrix} & \text{if } 0 \le X_{WB_t} \le \frac{D_{rm}}{m} \\ \begin{pmatrix} 0 \\ 0 \\ 0 \end{pmatrix} & \text{otherwise} \end{cases}$$ for West wall

Between window vector $\overrightarrow{CC'}$ and interior walls

$$\begin{pmatrix} x_{EC_t} \\ y_{EC_t} \\ z_{EC_t} \end{pmatrix} = \begin{cases} \begin{pmatrix} X_{EC_t} \\ Y_{EC_t} \\ Z_{EC_t} - \frac{H_{workplane}}{m} \end{pmatrix} & \text{if } 0 \le X_{EC_t} \le \frac{D_{rm}}{m} \\ \begin{pmatrix} 0 \\ 0 \\ 0 \end{pmatrix} & \text{otherwise} \end{cases}$$ for East wall

$$\begin{pmatrix} x_{NC_t} \\ y_{NC_t} \\ z_{NC_t} \end{pmatrix} = \begin{cases} \begin{pmatrix} X_{NC_t} \\ Y_{NC_t} \\ Z_{NC_t} - \frac{H_{workplane}}{m} \end{pmatrix} & \text{if } 0 \le Y_{NC_t} \le \frac{W_{rm}}{m} \\ \begin{pmatrix} 0 \\ 0 \\ 0 \end{pmatrix} & \text{otherwise} \end{cases}$$ for North wall

$$\begin{pmatrix} x_{WC_t} \\ y_{WC_t} \\ z_{WC_t} \end{pmatrix} = \begin{cases} \begin{pmatrix} X_{WC_t} \\ Y_{WC_t} \\ Z_{WC_t} - \frac{H_{workplane}}{m} \end{pmatrix} & \text{if } 0 \le X_{WC_t} \le \frac{D_{rm}}{m} \\ \begin{pmatrix} 0 \\ 0 \\ 0 \end{pmatrix} & \text{otherwise} \end{cases}$$ for West wall

Between window vector $\overrightarrow{DD'}$ and interior walls

$$\begin{pmatrix} x_{ED_t} \\ y_{ED_t} \\ z_{ED_t} \end{pmatrix} := \begin{cases} \begin{pmatrix} X_{ED_t} \\ Y_{ED_t} \\ Z_{ED_t} - \frac{H_{workplane}}{m} \end{pmatrix} & \text{if } 0 \le X_{ED_t} \le \frac{D_{rm}}{m} \\ \begin{pmatrix} 0 \\ 0 \\ 0 \end{pmatrix} & \text{otherwise} \end{cases}$$

...for East wall

$$\begin{pmatrix} x_{ND_t} \\ y_{ND_t} \\ z_{ND_t} \end{pmatrix} := \begin{cases} \begin{pmatrix} X_{ND_t} \\ Y_{ND_t} \\ Z_{ND_t} - \frac{H_{workplane}}{m} \end{pmatrix} & \text{if } 0 \le Y_{ND_t} \le \frac{W_{rm}}{m} \\ \begin{pmatrix} 0 \\ 0 \\ 0 \end{pmatrix} & \text{otherwise} \end{cases}$$

...for North wall

$$\begin{pmatrix} x_{WD_t} \\ y_{WD_t} \\ z_{WD_t} \end{pmatrix} := \begin{cases} \begin{pmatrix} X_{WD_t} \\ Y_{WD_t} \\ Z_{WD_t} - \frac{H_{workplane}}{m} \end{pmatrix} & \text{if } 0 \le X_{WD_t} \le \frac{D_{rm}}{m} \\ \begin{pmatrix} 0 \\ 0 \\ 0 \end{pmatrix} & \text{otherwise} \end{cases}$$

...for West wall

$$\begin{pmatrix} x_{E_t} \\ y_{E_t} \\ z_{E_t} \end{pmatrix} = \begin{cases} \begin{pmatrix} \frac{D_{rm}}{m} \\ \frac{W_{rm}}{m} \\ z_{NA_t} \end{pmatrix} & \text{if } x_{NA_t} = \frac{D_{rm}}{m} \wedge x_{ED_t} < \frac{D_{rm}}{m} \quad \text{for East-North wall corner} \\ \begin{pmatrix} \frac{D_{rm}}{m} \\ 0 \\ z_{ND_t} \end{pmatrix} & \text{if } x_{WA_t} < \frac{D_{rm}}{m} \wedge x_{ND_t} = \frac{D_{rm}}{m} \quad \text{for West-North wall corner} \\ \begin{pmatrix} 0 \\ 0 \\ 0 \end{pmatrix} & \text{otherwise} \end{cases}$$

$$\begin{pmatrix} x_{F_t} \\ y_{F_t} \\ z_{F_t} \end{pmatrix} = \begin{cases} \begin{pmatrix} \frac{D_{rm}}{m} \\ \frac{W_{rm}}{m} \\ z_{NB_t} \end{pmatrix} & \text{if } x_{NA_t} = \frac{D_{rm}}{m} \wedge x_{ED_t} < \frac{D_{rm}}{m} \quad \text{for East-North wall corner} \\ \begin{pmatrix} \frac{D_{rm}}{m} \\ 0 \\ z_{NC_t} \end{pmatrix} & \text{if } x_{WA_t} < \frac{D_{rm}}{m} \wedge x_{ND_t} = \frac{D_{rm}}{m} \quad \text{for West-North wall corner} \\ \begin{pmatrix} 0 \\ 0 \\ 0 \end{pmatrix} & \text{otherwise} \end{cases}$$

Coordinates of the selected points on the workplane

$$X_{j,t} = \begin{cases} 0.1 & \text{if } 1 \le j \le 5 \\ \frac{\frac{D_{rm} - 0.2m}{4} + 0.1\,m}{m} & \text{if } 6 \le j \le 10 \\ \frac{\frac{2\left(D_{rm} - 0.2m\right)}{4} + 0.1m}{m} & \text{if } 11 \le j \le 15 \\ \frac{\frac{3\left(D_{rm} - 0.2m\right)}{4} + 0.1m}{m} & \text{if } 16 \le j \le 20 \\ \frac{D_{rm} - 0.1m}{m} & \text{otherwise} \end{cases}$$

$$\Upsilon_{j,t} = \begin{cases} 0.1 \text{ m} & \text{if } j = 1 \vee j = 6 \vee j = 11 \vee j = 16 \vee j = 21 \\ \dfrac{\frac{W_{rm} - 0.2\text{m}}{4} + 0.1\text{ m}}{\text{m}} & \text{if } j = 2 \vee j = 7 \vee j = 12 \vee j = 17 \vee j = 22 \\ \dfrac{\frac{2\left(W_{rm} - 0.2\text{m}\right)}{4} + 0.1\text{m}}{\text{m}} & \text{if } j = 3 \vee j = 8 \vee j = 13 \vee j = 18 \vee j = 23 \\ \dfrac{\frac{3\left(W_{rm} - 0.2\text{m}\right)}{4} + 0.1\text{m}}{\text{m}} & \text{if } j = 4 \vee j = 9 \vee j = 14 \vee j = 19 \vee j = 24 \\ \dfrac{W_{rm} - 0.1\text{m}}{\text{m}} & \text{otherwise} \end{cases}$$

$$C'_{E_{j,t}} = \begin{cases} 0 & \text{if } x_{EA_t} = 0 \vee z_{EB_t} - z_{EA_t} \le 0 \\ \int_{x_{ED_t} - X_{j,t}}^{x_{EA_t} - X_{j,t}} \int_{\frac{z_{ED_t} - z_{EB_t}}{x_{ED_t} - x_{EB_t}} v + \left(z_{EB_t} - \frac{z_{ED_t} - z_{EB_t}}{x_{ED_t} - x_{EB_t}} x_{EB_t}\right)}^{\frac{z_{EC_t} - z_{EB_t}}{x_{EC_t} - x_{EB_t}} v + \left(z_{EB_t} - \frac{z_{EC_t} - z_{EB_t}}{x_{EC_t} - x_{EB_t}} x_{EB_t}\right)} \frac{\left(\frac{W_{rm}}{m} - \Upsilon_{j,t}\right) u}{\pi \left[(u)^2 + (v)^2 + \left(\frac{W_{rm}}{m} - \Upsilon_{j,t}\right)^2\right]^2} \, du \, dv & \text{otherwise} \\ + \int_{x_{ED_t} - X_{j,t}}^{x_{EA_t} - X_{j,t}} \int_{\frac{z_{EA_t} - z_{ED_t}}{x_{EA_t} - x_{ED_t}} v + \left(z_{ED_t} - \frac{z_{EA_t} - z_{ED_t}}{x_{EA_t} - x_{ED_t}} x_{ED_t}\right)}^{\frac{z_{EB_t} - z_{ED_t}}{x_{EB_t} - x_{ED_t}} v + \left(z_{ED_t} - \frac{z_{EB_t} - z_{ED_t}}{x_{EB_t} - x_{ED_t}} x_{ED_t}\right)} \frac{\left(\frac{W_{rm}}{m} - \Upsilon_{j,t}\right) u}{\pi \left[(u)^2 + (v)^2 + \left(\frac{W_{rm}}{m} - \Upsilon_{j,t}\right)^2\right]^2} \, du \, dv \end{cases}$$

$$C'N_{j,t} = \begin{cases} \int_{y_{NA_t}-\Upsilon_{j,t}}^{y_{ND_t}-\Upsilon_{j,t}} \int \left(\frac{z_{NC_t}-z_{NB_t}}{y_{NC_t}-y_{NB_t}}\right) v + \left(z_{NB_t} - \frac{z_{NC_t}-z_{NB_t}}{y_{NC_t}-y_{NB_t}} y_{NB_t}\right) \frac{\left(\frac{D_{rm}}{m} - X_{j,t}\right) u}{\pi\left[(u)^2 + (v)^2 + \left(\frac{D_{rm}}{m} - X_{j,t}\right)^2\right]^2} du\, dv \\ \quad \int \left(\frac{z_{ND_t}-z_{NB_t}}{y_{ND_t}-y_{NB_t}}\right) v + \left(z_{NB_t} - \frac{z_{ND_t}-z_{NB_t}}{y_{ND_t}-y_{NB_t}} y_{NB_t}\right) \\ + \int_{y_{NA_t}-\Upsilon_{j,t}}^{y_{ND_t}-\Upsilon_{j,t}} \int \left(\frac{z_{NB_t}-z_{ND_t}}{y_{NB_t}-y_{ND_t}}\right) v + \left(z_{ND_t} - \frac{z_{NB_t}-z_{ND_t}}{y_{NB_t}-y_{ND_t}} y_{ND_t}\right) \frac{\left(\frac{D_{rm}}{m} - X_{j,t}\right) u}{\pi\left[(u)^2 + (v)^2 + \left(\frac{D_{rm}}{m} - X_{j,t}\right)^2\right]^2} du\, dv \\ \quad \int \left(\frac{z_{NA_t}-z_{ND_t}}{y_{NA_t}-y_{ND_t}}\right) v + \left(z_{ND_t} - \frac{z_{NA_t}-z_{ND_t}}{y_{NA_t}-y_{ND_t}} y_{ND_t}\right) \\ 0 \text{ if } z_{NB_t} - z_{NA_t} \le 0 \\ 0 \text{ otherwise} \end{cases} \quad \text{if } x_{NA_t} = \frac{D_{rm}}{m} \wedge x_{ND_t} = \frac{D_{rm}}{m}$$

$$C'W_{j,t} = \begin{cases} 0 \text{ if } x_{WD_t} = 0 \vee z_{WB_t} - z_{WA_t} \le 0 \\ \int_{x_{WA_t}-X_{j,t}}^{x_{WD_t}-X_{j,t}} \int \left(\frac{z_{WC_t}-z_{WB_t}}{x_{WC_t}-x_{WB_t}}\right) v + \left(z_{WB_t} - \frac{z_{WC_t}-z_{WB_t}}{x_{WC_t}-x_{WB_t}} x_{WB_t}\right) \frac{\Upsilon_{j,t} u}{\pi\left[(u)^2 + (v)^2 + \left(\Upsilon_{j,t}\right)^2\right]^2} du\, dv \\ \quad \int \left(\frac{z_{WD_t}-z_{WB_t}}{x_{WD_t}-x_{WB_t}}\right) v + \left(z_{WB_t} - \frac{z_{WD_t}-z_{WB_t}}{x_{WD_t}-x_{WB_t}} x_{WB_t}\right) \\ + \int_{x_{WA_t}-X_{j,t}}^{x_{WD_t}-X_{j,t}} \int \left(\frac{z_{WB_t}-z_{WD_t}}{x_{WB_t}-x_{WD_t}}\right) v + \left(z_{WD_t} - \frac{z_{WB_t}-z_{WD_t}}{x_{WB_t}-x_{WD_t}} x_{WD_t}\right) \frac{\Upsilon_{j,t} u}{\pi\left[(u)^2 + (v)^2 + \left(\Upsilon_{j,t}\right)^2\right]^2} du\, dv \\ \quad \int \left(\frac{z_{WA_t}-z_{WD_t}}{x_{WA_t}-x_{WD_t}}\right) v + \left(z_{WD_t} - \frac{z_{WA_t}-z_{WD_t}}{x_{WA_t}-x_{WD_t}} x_{WD_t}\right) \\ \text{otherwise} \end{cases}$$

$$
C'EN_{j,t} = \left|
\begin{array}{l}
\displaystyle\int_{x_{ED_t}-X_{j,t}}^{x_{E_t}-X_{j,t}} \int_{\left(\frac{z_{EC_t}-z_{F_t}}{x_{EC_t}-x_{F_t}}\right)v+\left(z_{F_t}-\frac{z_{EC_t}-z_{F_t}}{x_{EC_t}-x_{F_t}}x_{F_t}\right)}^{\left(\frac{z_{ED_t}-z_{F_t}}{x_{ED_t}-x_{F_t}}\right)v+\left(z_{F_t}-\frac{z_{ED_t}-z_{F_t}}{x_{ED_t}-x_{F_t}}x_{F_t}\right)} \frac{\left(\frac{W_{rm}}{m}-\Upsilon_{j,t}\right)u}{\pi\left[(u)^2+(v)^2+\left(\frac{W_{rm}}{m}-\Upsilon_{j,t}\right)^2\right]^2}\,du\,dv \quad \text{if } x_{NA_t}=\frac{D_{rm}}{m} \wedge x_{ED_t}<\frac{D_{rm}}{m} \\
+\displaystyle\int_{x_{ED_t}-X_{j,t}}^{x_{E_t}-X_{j,t}} \int_{\left(\frac{z_{F_t}-z_{ED_t}}{x_{F_t}-x_{ED_t}}\right)v+\left(z_{ED_t}-\frac{z_{F_t}-z_{ED_t}}{x_{F_t}-x_{ED_t}}x_{ED_t}\right)}^{\left(\frac{z_{E_t}-z_{ED_t}}{x_{E_t}-x_{ED_t}}\right)v+\left(z_{ED_t}-\frac{z_{E_t}-z_{ED_t}}{x_{E_t}-x_{ED_t}}x_{ED_t}\right)} \frac{\left(\frac{W_{rm}}{m}-\Upsilon_{j,t}\right)u}{\pi\left[(u)^2+(v)^2+\left(\frac{W_{rm}}{m}-\Upsilon_{j,t}\right)^2\right]^2}\,du\,dv \\
+\displaystyle\int_{y_{NA_t}-\Upsilon_{j,t}}^{y_{E_t}-\Upsilon_{j,t}} \int_{\left(\frac{z_{F_t}-z_{NB_t}}{y_{F_t}-y_{NB_t}}\right)v+\left(z_{NB_t}-\frac{z_{F_t}-z_{NB_t}}{y_{F_t}-y_{NB_t}}y_{NB_t}\right)}^{\left(\frac{z_{E_t}-z_{NB_t}}{y_{E_t}-y_{NB_t}}\right)v+\left(z_{NB_t}-\frac{z_{E_t}-z_{NB_t}}{y_{E_t}-y_{NB_t}}y_{NB_t}\right)} \frac{\left(\frac{D_{rm}}{m}-X_{j,t}\right)u}{\pi\left[(u)^2+(v)^2+\left(\frac{D_{rm}}{m}-X_{j,t}\right)^2\right]^2}\,du\,dv \\
+\displaystyle\int_{y_{NA_t}-\Upsilon_{j,t}}^{y_{E_t}-\Upsilon_{j,t}} \int_{\left(\frac{z_{NB_t}-z_{E_t}}{y_{NB_t}-y_{E_t}}\right)v+\left(z_{E_t}-\frac{z_{NB_t}-z_{E_t}}{y_{NB_t}-y_{E_t}}y_{E_t}\right)}^{\left(\frac{z_{NA_t}-z_{E_t}}{y_{NA_t}-y_{E_t}}\right)v+\left(z_{E_t}-\frac{z_{NA_t}-z_{E_t}}{y_{NA_t}-y_{E_t}}y_{E_t}\right)} \frac{\left(\frac{D_{rm}}{m}-X_{j,t}\right)u}{\pi\left[(u)^2+(v)^2+\left(\frac{D_{rm}}{m}-X_{j,t}\right)^2\right]^2}\,du\,dv \\
0 \text{ if } z_{EC_t}-z_{ED_t}\le 0 \\
0 \text{ otherwise}
\end{array}
\right.
$$

$$C'WN_{j,t} = \begin{cases} \int_{x_{WA_t}-X_{j,t}}^{x_{E_t}-X_{j,t}} \int \left(\frac{z_{F_t}-z_{WB_t}}{x_{F_t}-x_{WB_t}}\right)v+\left(z_{WB_t}-\frac{z_{F_t}-z_{WB_t}}{x_{F_t}-x_{WB_t}}x_{WB_t}\right) \\ \qquad \int_{x_{WA_t}-X_{j,t}}^{x_{E_t}-X_{j,t}} \int \left(\frac{z_{E_t}-z_{WB_t}}{x_{E_t}-x_{WB_t}}\right)v+\left(z_{WB_t}-\frac{z_{E_t}-z_{WB_t}}{x_{E_t}-x_{WB_t}}x_{WB_t}\right) \\ \qquad\qquad \frac{\Upsilon_{j,t}\,u}{\pi\left[(u)^2+(v)^2+\left(\Upsilon_{j,t}\right)^2\right]^2}\,du\,dv \\ + \int_{x_{WA_t}-X_{j,t}}^{x_{E_t}-X_{j,t}} \int \left(\frac{z_{WB_t}-z_{E_t}}{x_{WB_t}-x_{E_t}}\right)v+\left(z_{E_t}-\frac{z_{WB_t}-z_{E_t}}{x_{WB_t}-x_{E_t}}x_{E_t}\right) \\ \qquad \int_{x_{WA_t}-X_{j,t}}^{x_{E_t}-X_{j,t}} \int \left(\frac{z_{WA_t}-z_{E_t}}{x_{WA_t}-x_{E_t}}\right)v+\left(z_{E_t}-\frac{z_{WA_t}-z_{E_t}}{x_{WA_t}-x_{E_t}}x_{E_t}\right) \\ \qquad\qquad \frac{\Upsilon_{j,t}\,u}{\pi\left[(u)^2+(v)^2+\left(\Upsilon_{j,t}\right)^2\right]^2}\,du\,dv \\ + \int_{y_{E_t}-\Upsilon_{j,t}}^{y_{ND_t}-\Upsilon_{j,t}} \int \left(\frac{z_{NC_t}-z_{F_t}}{y_{NC_t}-y_{F_t}}\right)v+\left(z_{F_t}-\frac{z_{NC_t}-z_{F_t}}{y_{NC_t}-y_{F_t}}y_{F_t}\right) \\ \qquad \int_{y_{E_t}-\Upsilon_{j,t}}^{y_{ND_t}-\Upsilon_{j,t}} \int \left(\frac{z_{ND_t}-z_{F_t}}{y_{ND_t}-y_{F_t}}\right)v+\left(z_{F_t}-\frac{z_{ND_t}-z_{F_t}}{y_{ND_t}-y_{F_t}}y_{F_t}\right) \\ \qquad\qquad \frac{\left(\frac{D_{rm}}{m}-X_{j,t}\right)u}{\pi\left[(u)^2+(v)^2+\left(\frac{D_{rm}}{m}-X_{j,t}\right)^2\right]^2}\,du\,dv \\ + \int_{y_{E_t}-\Upsilon_{j,t}}^{y_{ND_t}-\Upsilon_{j,t}} \int \left(\frac{z_{F_t}-z_{ND_t}}{y_{F_t}-y_{ND_t}}\right)v+\left(z_{ND_t}-\frac{z_{F_t}-z_{ND_t}}{y_{F_t}-y_{ND_t}}y_{ND_t}\right) \\ \qquad \int_{y_{E_t}-\Upsilon_{j,t}}^{y_{ND_t}-\Upsilon_{j,t}} \int \left(\frac{z_{E_t}-z_{ND_t}}{y_{E_t}-y_{ND_t}}\right)v+\left(z_{ND_t}-\frac{z_{E_t}-z_{ND_t}}{y_{E_t}-y_{ND_t}}y_{ND_t}\right) \\ \qquad\qquad \frac{\left(\frac{D_{rm}}{m}-X_{j,t}\right)u}{\pi\left[(u)^2+(v)^2+\left(\frac{D_{rm}}{m}-X_{j,t}\right)^2\right]^2}\,du\,dv \\ 0 \text{ if } z_{NC_t}-z_{ND_t}\le 0 \\ 0 \text{ otherwise} \end{cases} \quad \text{if } x_{WA_t} < \frac{D_{rm}}{m} \wedge x_{ND_t} = \frac{D_{rm}}{m}$$

$$C'room_{j,t} := \begin{cases} C'E_{j,t} \text{ if } C'E_{j,t} > 0 \\ C'EN_{j,t} \text{ if } C'EN_{j,t} > 0 \\ C'N_{j,t} \text{ if } C'N_{j,t} > 0 \\ C'WN_{j,t} \text{ if } C'WN_{j,t} > 0 \\ C'W_{j,t} \text{ if } C'W_{j,t} > 0 \\ 0 \text{ otherwise} \end{cases}$$

Workplane Illuminance due to direct daylighting

$$E'_{workplane_{j,t}} = C'_{room_{j,t}} \rho_{wall} E_{facadeb_t}$$

$$E_{wpb_t} = \begin{pmatrix} E'_{workplane_{1,t}} & E'_{workplane_{2,t}} & E'_{workplane_{3,t}} & E'_{workplane_{4,t}} & E'_{workplane_{5,t}} \\ E'_{workplane_{6,t}} & E'_{workplane_{7,t}} & E'_{workplane_{8,t}} & E'_{workplane_{9,t}} & E'_{workplane_{10,t}} \\ E'_{workplane_{11,t}} & E'_{workplane_{12,t}} & E'_{workplane_{13,t}} & E'_{workplane_{14,t}} & E'_{workplane_{15,t}} \\ E'_{workplane_{16,t}} & E'_{workplane_{17,t}} & E'_{workplane_{18,t}} & E'_{workplane_{19,t}} & E'_{workplane_{20,t}} \\ E'_{workplane_{21,t}} & E'_{workplane_{22,t}} & E'_{workplane_{23,t}} & E'_{workplane_{24,t}} & E'_{workplane_{25,t}} \end{pmatrix}$$

Final Workplane Illuminance

$$E_{workplane_t} = E_{wpb_t} + E_{wpd_t}$$

$kk = 1,2 \ldots 5 \qquad jj = 1,2 \ldots 5$

$Min_t = min\left(E_{workplane_t}\right)$ ...minimum workplane illuminance

$Max_t = max\left(E_{workplane_t}\right)$ ...maximum workplane illuminance

$$E_{mean_t} = \sum_{jj=1}^{5} \sum_{kk=1}^{5} \left(\frac{E_{workplane_t}}{25}\right)_{jj,kk}$$ ...Average workplane illuminance

Coordınates of the selected workplane poınts

$$\mathrm{Drm} = \frac{1}{m}\begin{bmatrix} 0\ 1m & \dfrac{D_{rm} - 0\ 2m}{4} + 0\ 1m & \dfrac{2\left(D_{rm} - 0\ 2m\right)}{4} + 0\ 1m & \dfrac{3\left(D_{rm} - 0\ 2m\right)}{4} + 0\ 1m & D_{rm} - 0\ 1m \\ 0\ 1m & \dfrac{D_{rm} - 0\ 2m}{4} + 0\ 1m & \dfrac{2\left(D_{rm} - 0\ 2m\right)}{4} + 0\ 1m & \dfrac{3\left(D_{rm} - 0\ 2m\right)}{4} + 0\ 1m & D_{rm} - 0\ 1m \\ 0\ 1m & \dfrac{D_{rm} - 0\ 2m}{4} + 0\ 1m & \dfrac{2\left(D_{rm} - 0\ 2m\right)}{4} + 0\ 1m & \dfrac{3\left(D_{rm} - 0\ 2m\right)}{4} + 0\ 1m & D_{rm} - 0\ 1m \\ 0\ 1m & \dfrac{D_{rm} - 0\ 2m}{4} + 0\ 1m & \dfrac{2\left(D_{rm} - 0\ 2m\right)}{4} + 0\ 1m & \dfrac{3\left(D_{rm} - 0\ 2m\right)}{4} + 0\ 1m & D_{rm} - 0\ 1m \\ 0\ 1m & \dfrac{D_{rm} - 0\ 2m}{4} + 0\ 1m & \dfrac{2\left(D_{rm} - 0\ 2m\right)}{4} + 0\ 1m & \dfrac{3\left(D_{rm} - 0\ 2m\right)}{4} + 0\ 1m & D_{rm} - 0\ 1m \end{bmatrix}^{T}$$

$$\mathrm{Wrm} = \frac{1}{m}\begin{bmatrix} W_{rm} - 0\ 1m & \dfrac{3\left(W_{rm} - 0\ 2m\right)}{4} + 0\ 1m & \dfrac{2\left(W_{rm} - 0\ 2m\right)}{4} + 0\ 1m & \dfrac{W_{rm} - 0\ 2m}{4} + 0\ 1m & 0\ 1m \\ W_{rm} - 0\ 1m & \dfrac{3\left(W_{rm} - 0\ 2m\right)}{4} + 0\ 1m & \dfrac{2\left(W_{rm} - 0\ 2m\right)}{4} + 0\ 1m & \dfrac{W_{rm} - 0\ 2m}{4} + 0\ 1m & 0\ 1m \\ W_{rm} - 0\ 1m & \dfrac{3\left(W_{rm} - 0\ 2m\right)}{4} + 0\ 1m & \dfrac{2\left(W_{rm} - 0\ 2m\right)}{4} + 0\ 1m & \dfrac{W_{rm} - 0\ 2m}{4} + 0\ 1m & 0\ 1m \\ W_{rm} - 0\ 1m & \dfrac{3\left(W_{rm} - 0\ 2m\right)}{4} + 0\ 1m & \dfrac{2\left(W_{rm} - 0\ 2m\right)}{4} + 0\ 1m & \dfrac{W_{rm} - 0\ 2m}{4} + 0\ 1m & 0\ 1m \\ W_{rm} - 0\ 1m & \dfrac{3\left(W_{rm} - 0\ 2m\right)}{4} + 0\ 1m & \dfrac{2\left(W_{rm} - 0\ 2m\right)}{4} + 0\ 1m & \dfrac{W_{rm} - 0\ 2m}{4} + 0\ 1m & 0\ 1m \end{bmatrix}$$

Appendix H:

Artificial Lighting Control Strategies

Artificial lighting control

Workplane illuminance values for the three luminaires (at full power)

$$E1_t = \begin{pmatrix} 139 & 194 & 220 & 194 & 139 \\ 156 & 214 & 240 & 214 & 156 \\ 140 & 182 & 200 & 182 & 140 \\ 109 & 133 & 142 & 133 & 109 \\ 80 & 102 & 109 & 102 & 80 \end{pmatrix} \text{lx for luminaire Lum1}$$

$$E2_t = \begin{pmatrix} 121 & 153 & 176 & 153 & 121 \\ 144 & 185 & 209 & 185 & 144 \\ 153 & 204 & 235 & 204 & 153 \\ 141 & 186 & 213 & 186 & 141 \\ 117 & 150 & 165 & 150 & 117 \end{pmatrix} \text{lx for luminaire Lum2}$$

$$E3_t = \begin{pmatrix} 80 & 102 & 109 & 102 & 80 \\ 109 & 133 & 142 & 133 & 109 \\ 140 & 182 & 200 & 182 & 140 \\ 156 & 214 & 240 & 214 & 156 \\ 139 & 194 & 220 & 194 & 139 \end{pmatrix} \text{lx for luminaire Lum3}$$

$E_{art_t} = E1_t + E2_t + E3_t$ workplane illuminance due to electric lighting

$$E_{art\_mean_t} = \sum_{jj=1}^{5} \sum_{kk=1}^{5} \left(\frac{E_{art_t}}{25} \right)_{jj,kk}$$ Average workplane illuminance due to electric lighting

i) On-Off control

$$Fonoff_t = \begin{cases} 1 & \text{if } E_{mean_t} < 500\text{lx} \\ 0 & \text{if } E_{mean_t} \geq 500\text{lx} \end{cases}$$

$$Eonoff_t = Fonoff_t E_{art_t} + E_{workplane_t}$$

$$Eonoff_{luminaire_t} = Eonoff_t - E_{workplane_t}$$

ii) Unison dimming control

$$Funison_t = \begin{cases} \dfrac{E_{art\_mean_t} - E_{mean_t}}{E_{art\_mean_t}} & \text{if } 0 < \dfrac{E_{art\_mean_t} - E_{mean_t}}{E_{art\_mean_t}} \leq 1 \\ 0 & \text{otherwise} \end{cases}$$

$$Eunison_t = Funison_t E_{art_t} + E_{workplane_t}$$

$$Eunison_{luminaire_t} = Eunison_t - E_{workplane_t}$$

Artificial lighting energy consumption

Experimental equation of luminaires' energy consumption as a function of percent luminous flux (O'Neill,2008)

$tt = 7,8 \ldots 18$

Number of Luminaires

$$Lum = \begin{cases} 3 \text{ if } W_{rm} = 4m \wedge D_{rm} = 4m \\ 4 \text{ if } W_{rm} = 4m \wedge D_{rm} = 5m \\ 4 \text{ if } W_{rm} = 4m \wedge D_{rm} = 6m \end{cases}$$

i) On-Off control

$$Ponoff_{luminaires_t} = \begin{cases} \left[0.5477 \left(100 \, Lum \, Fonoff_t\right) + 11.909\right] W \text{ if } Fonoff_t > 0 \\ 0W \text{ otherwise} \end{cases}$$

$$Energy_{onoffhr_{tt}} = \frac{\left(Ponoff_{luminaires_{tt}} + Ponoff_{luminaires_{tt+1}}\right) hr}{2}$$ hourly energy consumption

$$E_{energyonoff} = \sum_{tt} Energy_{onoffhr_{tt}}$$ daily energy consumption (from 7.00 to 19.00)

ii) Unison dimming control

$$Punison_{luminaires_t} = \begin{cases} \left[0.5477 \left(100 \, Lum \, Funison_t\right) + 11.909\right] W \text{ if } Funison_t > 0 \\ 0W \text{ otherwise} \end{cases}$$

$$Energy_{unisonhr_{tt}} = \frac{\left(Punison_{luminaires_{tt}} + Punison_{luminaires_{tt+1}}\right) hr}{2}$$

$$E_{energyunison} = \sum_{tt} Energy_{unisonhr_{tt}}$$

Appendix I:

Daylighting/Lighting Model Outputs

Results

Daylight workplane illuminance distribution

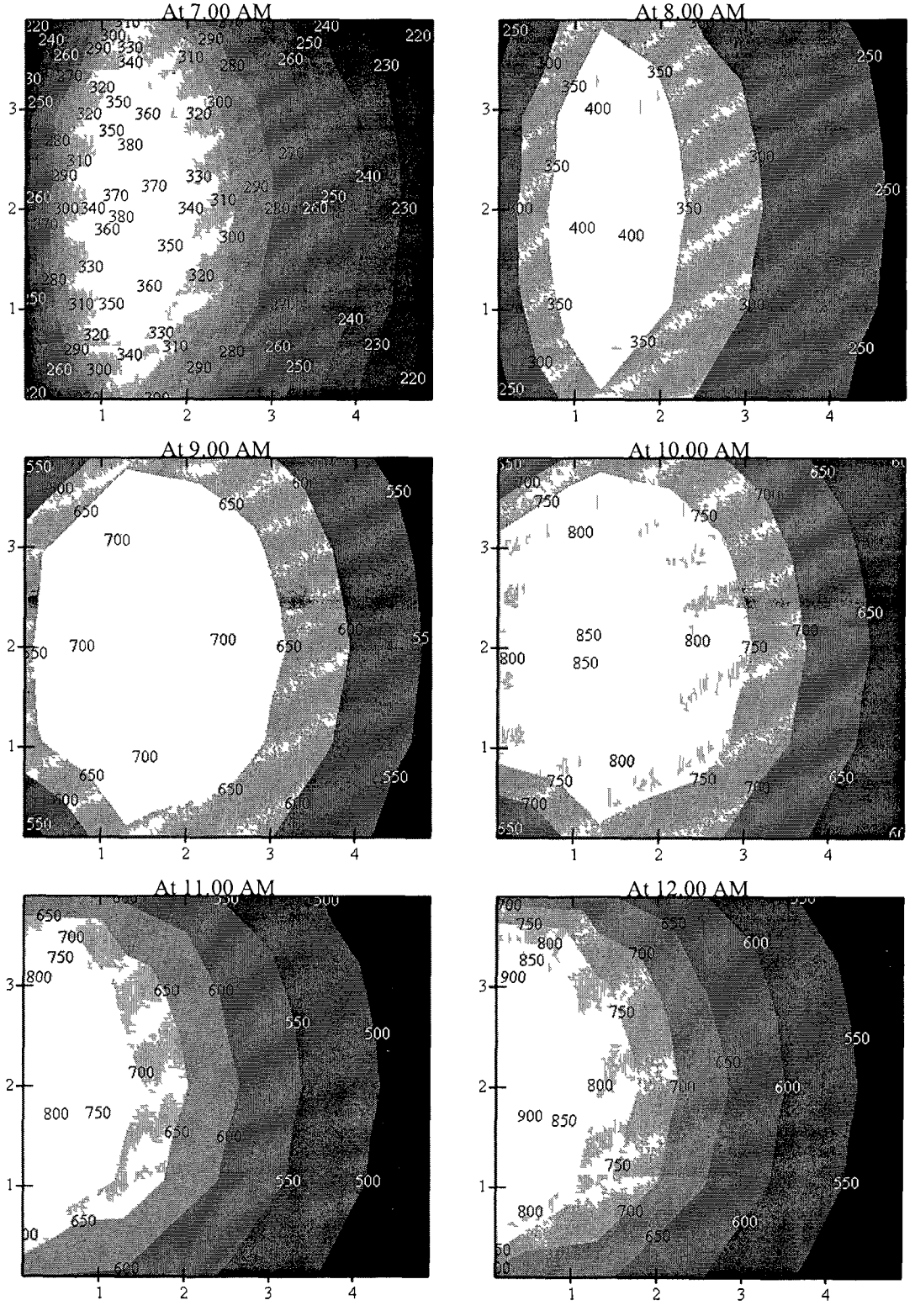

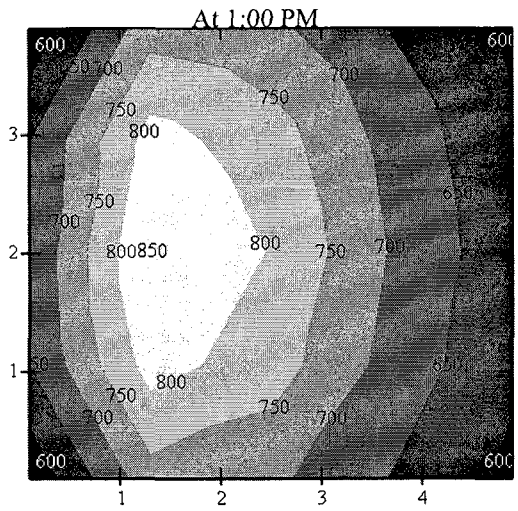
At 1:00 PM

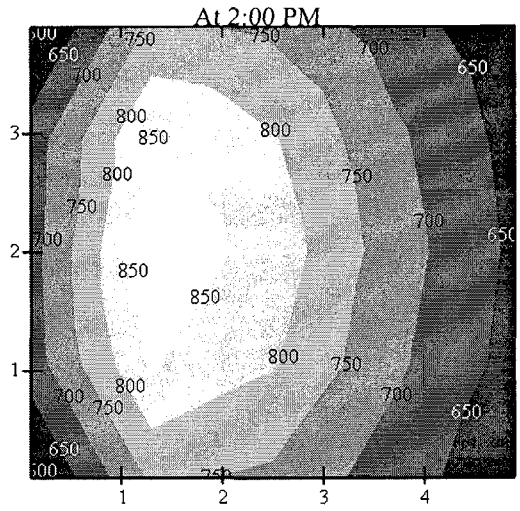
At 2:00 PM

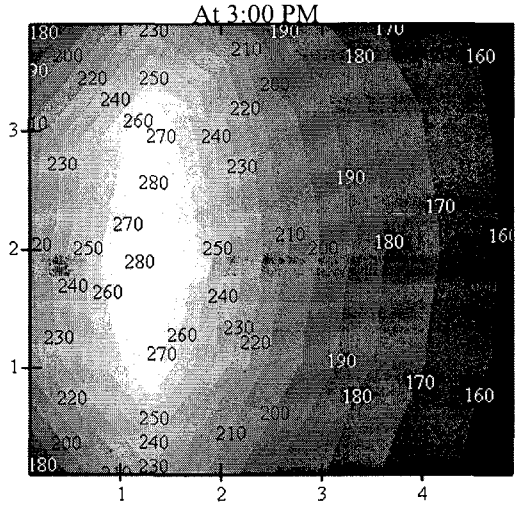
At 3:00 PM

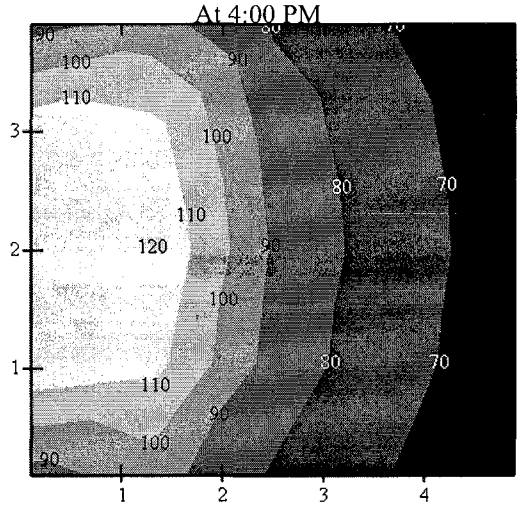
At 4:00 PM

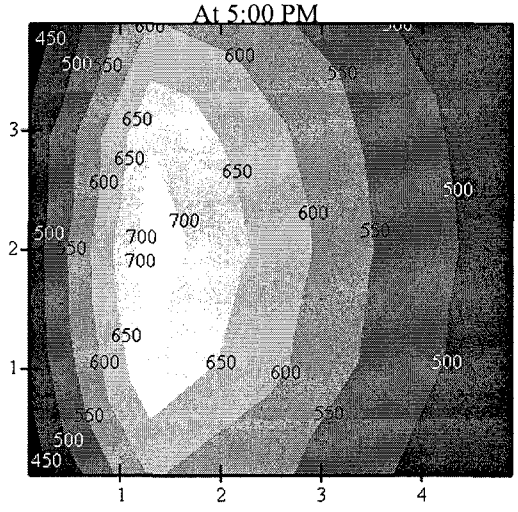
At 5:00 PM

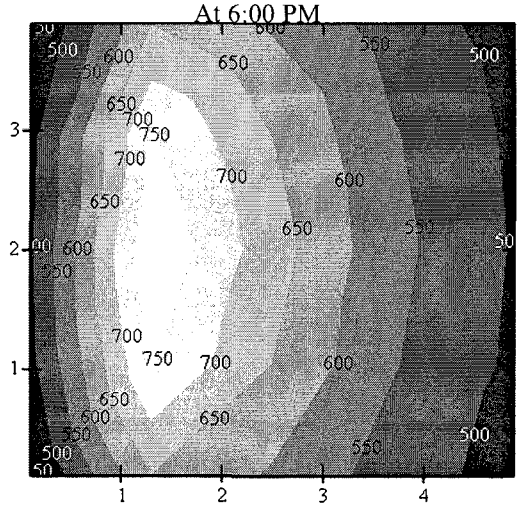
At 6:00 PM

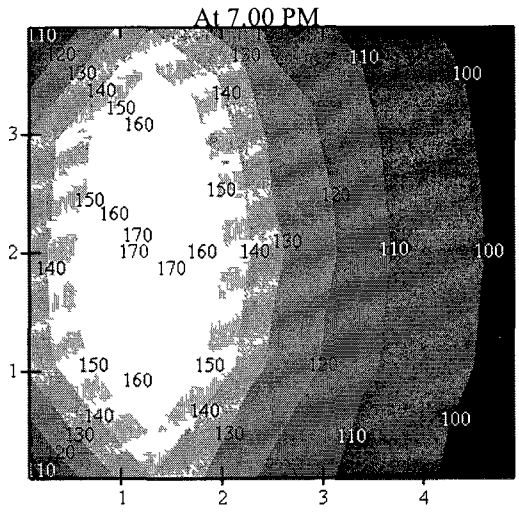

Shade Position and dimming factor